Design of a sustainable archive for the preservation of a nitrate film collection

Document Version:
Publisher's PDF, also known as Version of Record (includes final page, issue and volume numbers)

Please check the document version of this publication:

• A submitted manuscript is the version of the article upon submission and before peer-review. There can be important differences between the submitted version and the official published version of record. People interested in the research are advised to contact the author for the final version of the publication, or visit the DOI to the publisher's website.
• The final author version and the galley proof are versions of the publication after peer review.
• The final published version features the final layout of the paper including the volume, issue and page numbers.

Link to publication

Design of a sustainable archive for the preservation of a nitrate film collection

22nd February 2023

Daria Zendri

EINDHOVEN UNIVERSITY OF TECHNOLOGY

Stan Ackermans Institute

SMART BUILDINGS & CITIES

Design of a sustainable archive for the preservation of a nitrate film collection

By

Daria Zendri

A thesis submitted in partial fulfillment of the requirements for the degree of

Engineering Doctorate (EngD)

The design described in this thesis has been carried out in accordance with the TU/e
Code of Scientific Conduct

Dr.ir. Roel Loonen, university supervisor

MA Walter Swagemakers, company advisor

Eindhoven, the Netherlands

February 2023

This thesis has been established in collaboration with

Summary

The Eye Filmmuseum is the national film institute and museum for film heritage and film art in the Netherlands. Approximately 8% of Eye's total film collection consists of nitrate film, a material used for motion picture film, that becomes unstable when good climate conditions such as low temperature, around 2°C, and low relative humidity, between 20 and 30% are not maintained. If big quantities of deteriorated nitrate are stored together, they may spontaneously ignite. Nitrate film burns quickly, produces poisonous smoke containing toxic fumes and, once it is burning, it is hard to put out. Since the collection is currently held in old bunkers that cannot provide a proper climate, the Eye Filmmuseum wants to move its collection to a new depot that meets the requirements for a good preservation of the nitrate film collection. This EngD project aims at creating a set of recommendations for the configuration of a new nitrate archive for the Eye Filmmuseum. Solutions for different aspects of the building are explored, including materials, cooling strategies, dehumidification and ventilation, fire safety, energy efficiency, environmental impact, and costs.

Different nitrate archives from different countries are examined, to identify best-practices in terms of materials, cooling and dehumidification strategies, fire safety systems and costs. Moreover, standards from ISO, NFPA and Kodak are investigated to understand the specific building requirements of a nitrate archive.

The material considered for the building structure is Cross Laminated Timber, due to its good hygrothermal properties, its renewability, and for its behavior in case of fire. Passive cooling strategies are analyzed; shading elements, such as a roof canopy, protect the building from direct solar irradiance. Low emissivity and reflective materials can further lower the cooling demand of the building. Energy efficient mechanical cooling can be provided by an air chiller or heat pump; a desiccant wheel is the most efficient system for dehumidification, considering low temperature and low relative humidity requirements.

For fire safety, two different fire tests are examined, one to assess the behavior of nitrate fire, and the second to assess the behavior of a CLT building subjected to fire. For the collection storage, two types of shelves are considered, movable and fixed, which require different building design and fire suppression systems. Movable shelves require compartmentation, to avoid the spread of fire in the adjacent vault; this is done by using rock mineral wool, a non-flammable material. Fixed shelves are open faced and made with steel-clad insulation material, which prevents the fire from spreading from the shelves to the vault. Additionally, with the use of a fire suppression system, the compartmentation is not necessary. Due to the different requirements, the two types of shelves lead to two different building configurations. In both designs, fire doors and explosion vents are necessary.

To assess the yearly electricity demand of the archive building, considering its indoor climate requirements, an outline of the building shape+ is created, according to the collection size, and building energy simulations are run. To cover yearly electricity demand, different number of photovoltaic panels are also considered in the simulation. The PV system is coupled with batteries of different sizes to increase the self-consumption of electricity and lower the dependency from the grid. The payback time for each combination of PVs number and battery size is assessed. The results show that the building with only PVs have higher import from the grid than self-consumption, while a building with both PVs and batteries have lower import from the grid compared to the self-consumed electricity. Considering the same number of PVs and different battery sizes, the amount of electricity imported from the grid decreases as well as the electricity sold to the grid, while self-consumption increases.

The payback time of each PV system size and battery capacity combination was calculated. The results show that any number of PV modules installed have approximately the same payback period. For the case with batteries, on average the bigger the battery, the longer the payback time. When taking into account only one battery size, if the number of PV panels increases, the payback time is shorter. When big batteries are coupled with less PVs, the payback time shows that the system is not viable.

The sensibility of a thermal energy storage using ice slurry for the archive building was explored. By using the surplus electricity produced by the PV system during the day, ice slurry is produced and stored in tanks. During the night, when there is no electricity production, the ice slurry melts and provides free cooling to the vaults. Considering different number of PV panels, the cooling capacity of such systems seems to be enough to cover the night cooling demand of most days during the entire summer.

The behavior of an emergency battery is analyzed, to bridge the cooling demand during possible blackouts. It was calculated that an emergency battery of at least 20 kWh can help to provide enough electricity to the system for at least 26 h, considering a building with and without fixed battery and with blackouts happening both in summer and in winter.

The environmental impact of the building was analyzed for different aspects. The impact of the CLT structure of the building was compared to two other building structure types, namely concrete and lightweight timber frame, considering embodied energy and embodied carbon. The data is collected from Environmental Product Declarations of different materials. Results show that, on average, concrete has the highest impact, followed by CLT; lightweight timber frame has the lower impact.

The carbon payback time of PVs and battery is calculated. Overall, the best performance is given by smaller batteries; when considering PVs and batteries, smaller batteries give on average a shorter carbon payback time. Considering different number of PVs with the same battery size, the higher the number of PVs, the longer the carbon payback; implemented batteries can save up to three times the amount of CO_2.

Considering the Dutch goal of reduction of greenhouse gases to almost zero by 2050, the difference between current carbon payback and future carbon payback for PVs and batteries was assessed. Choosing lower embodied carbon solutions in the early design phase, will compensate the reduction of carbon through the years given by the transition of the grid toward renewable energy sources.

Finally, a cost estimation of the different scenarios is made; the amount of materials used for each scenario is calculated and the costs of each material are collected from supplier. A tool was used to assess indirect and additional construction costs. A range of the estimation of each scenario is given, and the cost is compared to two nitrate archives, built in the last decade, considering the rise in construction cost.

Table of contents

1 Introduction

1.1 The Eye Filmmuseum

The Eye Filmmuseum is the national film institute and the only museum for film heritage and film art in the Netherlands. Over the past 70 years, Eye has acquired an internationally leading collection that spans the entire history of film, up to and including the most recent Dutch films. The collection contains approximately 50,000 film titles (60% of which are international), 700,000 photographs, 82,000 posters, 7,000 sheet music items, some 200 archives of filmmakers and organizations, approximately 1,500 devices and an extensive library collection. In 2016, the new Eye Collection Centre opened, where the Eye collection has a safe depot under the best possible storage conditions. However, the safety and storage conditions of the nitrate film collection, which cannot be stored in the Eye Collection Centre for safety reasons, are currently far from optimal.

1.2 The nitrate film collection and its preservation

Approximately 8% of Eye's total film collection (around 27,000 cans) consists of nitrocellulose carriers, so-called nitrate film. Nitrate refers to a group of early transparent plastic film supports that were common between the end of the nineteenth century and up to the early 1950s. Nitrate film was used for still photographic negatives, as well as motion picture film. Most nitrate consists of a flexible sheet or roll of cellulose nitrate film base with a silver gelatin photographic emulsion [1]; more modern film is acetate or polyester-based.

As it deteriorates, nitrate releases highly acidic nitrogen oxide gases which are harmful for the collection. Not only heat and poor ventilation are bad for nitrate film: this material absorbs humidity, which accelerates its decomposition. In advanced stages of decomposition, self-ignition of nitrate film can take place at temperatures as low as 38°C [2]. Nitrate film burns extremely quickly, with a hot and intense flame; it produces very dense, poisonous smoke containing copious amounts of nitrogen dioxide fumes; unlike other flammable materials, nitro-cellulose does not need oxygen and, once it is burning, it is hard to put out [2].

Figure 1. Left: healthy nitrate film [picture taken by author]; right: highly decomposed nitrate film [3]

According different studies [4] keeping nitrate film under the right climatic conditions slows down its decomposition and gives the collection a longer life; the proper climate conditions for nitrate film is below 2°C and approximately 35% Relative Humidity (RH). To safeguard the collection, it is fundamental to store it in a conditioned environment, keeping the film away from any source of heat, for example radiators and light bulbs [1]. Moreover, temperature and humidity should not increase or decrease more than 1°C and 1% per hour, respectively.

1.3 Current state of the Eye Filmmuseum's nitrate archives

Eye's nitrate film collection is currently divided in three different locations of the Netherlands: Overveen, Heemskerk and Castricum. None of the three meet the requirements for the proper preservation of nitrate film.

Figure 2. Current eye's nitrate bunkers. 1) Overveen; 2) Heemskerk; 3) Castricum.

All three storage spaces are old bunkers, respectively built in 1971, 1941 and 1939. The vaults in Castricum and Hemskeerk have no cooling system, only dehumidification, and presents temperatures between 14 and 19 all year round. The vaults in Overveen, despite cooling and dehumidification system, have temperature and RH above the advised threshold. Moreover, all three present other problems, such as mold growth due to bad insulation. In spite of a very low probability, should a fire occur in one of the vaults, it would affect a lot of vulnerable objects found in the surroundings, such as buildings and roads; for this reason, fatalities due to formation and spread of toxic combustion gases cannot be excluded. In addition, the bunkers are located in the protected dune area of Kennemerland (Natura 2000), and a fire could cause significant damage to the environment.

1.3.1 Overveen

Figure 3 and Figure 4 represent respectively the plan and sections of the archive in Overveen. The building consists of eight vaults, where the nitrate film is preserved, and a technical room, adjacent to vault number 8. As depicted in Figure 4, section B-B, an escape system was designed so that, in case of fire, the flames are redirected away from the building in a controlled way.
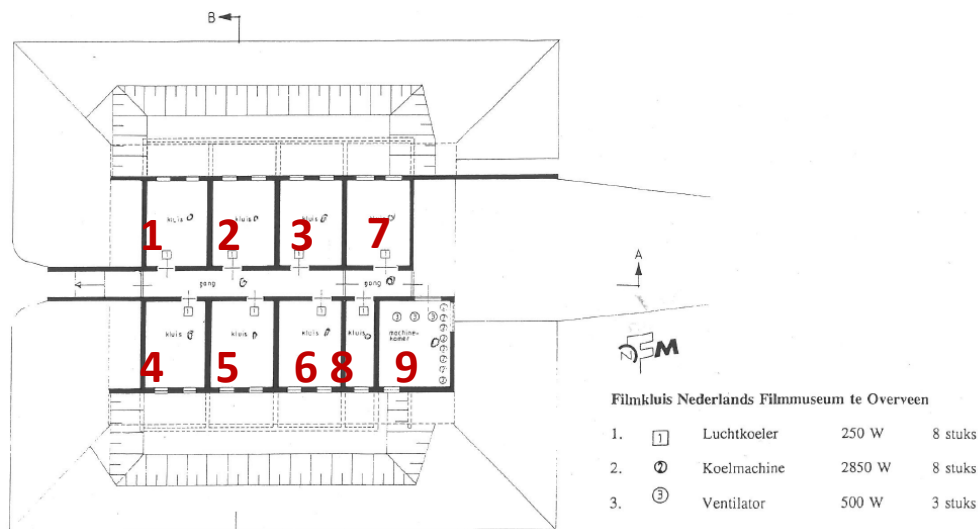
Figure 3. Plan of the archive in Overveen. 1-8: archive storage; 9: technical room.

Filmkluis Nederlands Filmmuseum te Overveen

1.	▢	Luchtkoeler	250 W	8 stuks
2.	②	Koelmachine	2850 W	8 stuks
3.	③	Ventilator	500 W	3 stuks

doorsnede A-A

doorsnede B-B
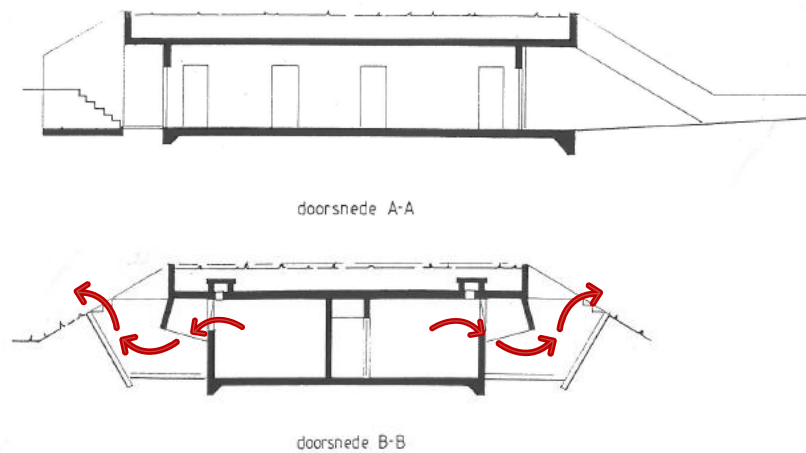
Figure 4. Sections of the archive in Overveen

The Eye Filmmuseum carried out an analysis of the building performance, assessing that the building, at the current state, cannot properly preserve the nitrate collection, and no changes can be made that will improve the climate condition of the vaults. The main points from the analysis, represented in Figure 5 to Figure 8, are the following:

- The climate conditions are well above the ISO norm 10356:1996 (2°C, 30% RH);
- Cells 2 and 8 are above the threshold for mold and there is mold growth in several cells;
- The climate in cell 8 does not seem to be under control and fluctuates a lot. This is most likely due to the cooling system in the technical room, that is adjacent to cell 8;
- Due to abrupt heating moments, given by bad system functioning or fluctuations, several condensation incidents have been reported. That is bad for the collection: condensation is a trigger for decomposition;
- The cells in the southern side (3 and 7), are more sensitive to outside temperatures: in the heat wave (2018) the temperature has gone up, while the other cells remained stable.
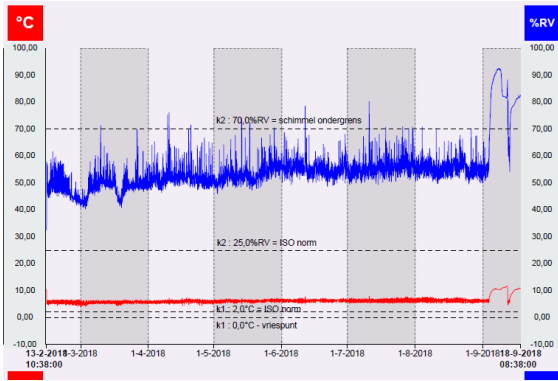
Figure 5. Temperature and RH in vault 2
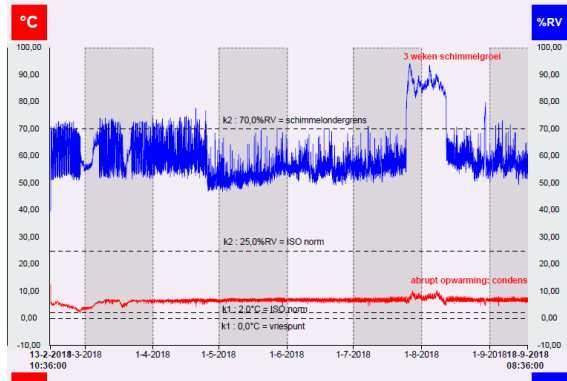
Figure 6. Temperature and RH in vault 3
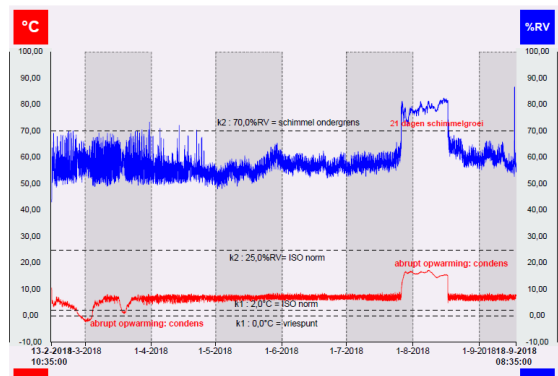
Figure 7. Temperature and RH in vault 7
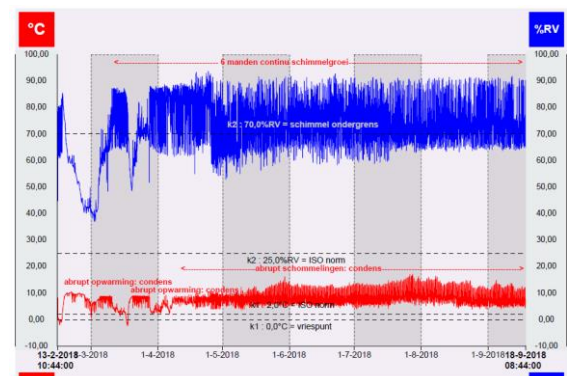
Figure 8. Temperature and RH in vault 8

12

2 Design process

2.1 Project problem statement

Since the current archives can no longer meet the proper climate conditions for the nitrate film collection, the Eye Filmmuseum wants to move its collection to a new depot that meets all the above-mentioned requirements, and has looked at newly built nitrate vaults within its network of film archives and museums. They selected the nitrate depot built by the Austrian Film Archive in 2010 as an inspiring examplehe depot is based on a construction of Cross Laminated Timber (CLT), a renewable material with low carbon impact and good hygrothermal properties.

The current nitrate film collection of the museum comprises 27,000 cans; the Eye Filmmuseum foresees a growth of roughly 30% in the next years, hence the capacity for the archive should be for 40,000 cans. The vaults where the collection is held should have a temperature of 2°C and a relative humidity between 20 and 30%. The design of the archive should achieve high energy efficiency through sensible material choice, active cooling systems and passive cooling strategies. To cover the electricity demand of the archive building, energy production and storage should be considered. Although the chance of fire is low, the design should allow to save as much of the collection as possible, while ensuring the safety of people and surroundings.

This EngD project aims at creating a set of recommendations for the design of a new nitrate archive for the Eye Filmmuseum. Different aspects and needs for this type of building are analyzed: preservation of the collection through proper indoor climate conditions and fire safety, also considering energy and cost efficiency, and environmental impact.

The insights are based on a wide variety of design-driven research activities, combining knowledge from the Eye Filmmuseum regarding nitrate film, with different kinds of simulations and calculations. The findings elaborate on topics such as the influence of material choice regarding indoor clime conditions, fire safety, and environmental performance; renewable energy systems, their return of investment and carbon payback; overall energy efficiency considering materials and passive cooling strategies.

2.2 Methodology

The project started with an analysis of a large selection of state-of-the-art nitrate archives built by different institutes and museums worldwide. The research continued around three topics: materials, cooling strategies and fire safety. For the latter, different fire tests were analyzed, and feedback was received by a fire safety specialist, lecturer at TU/e. Moreover, input was given by the Eye advisors regarding nitrate film, its behavior in different conditions, and its characteristics.

After the first analysis, an outline of the building shape according to the collection size was created. A virtual model for each scenario was made, with the materials and characteristics given by the results of the initial research.

Simulations were run to assess the electricity consumption of the building, considering the strict climate conditions requirements. The simulations were used as a tool to support the research findings regarding lowering the electricity demand through passive cooling strategies and system design. Once the model was finalized, a suitable PV system was analyzed for the building, to cover the yearly electricity consumption. The PV system was then coupled with batteries of different sizes to increase the self-consumption and lower the dependency from the grid. The payback time for each combination of PVs number and battery size was calculated.

The environmental impact of the CLT structure was assessed and compared to two other building construction types, namely concrete and lightweight timber frame. The carbon payback of PVs and battery system and for different insulation thicknesses was calculated.

A presentation at the Eye Filmmuseum at the end of the first year was organized to present the project and get feedback from different stakeholders, including heritage inspectors, heritage climate specialists, infrastructure policy makers, collection specialists, and researchers.

Constant feedback was received by the university supervisor regarding the technical aspects, through weekly progress meetings, while practical knowledge on the nitrate collection was given by the advisors of Eye Filmmuseum through monthly progress meetings.

Figure 9 shows a graphical outline of the design process that was followed during this project. The outcomes of each of the investigations is described in the content chapters 3-11. The results of the individual steps are synthesized in chapter 12: Design recommendations for a safe and energy-efficient nitrate archive building. Finally, this report also includes a large number of appendices where the interested reader can find more detailed information about the research, calculations, and graphs regarding the different chapters.
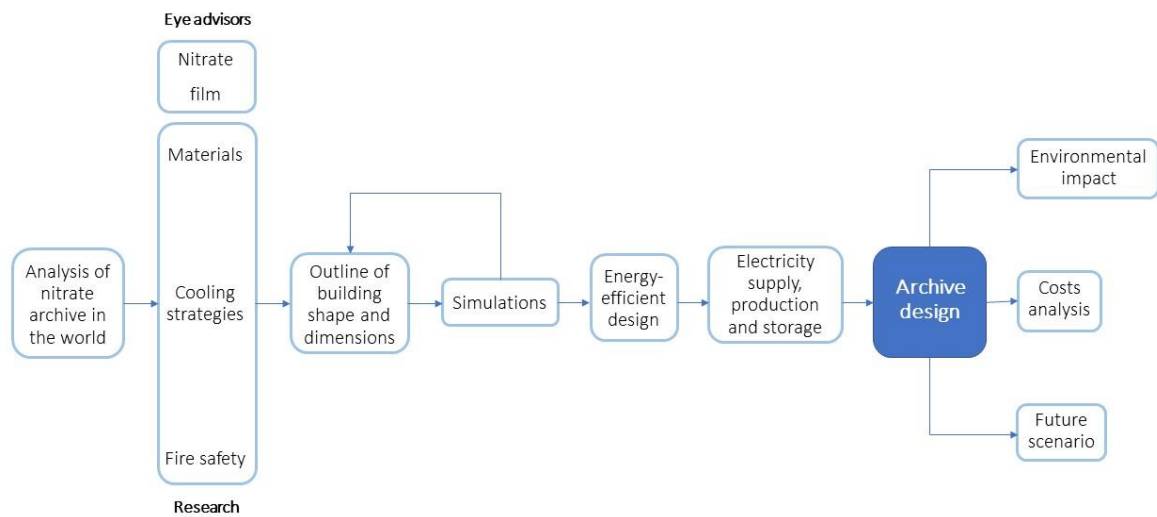
Figure 9. Project methodology

3 Nitrate archives – Standards and reference projects

3.1 Current standards and guidelines

Both ISO (International Organization for Standardization) and the NFPA (National Fire Protection Association) published norms regarding storage and handling of nitrate film: the ISO norm 10356 and the NFPA 40. While the ISO is international and operates around the world in 165 countries, the NFPA is based in the United States and operates only in a few countries, Europe excluded [5].

Through the years, the US has had several nitrate film fires, which led to the loss of plentiful film material [4][5] and consequently brought to the creation of more stringent regulations, thoroughly described in the NFPA 40. Since these rules do not apply to Europe, the NFPA 40 was used in this research as indications of dimensions for the design of the archive, together with the ISO norm 10356 [8].

Moreover, the leading manufacturer of film and photographic supply Eastman Kodak Company, better known as Kodak, has created several guidelines for properly preserve film collections, among which nitrate film.

In Sections 3.1.1, 3.1.2 and 3.1.3 the main points of these documents are summarized.

3.1.1 ISO 10356:1996 – Cinematography: Storage and handling of nitrate-base motion-picture films

The document that regulates nitrate film is the ISO 10356:1996 – Cinematography: Storage and handling of nitrate-base motion-picture films [9]; the main points taken are the following:

Rolls of nitrate-base film that have not yet deteriorated shall be placed in individual metal cans (aluminum or stainless steel) with fitted but unsealed closures until they can be duplicated to safety film. Storage rooms and chambers should contain only nitrate-base film. Storage rooms should be equipped with appropriate ventilating systems, fire sensors, water sprinklers, etc. so that any possible conflagration can be confined to that room. These rooms should be constructed and ventilated so that toxic and flammable fumes and gases cannot reach other rooms.

Recommended climatic conditions for storage are given in Table 1.

Table 1. Recommended climatic conditions

Storage	Maximum temperature (°C)	Relative humidity (%)
Short term*	25	25 to 50
Long term	2	20 to 30

* For example, examination, cleaning, or duplication

The different deterioration speeds of nitrate-base film cannot be explained completely, although many factors are known to influence the stability. These are:

- Inner stability and degree of purity of the cellulose nitrate;
- Keeping temperature – the deterioration speed doubles for each 5°C temperature increase;
- Humidity content of the film;
- Content of nitrogen oxides in the film;
- Acid gases from the air.

3.1.2 NFPA 40:2019 – Standard for the Storage and Handling of Cellulose Nitrate Film

NFPA is the National Fire Protection Association, the international organization devoted to eliminating death, injury, and economic loss due to fire, electrical and related hazards. The main points taken from the NFPA 40:2019 – Standard for the Storage and Handling of Cellulose Nitrate Film [10] are the following:

Chapter 4: Construction Requirements and Arrangements of Buildings

- Construction
  - Nitrate film shall be stored or handled only in buildings of Type I construction, as define in NFPA 220 (Type I: Non-combustible (or limited combustible) construction material with a high level of fire resistance, typically concrete construction);
  - Decomposition vents and explosion vents shall be of non-combustible construction;
  - All rooms where nitrate film is stored or handled shall be separated from each other and from all other parts of the building by partitions having fire resistance rating at least 1 hour;
  - Explosion venting shall be provided in the ratio of 0.09 m^2 of free vent area per each 1.4 m^3 of room or vault volume;
  - The minimum aisle width for film vaults shall be 760 mm.

Chapter 5: Fire Protection

- Automatic sprinklers
  - The purpose of this protection is to prevent fire or heat from affecting storage that is not initially involved in a fire;
  - Every room where nitrate is stored in quantities greater than 23 kg, or 3050 m, shall be protected by an automatic sprinkler system that is installed in accordance with the requirements of NFPA13 group II extra hazard occupancies (*defined as occupancies or portions of other occupancies with moderate to substantial amounts of flammable or combustible liquids or occupancies where shielding of combustible is extensive).

Chapter 6: Storage of Nitrate Film

- Extended term storage vaults
  - Walls and floors of vaults shall be of Type I construction and shall not have less than 4-hour fire resistance;
  - Extended term storage vaults shall comply with 6.3.1.3, 6.3.1.4, 6.3.1.5:
    - 6.3.1.3 Where the ceiling of a vault is a bearing floor, it shall have fire resistance of at least 4 hours;
    - 6.3.1.4 Where the vault walls extend 0.9 m or more above the roof, the vault roof and ceiling shall be permitted to be constructed of non-combustible materials and shall be permitted to serve as an explosion vent;
    - 6.3.1.5 Vaults shall be provided with drains or scuppers to carry automatic sprinkler discharge directly to the outside of the building;
  - Door openings in extended term storage vaults shall be protected with automatic, self-closing door assemblies having fire protection rating of 3 hours;
  - Shelves and vertical barriers shall be of non-combustible insulating material that is at least 9.5 mm thick or of hardwood construction that is at least 25 mm thick;
  - Racks shall be designed in relation to the sprinkler system so that the open face of each rack structure shall be protected by the sprinkler system.

3.1.3 KODAK – Storage and Handling of Processed Nitrate Film

On the official website of Kodak [2], it is possible to find guidelines on how to properly handle processed nitrate film. Following the most important principles:

- Storage vaults and conditions
  - Store negatives only in small quantities and in different locations. The production of chemical vapors and heat from large concentrations of nitrate films demands special storage conditions with a special exhaust and ventilation system;
  - Never store any nitrate-base materials in sealed containers or without ventilation. Such dead storage simply increases the rate of decomposition. Pack the reels loosely in ventilated metal boxes or cabinets.
  - For longer storage, use an approved (by local competencies) storage vault;
  - Important principle supporting the regulations are:
    - Elimination of all possible means of starting a fire;
    - Control of, and protection against, the spread of fire;
    - Segregation of large quantities of film into small, protected units;
    - Ample provision for safety to human life;
    - Proper ventilation and exhaust system;
  - Vaults for long term storage are limited to 28 m^3 with a vent area of at least 1.7 m^2, and with no less than eight sprinklers;
  - Shelves in long term film vaults should be divided into individual compartments not less than 1.90 cm thick non-combustible insulating material. Each compartment should hold only one, or at most two, film containers;
  - Automatic fire dampers should be installed in the air ducts so that a fire in one vault will not spread to another and so that the toxic gases given off will not be distributed to other rooms but will be vented outside.

Other features that need particular attention during the design of the archives are self-closing doors, exits, vents, the electrical systems, the heating equipment, and the automatic sprinklers of the fire system.

The ceiling water sprinklers should be directed so that all shelves will be drenched in the event of fire. The individual containers will protect the film from water damage. Automatic fire dampers should be installed in the air ducts so that a fire in one vault will not spread to another and so that the toxic gases given off will not be distributed to other rooms.

3.2 Examples of nitrate archives

There are a few examples of nitrate film archive already built around the world. The information regarding these archives is limited; the majority of the nitrate film archive are found in Europe, with two in the UK, one in Denmark, Sweden, Austria and Italy, followed by north America, with four in the US and one in Canada, two in Oceania – one in Australia and one in New Zealand – and finally a small section in Japan.

Three of these archives show different solutions for the proper conservation of nitrate film collections: the MoMA's Celeste Bartos Film Preservation Center in the US, the British Film Institute's Master Film Store in the UK, and the archive of Filmarchiv Austria.

3.2.1 Celeste Bartos Film Preservation Center

The Celeste Bartos Film Preservation center opened in 1996 and is located in Pennsylvania, US. The Museum of Modern Art's Department of Film has more than 30,000 films, 5,000 of which are made of nitrate, preserved in a 730 m^2 building.

Figure 10. Celeste Bartos Film Preservation Center, USA

Figure 10 shows the archive building. The corrugated white volumes contain the HVAC system; the white panels above are explosion vents, required by federal law, that open in case of fire to release the pressure outside the vault and maintain the structural integrity.

The building offers a flexible system of temperature- (35 °F (=1.6°C)) and humidity- (30%) controlled vaults (34 vaults for nitrate). Moreover, there are two conditioning vaults that are used to acclimatize the films before storing them in the vaults. Each vault is isolated from the adjacent vaults by concrete.

Figure 11. Shelves made of cubbyholes, with two cans for each compartment

Figure 11 shows the shelves that are used: cubbyholes are created so that cans are divided two by two. The shelves are made of steel-clad insulated material and are sealed up with a temperature-caulking material, so that if a reel burns in one cubbyhole, any adjacent cubbyhole will not reach the ignition temperature.

Every vault has 16 sprinkler heads, placed on the ceiling that, in case of fire, would completely fllod the face of the shelves, further cooling and cutting the fire [11].

Figure 12. Aerial view of the Celeste Bartos Film Preservation Center

3.2.2   Filmarchiv Austria's nitrate archive [11]

The Filmarchiv Austria's depot is the first nitrate archive entirely made of Cross Laminated Timber (CLT). The 250 m² building was completed in 2010; it has two floors, with the lower housing the film collection and the upper containing the air-conditioning system designed as a compact explosion-proof unit. The ground floor is divided into three separate storage vaults, with a fourth room at the entrance for the acclimatization of the film reels (Figure 13).
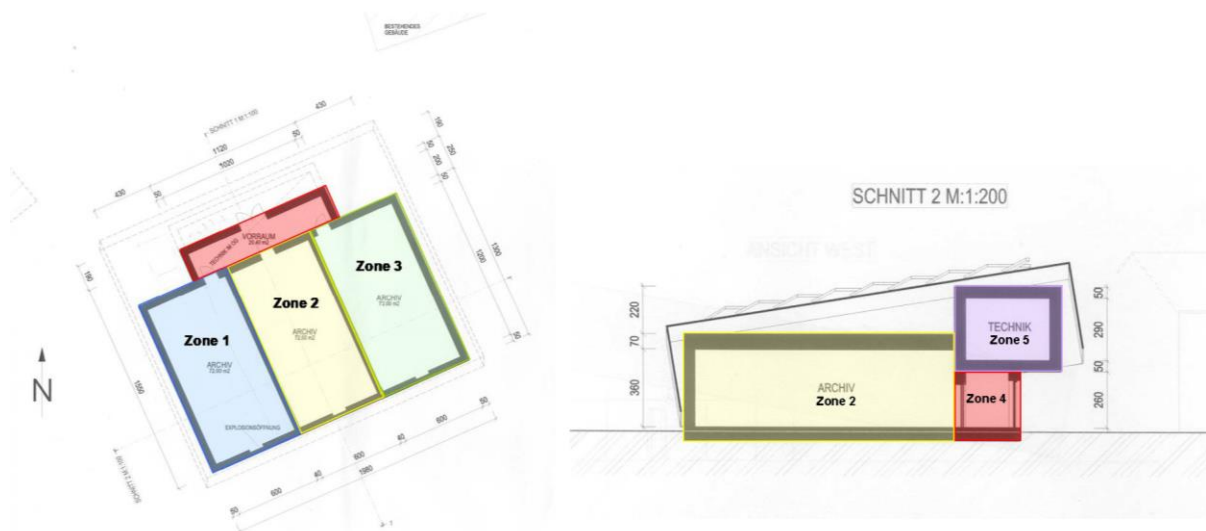
Figure 13. Floor plan and section of the nitrate film archive

The vault provides mobile shelving space for 70,000 cans in a storage conditioned with 0-2°C temperature and 35% RH (with 40% RH set as an acceptable maximum). Cold air is blown in at the top of the chambers and sinks gradually downwards, regulating temperature and humidity. The nitrous gases that emanate from the degrading film are heavier than air and accumulate on the floor of the chambers; these are carried out of the vault by the ventilation system. The storage space has an air exchange rate of 0.02 per hour, which means that the entire atmosphere of each vault is exchanged once every 48 hours; this is done because ventilation – together with temperature and humidity – plays a large role in both preventing nitrate decomposition as well as slowing it down where it already exists.

The walls of the vaults are made of CLT and are 350 mm thick, with an insulation layer composed of a 200mm thick chamber filled with shredded paper. Channels milled into the wooden boards enclose air between the layers of the panels and work as an additional insulation. A sheet

of parchment placed between the wall's layers act as a kind of vapor barrier, but without fully sealing off the vault's chambers. To keep the surface untreated and the microclimate within the storage chambers as free from polluting agents as possible, the walls' layers are connected by dowels made of dried-out beech wood.

The building runs on a cooling system based on heat pump technology and using four counter-current air flows. Incoming air is channeled through wheels containing silica crystals as a dehumidifier. It is thus possible to regulate temperature and humidity levels within the three storage chambers solely by blowing in conditioned air. Explosion-proof lighting are installed in the vaults, positioned as far away as possible from the film reels.

Figure 14. Façade of the nitrate vault in Laxenburg, Austria

The roof was positioned to allow as much exposure to the sun as possible; the hollow area between the top floor ceiling and the roof prevents the sun from shining directly onto the top of the storage chambers. The sides of this area are faced with a fine metal grid rather than solid sheet-metal, which means that air can circulate through them, allowing the strong winds to work as another cooling element.

In accordance with fire-department requirements, the walls of each chamber are designed to divert the explosive energy of any nitrate fire towards an area as far away as possible from office buildings and other working spaces (also shown in Figure 15). Internal and external fire detectors are linked directly to the local fire department, setting off automatic alarms if smoke or flames are registered.

Figure 15. Aerial view of the nitrate film in Laxenburg

3.2.3   British Film Institute's Master Film Store [12]–[15]

Completed in 2011, the 3000-square meters archive has been built on a nuclear bunker site in the countryside and holds more than 450,000 cans of the nation's film, both acetate and nitrate.

The film is stored at -5°C and at 35% RH; at these low temperatures, the chance of nitrate film self-igniting is very low. The collection is stored in 30 compartments, with more than 6,000 cans each.
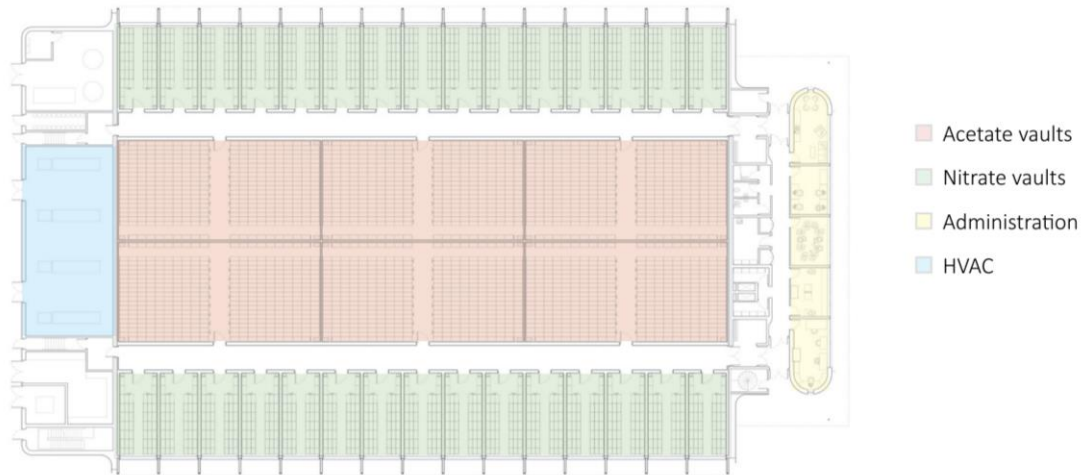
Figure 16. Floor plan of the Master Film Store

As Figure 16 shows, the main section has acetate film stored in the center, and nitrate film along two edges. Technical equipment is at the rear, including dehumidification plant and back-up boilers. At the front is an administration building, with an acclimatization room for film taken out of storage. This part of the building is thermally separated from the rest; the refrigeration plant is on the roof.
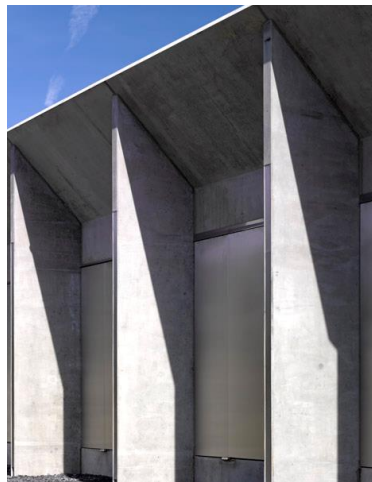
Figure 17. Explosion vents of the nitrate vaults

The external walls of the nitrate vaults comprise explosion vents (Figure 17). They are held up by chains with fusible links, which means that if the temperature internally reaches 70°C, the doors, which are hinged at the bottom, will drop down and the flames will spread across the adjacent landscaped area (Figure 18). Moreover, the shape of the façade makes sure that the flames are directed away from the building, in order to preserve the façade and the equipment located on the roof.

Figure 18. Aerial view of the British Film Institute's Master Film Store

The doors to access the vaults are designed with two-hour hydrocarbon fire resistance, to prevent fire from one cell to ignite film in a neighboring cell through the corridor. The cells are constructed of high-quality reinforced concrete panels, to achieve high airtightness with only 0.3 ac/h.

Figure 19. British Film Institute, UK

The high levels of insulation, with a U-value of 0.1 W/m^{2}k for walls, roof, and exposed floors, mean that, once the cells reach their operational temperature, their refrigeration demand can be kept to a minimum. The high thermal mass construction method and the air permeability provide a very stable internal environment. The reflective cladding material helps keeping solar gains low.

The refrigeration equipment was designed to be as efficient as possible; the main energy demand comes from the four desiccant wheels that dry the air down to 35% RH. These wheels, each about 1.5 meters in diameter, while slowly turning, they remove the water from the chilled air that travels through them. The desiccant then must be heated to 140°C to dry it out again, with fresh air passed through to remove the liquid. A heat recovery loop was introduced to the system, which takes waste heat from the chillers and supplies it to the desiccant wheels, reducing their energy demand. The back-up boilers are only for use in case of failure, or if external temperatures fall well below -5°C, in which case no refrigeration will be needed so there will be no heat waste. The annual energy consumption is 42.40 kWh/m².
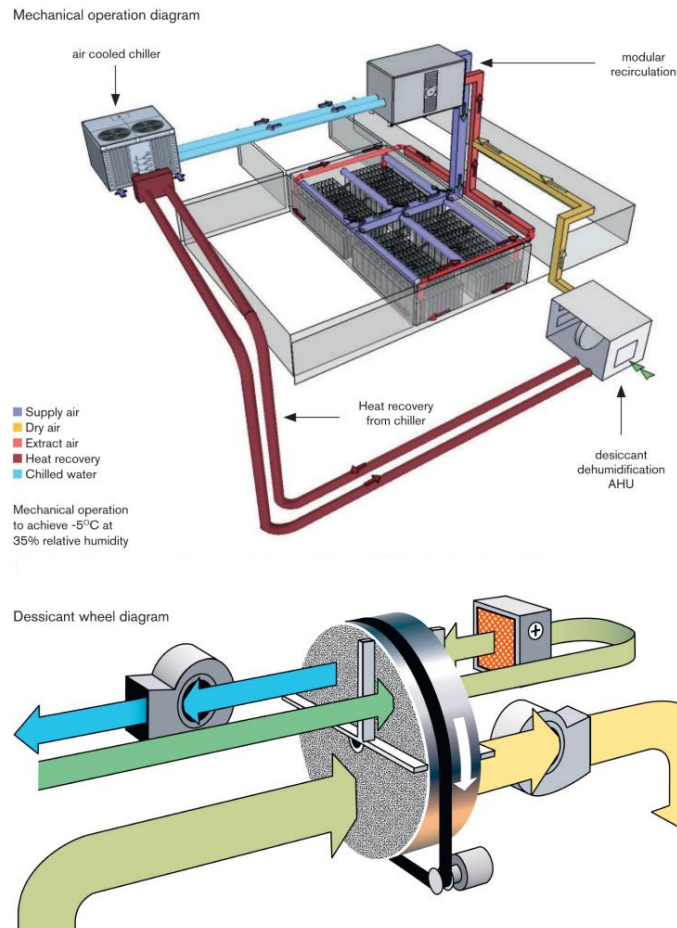
Figure 20. Mechanical operational diagram

3.2.4   Recommendations based on the three case studies

From the previous example, several things can be considered good practice for a nitrate archive design, which are shown in Table 2.

Table 2. Recommendations from the three archives

	Celeste Bartos	Filmarchiv Austria	British Film Institute
Energy efficient design		· Inclined roof for shading and PV placement · Distance between vaults and HVAC room	· Distance between offices and vault
Materials		· CLT for thermal stability and insulation	· Reflective façade cladding
Fire safety	· Insulated shelves · Sprinkler system · Explosion vents · Empty space on the side of the vaults for safety in case of explosion	· Explosion vents · Empty space on the side of the vaults for safety in case of explosion	· Shape of façade to redirect the flames · Explosion vents · Empty space on the side of the vaults for safety in case of explosion
Systems		· Rotary desiccant wheel · Heat pump with heat recovery and recirculation	· Rotary desiccant wheel · Efficient cooling system with chiller · Heat recovery and recirculation

23

4 Materials

Thermal inertia is needed in buildings to mitigate the daily temperature cycles. For this, two strategies can be implemented: design walls with materials that have a high heat capacity, to delay heat flow; add thermal insulation, to reduce heat loss or gain through the house envelope. [16].

4.1 Cross laminated Timber (CLT)

CLT is a product consisting of multiple timber layers, perpendicularly face-glued together to form structural wall and flooring system. Its production has increased over the years since 2005 and it has become widely used in construction [17].

Figure 21. Image of CLT panel

The Eye Filmmuseum took the Austrian archive as a good example for their project. CLT seems to be a good solution for many different reasons: it has good hygrothermal properties and has the ability to act as an additional insulator, having low thermal conductivity, leading to low heating and cooling energy demand [18]. It is a renewable material and, through carbon sequestration, contributes to lower the carbon footprint of buildings.

The CLT used for the Austrian archive's structure is manufactured by a pioneer in the field of timber construction. The company developed a special process of combining layers of untreated wood that create the panels; the panels are held together not with glue, but with beech dowels; these create a pollution-free environment for the film collection, since the use of glue to connect each layer is avoided.

The use of prefabricated panels results in a faster construction compared to e.g., concrete, where a certain amount of waiting time is necessary for the concrete to dry. Shorter construction time means lower costs.

According to Kukk at el. [19], a CLT external wall composed of 5 layers should have an initial low moisture content, around 13%, that should be maintained during construction and service life, which is fundamental to provide airtightness to the building.

The thicknesses of CLT panels varies from 60 mm to 320 mm, according to different CLT suppliers [20] [21]. Taking the example of Austria, it was decided to use 300 mm for the outer walls and 240 mm for the roof.

4.2 Insulation

The more insulation is used in the exterior envelope, the less heat is transferred into or out of the building due to temperature difference between interior and exterior [22]. Different insulation materials were taken into account, both bio-based and not biobased. Considering the highly

flammability of the nitrate film collection, it was important to opt for a non-flammable material and, for this reason, the bio-based insulation materials were not considered, since all rated E according to the European Standard EN 13501-1 for the fire classification of building materials [23]. Rock mineral wool was hence chosen as a proper insulation material; it is classified as A1 – non-combustible material, with S1 – low smoke production and D0 – no flaming droplets or particles [24] [25]; moreover, being permeable, it allows water and vapor to escape.

4.3 Concrete flooring

A completely non-flammable material, concrete, was used for the floor, to avoid the spreading of fire to other vaults.

During construction phase, it is fundamental to allow concrete adequate drying time, before closing off the building and moving in the collection. The high moisture evaporation levels of concrete could be released inside the building increasing the RH, causing the dehumidification system to overwork. Moreover, if the collection is present, the moisture would be absorbed by the nitrate film and could cause faster decomposition.

4.4 Material thicknesses

The calculation of different thicknesses for the insulation layer were made (Appendix 13.3.1), considering the minimum requirement for passive buildings in the Netherlands, where R_c should be between 8 and 10 (m²K)/W [26][27]. 300 mm CLT and 200 mm were chosen for the wall, 240 mm CLT and 250 mm insulation for the roof; these result in a R_c value of 8.7 and 9.5 (m²K)/W, respectively.

Table 3. Calculation of wall's U-value for different insulation thicknesses

	Insulation		CLT			
	Thermal conductivity [W/(m*k)]	Thickness [m]	Thermal conductivity [W/(m*k)]	Thickness [m]	Total thickness [m]	R-value [(m²K)/W]
Wall	0.035	0.20	0.11	0.30	0.50	8.7
Roof	0.035	0.25	0.11	0.24	0.49	9.5

5 Indoor climate

5.1 Building cooling

For good preservation, nitrate film needs to be kept at a constant temperature of 2°C.

Heat gains in buildings can be internal or external; internal heat gain sources are human activities, appliances, lighting; external heat gains are solar radiations and ambient temperature [28]. For the archive building, only the latter are a concern.

There are two ways to keep a building cool: through active cooling and/or passive cooling. Active cooling is defined as the mechanical equipment to satisfy the needs of cooling within a building, that is not provided by nature [29]. Passive cooling are those strategies that are used to prevent heat from entering the building, or to remove it once it has entered. These can reduce the peak cooling load in buildings, thus reducing the size of air conditioning equipment and the period for which it is generally required [22].

5.1.1 Passive cooling strategies

Other than insulating the building, there are other strategies that were considered to keep the building cooler; these will be analyzed in the following paragraph.

5.1.1.1. Building shading

Shading is one of the passive techniques that protects buildings from solar heat gains and is considered an important aspect in designing energy efficient buildings [28].

In general, shading is provided by building elements, like overhangs, horizontal louvers, light shelves, to control the solar gains of building through windows. For the nitrate building, windows are not designed so that the collection is protected from the solar gains; nevertheless a roofing element can be considered to create shading and lower the cooling demand of the building in the summer, when solar radiation is high.

Shading the roof is a strategy thus reducing heat gain [22]. The conventional approaches to reduce the heat flux via roof include false ceilings, insulations, increasing the roof thickness, or using roof coatings [30].

Since the roof receives the highest portion of solar radiation, the most effective method to limit the solar gains is to shade by constructing a second roof over the first. The outer roof reaches high temperatures, and it is therefore fundamental to separate it from the inner roof, allow the dispersion of heat from the space between the two, and use a reflective surface on them both. For optimal efficiency, the surface of the outer roof should be of light color, hence with low emissivity [31]. Air cavities within an attic space reduce the solar heat gain factor, thereby reducing space-conditioning loads. The performance improves if the void is ventilated. [22]

To further protect the vaults from solar gains through walls, it is recommended to position the office block in the south side of the building.

5.1.1.2. Low emissivity and reflective material

A reflective or cool roof is a conventional roof with a solar reflective material on the exterior surface. The high solar reflectance and thermal emittance of the coating helps the surface to maintain cooler temperatures, compared to conventional roofs under the same conditions. This measure is simple to apply, since the optical properties can be controlled just by acting on the surface of the roof, generally changing the color or by using high reflective materials, also called cool materials [32]. Reflective materials applied to exterior building components can reflect the

solar energy year-round, lowering the cooling load of buildings. A cool roof has potential to reduce the daily heat gain. Most common cool white materials are liquid applied coatings and can lower the surface temperature between 5 and 13°C with respect to their matching conventional colors [32]. Decreasing the temperature of opaque components reduces the heat flow onto the building, leading to energy savings in air-conditioned buildings.

5.1.2   Mechanical cooling

The vaults containing the nitrate collection archive needs to be between 0 and 2°C, which makes it necessary to implement mechanical cooling in the building.

5.1.2.1.   Cooling systems

Two systems that were used by the Austrian archive and the BFI's Master Store are heat pump and air-cooled chiller, respectively. A heat pump is a device that can heat a building by transferring thermal energy from the outside using a refrigeration cycle; heat pumps can also operate in the opposite direction, cooling the building by removing heat from the enclosed space and rejecting it outside. Air-cooled chiller has the same functionality, it absorbs heat from the building and reject it to the outdoor, by means of a refrigerant.

Ice slurry was also analyzed as a secondary cooling system for the archive. A thorough explanation can be found in Section 8.3.

5.1.3   Building ventilation

Ventilation is another important aspect that is needed to clear the vaults from the nitrous gases that are produced by the nitrate film collection [1]. If not properly ventilated, the gaseous by-product released by the nitrate film can accelerate the decomposition process.

Taking the example of both the Austrian archive and the BFI Master Store, cold air coming from the AHU should be blown in at the top of the chambers; this sinks gradually downwards, regulating temperature and humidity. The heavier-than-air nitrous gases emanating from the degrading film stock accumulate at the floor of the chambers and are carried out of the vault by the ventilation system, through an outlet placed near the floor. Since the vaults are rarely accessed by people, the ventilation rate can be kept as low as 0,042 ac/h, which means that the air inside one vault is exchanged once per day. Having a higher ventilation rate would require higher dehumidification loads and would increase thermal losses. The Austrian film archive's ventilation rate is 0,02 ac/h, which means that air is exchanged once every 48 hours.

To further decrease heat losses and avoid infiltration, the building should have a high airtightness. According to articles regarding the Austrian archive, an infiltration rate of 0,06 ac/h was achieved [11].

5.1.4   Building dehumidification

The nitrate collection requires a stable Relative Humidity, between 20 and 30%, as stated in the ISO norm and NFPA 40. There are different dehumidification strategies that can be applied according to the climate and building typology. According to Pillai et al, desiccant dehumidification and direct expansion/desiccant are more applicable in mixed-humid climates (see Figure 22).
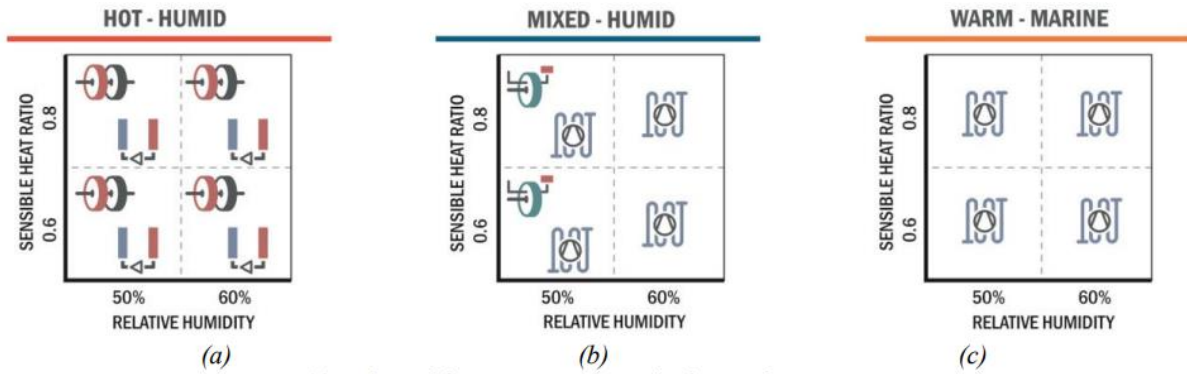
Figure 22. Dehumidification strategies for different climates [33]

Desiccant dehumidification makes use of the properties of chemical substances, such as silica gel, to absorb moisture from the air. As shown in Figure 23 outside air, after passing through an enthalpy wheel, passes over a pre-cooling coil, that reduces the air temperature; pre-cooled air then blows through a moving honeycomb wheel containing the water-absorbing chemicals, where it goes through an isenthalpic process. During this process, the moisture content of the air is reduced, and the temperature increases. The high temperature air then passes over a post-cooling coil to cool it down to the required supply temperature. As the wheel rotates, it then passes through a separate stream of heated "regeneration" air that is vented to the outdoors. This "regeneration" stream causes the chemicals to release the moisture, so by the time the wheel completes a revolution, the chemicals are again ready to absorb moisture. Since this system needs a high-grade heat to regenerate the desiccant, it is more efficient if the space needs to be maintained at a low RH, namely lower than 50% [33][34][35].
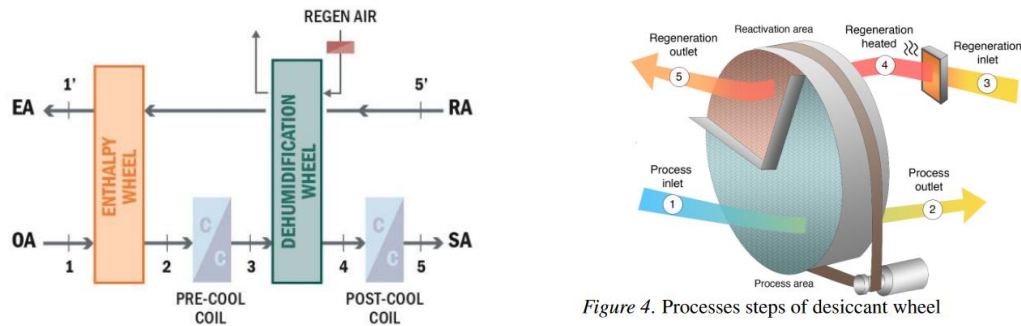

Figure 4. Processes steps of desiccant wheel

Figure 23. Left: schematic of desiccant dehumidification system [33];

Right: process steps of desiccant wheel [34]

Direct expansion/desiccant has a different functioning. When a sensor detects that the room is too warm, the stream of air passes through a cold coil before being supplied to the space. The coil is cooled by a flow of cold water supplied by a chiller or by evaporation of a refrigerant that is provided by a remote compressor/condenser unit (known a DX cooling). If the temperature of the cooling coil is below the dew point temperature of the air, moisture will condense on the coil, thereby dehumidifying the air. In case where the desires space dew point temperature is quite low (e.g. 8°C) at least some of the air must be cooled to that temperature. In buildings were the temperature needs to be adjusted for human comfort, 8°C is colder than the desired space temperature, hence this sub-cooled must be reheated. Such arrangements are called sub-cool/reheat systems [35].
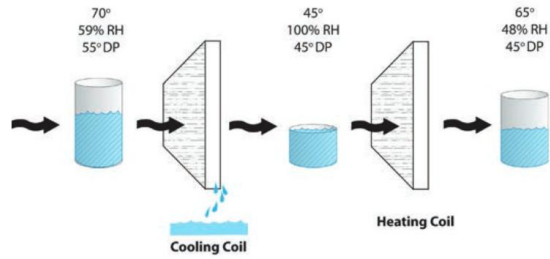
70°
59% RH
55° DP

45°
100% RH
45° DP

65°
48% RH
45° DP

Cooling Coil

Heating Coil

Figure 24. DX cooling schematic

The Filmarchiv Austria's depot and BFI's Master Store have both the desiccant wheel as dehumidification system, and it seems to keep the humidity levels according to the requirements. The Eye's archive in Overveen uses the DX cooling as desiccant method and, as Figure 5 - Figure 8 in Section 1.3.1 shows, the RH levels are high, above the advice threshold that the standards advise. Hence, the desiccant wheel seems to be the best choice for the dehumidification system of the archive building.

6 Fire safety

During deterioration, nitrate film produces highly acidic nitrogen oxide gases, which are harmful for the surroundings, for the people and for the environment; if not released, these gases stay captured in the storage area and, in case they build up, they cause an autocatalytic reaction that speeds decomposition of the nitrate material. The reaction produces heat, which further acts on the available gases and humidity, and the environment around the film becomes toxic. When high quantities of deteriorated nitrate are stored together, they might ignite spontaneously [1]. In the past, many films recorded on nitrate film were lost, because collections were stored improperly causing fire in archives, which also led to casualties and harm to the environment. For these reasons, it is important to design an archive building that, in case of fire, can save as much of the collection as possible, preserve the environment and avoid casualties.

For this project, the behavior of CLT in case of fire was analyzed through different researches [36][37][38][39][40] and through a test performed on a natural full-scale CLT building. This was carried out by a collaboration between CNR-IVALSA (Institute for the Valorization of Wood and Tree Species, Trentino-Alto Adige, Italy) and the Japanese Building Research Institute in Tsukuba, to analyze the performance of a CLT building in case of fire.

A second test, carried out by the Imperial War Museum, was studied; with the goal of assessing the feasibility of a specific nitrate archive design, a big quantity of nitrate film was ignited in a concrete dummy storage.

Two different types of shelves are considered for the archive, which require two different building configurations. Finally, the requirements for the openings, namely door and explosion vents, are investigated.

6.1   CLT and fire

When using bio-based materials, construction must be designed and built in a way that, in case of fire, load bearing capacity can be assumed for a specific period of time, generation and spread of fire and smoke is limited, and spread of fire to neighboring construction is limited [36].

The characterization of the fire behavior of building products and building assemblies is based on the following criteria:

- Where mechanical resistance is required, structures shall be designed and constructed in such a way that they maintain their load-bearing function during the relevant fire exposure (load-bearing R).
- Where fire compartmentation is required, the elements forming the boundaries of the fire compartment, shall be designed, and constructed in such a way that they maintain their separating functioning during the relevant fire exposure. This includes ensuring that integrity failure does not occur (integrity E) and ensuring that insulation failure does not occur (insulation I) [36].

When exposed to fire and after an initial heating phase, timber starts a process of thermal degradation, known as pyrolysis. This begins to take place at about 260-300 °C [37]; it produces combustible gasses and results in loss of mass of timber due to evaporation and moisture migration [38]. After this phase, a char layer - the remaining layer of burnt wood which becomes deeper as pyrolysis continues - is formed on the fire-exposed surface, as shown in Figure 25. The char layer acts as a natural insulator for the underlying timber, due to its low effective thermal conductivity [39], and provides thermal protection to the timber beneath the char. This results in a steep in-depth gradient in the uncharred timber and a shallow penetration depth. According to

Wiesner at al. [40], thermal penetration depth is typically 25 to 35 mm at any time between 30 to 90 min during standard fire exposure.
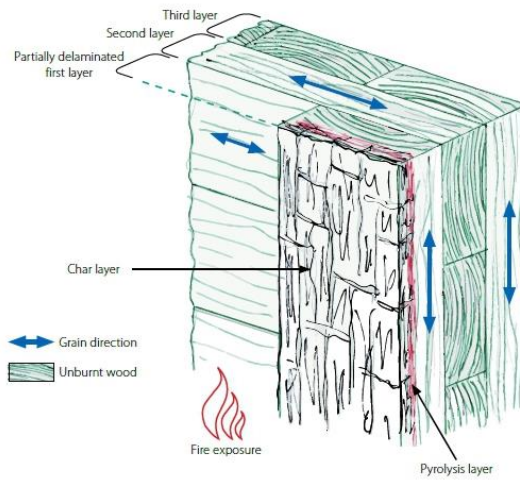

Figure 25. CLT panel exposed to fire [41]

Due to fire exposure or in case of failure of the adhesive, the outermost charred layer can detach from the panel; this results in the loss of the insulation and protection provided by the charred layer to the rest of the underlying timber. Virgin wood is hence exposed to fire, making it reignites [41]. This process continues layer by layer, until fire is artificially extinguished.

6.1.1   SOFIE project

With the goal of assessing the structural behavior of timber buildings made of prefabricated cross-laminated timber panels, an extensive research project called SOFIE was carried out [42]. A natural full-scale fire test was performed in a 3-storey timber building, with an area of 7x7 m^2 and a height of 10 m. The building was constructed with 85 mm thick CLT timber wall and 142 mm thick CLT panels for the floors, connected to the walls by means of steel brackets and screws. The south and the west facades of the test building were covered with insulating and finishing materials, while on the north and the east sides of the building the CLT walls remained uncovered. A room located on the first floor, on the north-west corner, was designated as the fire room. It presented two windows openings and a door, which was certified with fire resistance of 60 minutes and remained closed during the fire test.

Figure 26 and Figure 27 show the plans of each floor and the elevations, while Figure 28 shows the cross-section of the walls and the floor of the fire room.
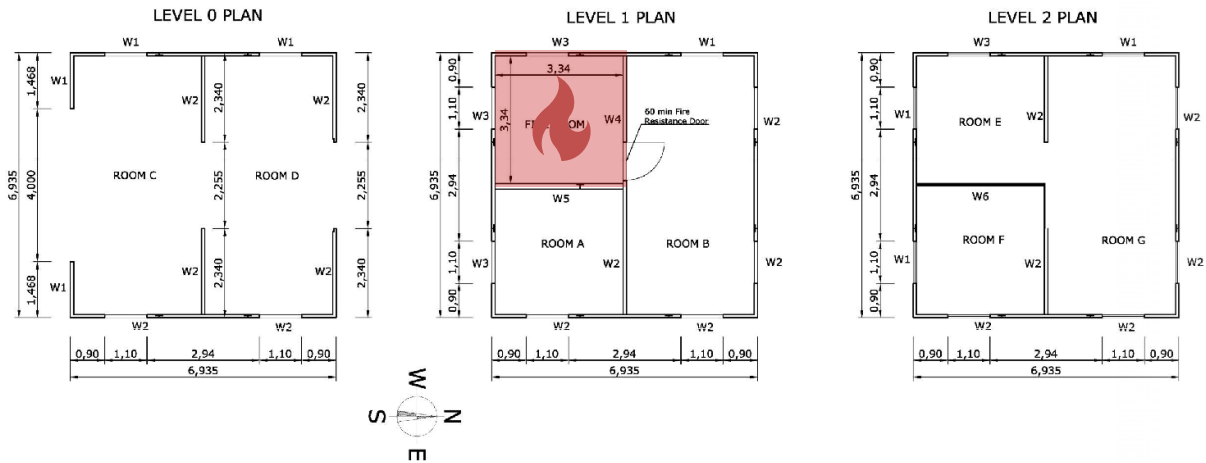
Figure 26. Plans of 3-storey timber building for the natural full-scale fire test [42]
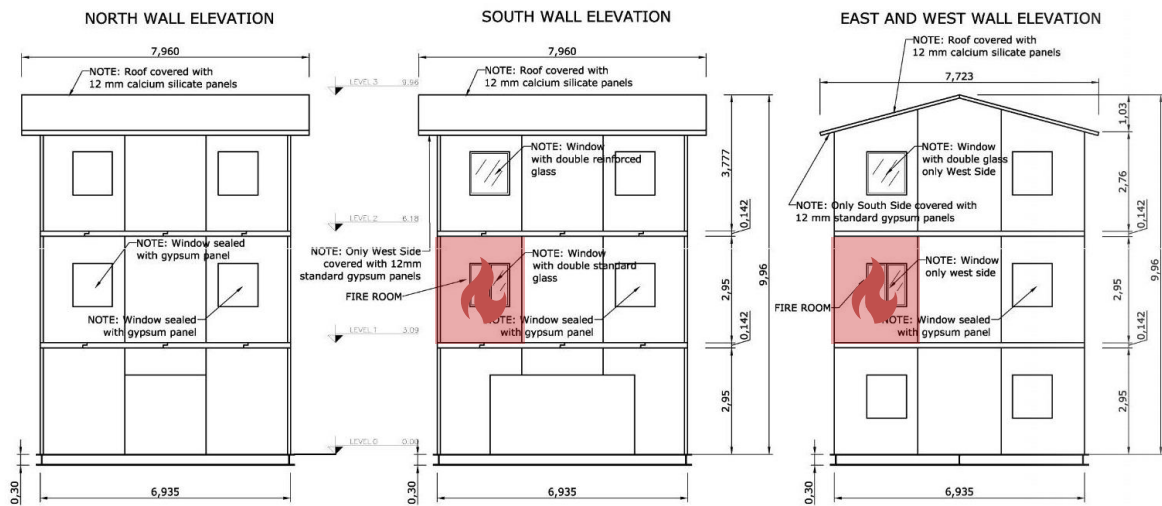

Figure 27. Elevations of 3-storey timber building for the natural full-scale fire test [42]
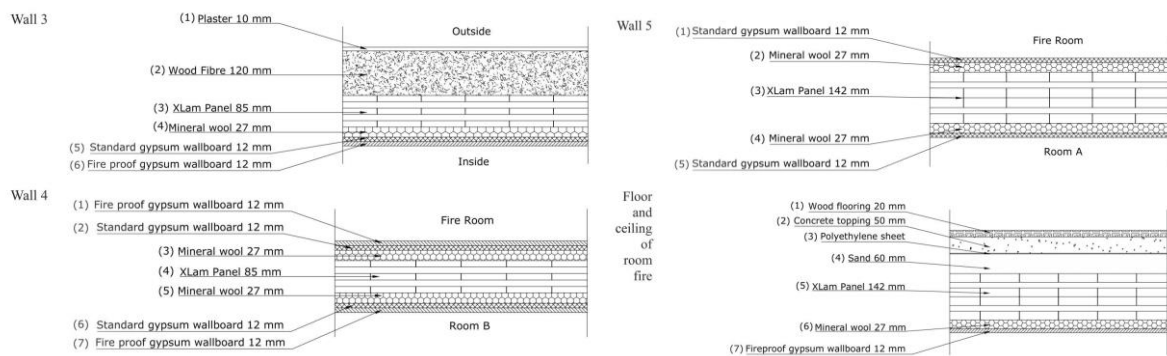

Figure 28. Cross-section of the walls and floors of the fire room

During the test, the temperature at different locations was constantly measured and recorded with thermocouples, which were located on the room surfaces and within the wall, ceiling, and floor layers. Moreover, a column of five thermocouples was used to measure the temperature in the middle of the room at different heights. The fire room was equipped with two typical

mattresses made of polyurethane and several wooden cribs, which were ignited with common fire starts.

OUTCOME

After ignition, fire grew slowly due to low ventilation in the fire room. After about 36 minutes, the collapse of both south and west windows occurred, and the fire intensity inside the room and the external burning out of the windows became more severe (Figure 29).

Figure 29. Fire development after about 32 minutes (left) and after 40 minutes (right) after ignition

After 53 minutes the door of the fire room fell off, leading to smoke penetration into the adjacent room. After 55 minutes the fire intensity started declining and after 60 minutes the fire was controlled and manually extinguished by firefighters, as planned. The window openings of the room above the fire room did not fail and thus no fire spread into the upper level was observed.

Figure 30 shows the room temperatures measured in the middle of the fire room by the thermocouples. A non-uniform temperature distribution over the height of the fire room was measured with the highest temperature close to the ceiling and the lowest temperature close to the floor. After about 35 minutes all temperatures rose within a few minutes to flashover, confirming the increased fire intensity observed during the test.
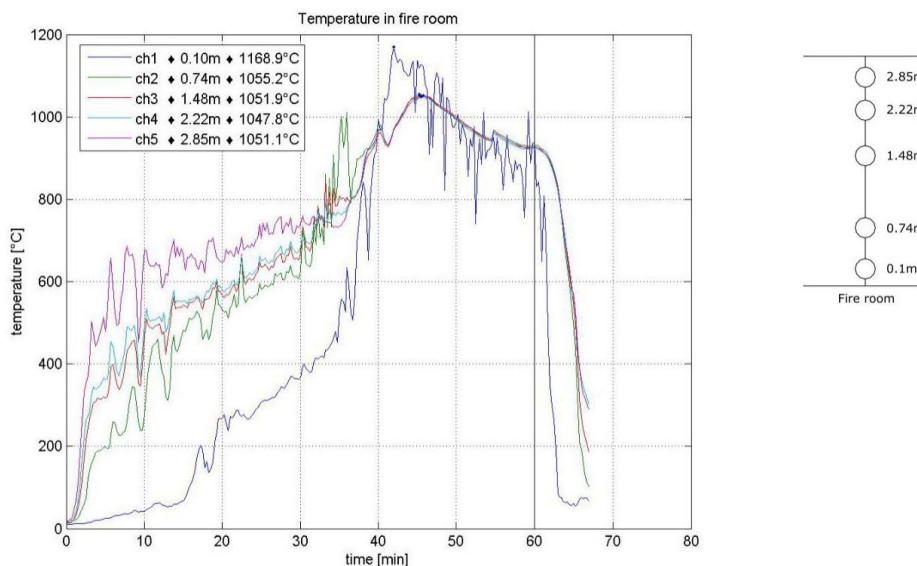

Figure 30. Temperatures measured in the middle of the fire room at different heights (left): 0.1, 0.74, 1.48, 2.22 and 2.85m.

Figure 31 shows the temperature measured at the interface of the different layers that compose the north side wall, which separates the fire room with the adjacent room B. The temperature behind the two layers of gypsum plasterboard grew very rapidly after about 47 minutes; it is assumed that both gypsum layers failed after about 57 and 53 minutes, respectively. Based on the rapid increase of temperature measured behind the rock wool insulation, it can be assumed that it fell off quite immediately after being exposed to fire.
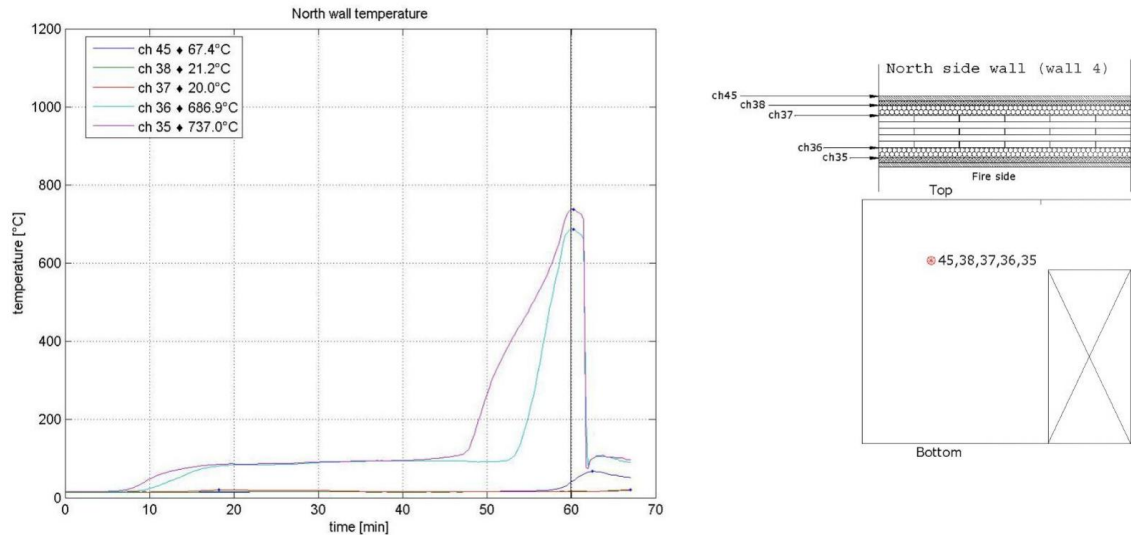

Figure 31. Temperatures measured at the interface of the different layers of the north side wall

In the room above the fire compartment no elevated temperatures were measured and no smoke was observed. The room adjacent to the fire room shows constant temperature throughout the test, which means that CLT prevent the transfer of heat from one room to the other. In conclusion, the test has confirmed that with pure structural measures it is possible to limit the fire spread to one room even for timber structures.

6.2   Imperial War Museum fire test

In 2000, the Imperial War Museum commissioned a full-scale fire test to assess the performance of the design of their not-yet-built archive building. The test building comprised a test cell to the full building design specification, with a dummy cell on either side and other features of the design, such as the corridor. Figure 33 shows the plan of the test building. The walls of the test cell – cell 2 – are made of reinforced concrete, while the rest was constructed with blockwork. The test cell was fitted with a four-hour fire-resisting door. The test cell was fitted out with representative shelving where approximately 500 film cans were placed. An explosion vent was placed in the outer wall of cell 2 and two cans with nitrate film were placed in the adjacent cells, near the partition wall.

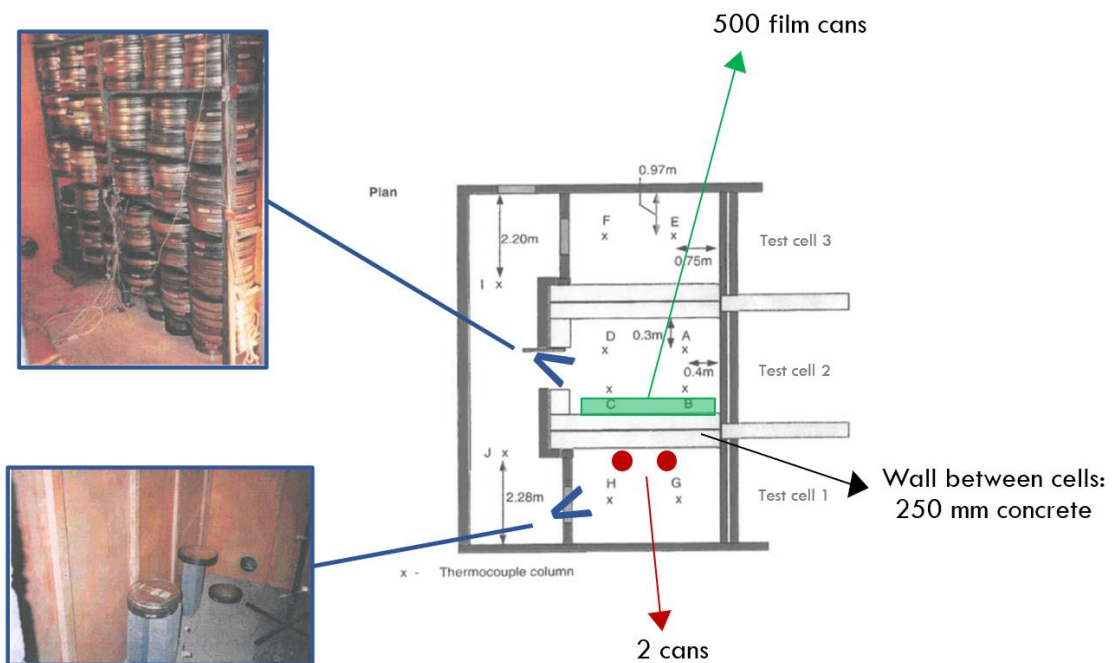*Figure 32. Exterior view of front of facility.*

Figure 33. Floor plans of dummy and placement of the cans

To measure the temperature inside the cells at any time, thermocouples were used (Figure 34):

- Test cell
  - 4 columns each of 6 thermocouples
  - 12 thermocouples, 2 each in either wall, door, vent, floor, and ceiling
- Adjoining cells (both)
  - 2 columns each of 6 thermocouples
  - 12 thermocouples, 2 each in either wall, door, vent, floor, and ceiling
  - 2 targeted cans, with 2 thermocouples inside and 2 surface thermocouples outside
- Corridor
  - 2 columns each of 6 thermocouples

Other devices used are a camera to record a video inside the test cell 2 and a pressure measuring device.
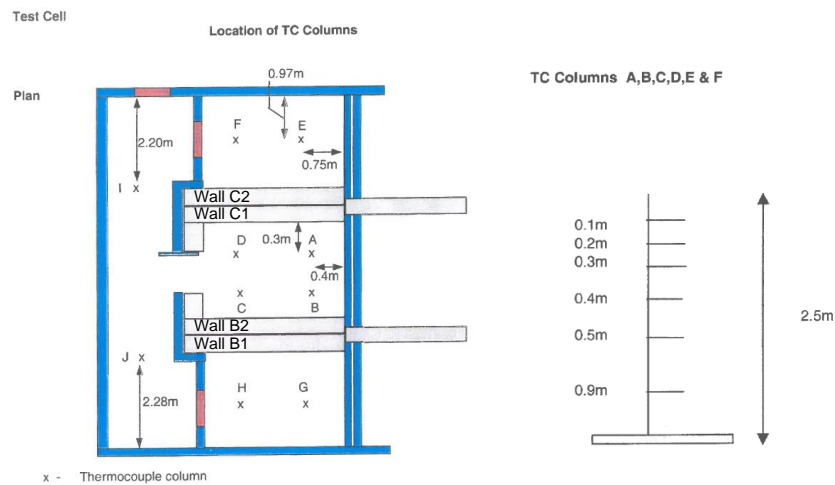

Figure 34. Left: location of thermocouple columns (A-J); right: measurement points of thermocouple column

The fire was started using heater pads on a "source" film can. 6 minutes and 53 seconds later smoke could be seen coming from the source film can and, 12 seconds later, flames. Smoke was seen flowing from out of the vent opening outside of the test cell at the same time and flames followed 47 seconds later. Flames emerged from the test cell for a further 4 minutes, with external flame lengths that peaked briefly at around 20 meters (Figure 35).

ANALYSIS OUTCOME

The fire initiated when the interior of the source film can reached around 280°C, and developed very rapidly, with temperature within burning film can reaching 1150°C. The fire cell air temperature peaked at around 875°C but decreased quickly. The pressure was 90 Pa. Right after the explosion, the vent opened and fire developed; the temperature in the fire cell rose to around 800°C and kept constant for a certain period, before decreasing. The surface temperature within cell 2 registered a very small initial increase, but later rose to around 700°C.

Figure 35. Fire at peak

In the adjoining cells, the target can did not register the fire at any stage and air and wall temperatures in cell 1 remained constant. In cell 3 the air temperature rose by about 1°C, the wall temperature remained constant, but the vent temperature rose by 3.5°C, most likely causing the air temperature rise of the cell. Temperatures in the corridor rose briefly by 2°C, probably as a

result of hot gases being blown through the door. The film in the can in cell 3 remained unaffected, as shows Figure 37.
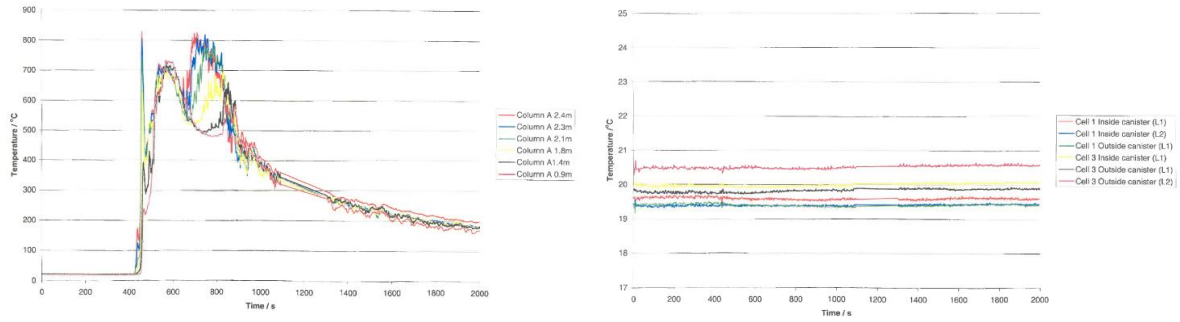

Figure 36. Left: temperature according to thermocouple column - Cell 2 Column A (fire room); Right: temperature of the cans in the adjacent cells

Figure 37. Undamaged film inside can from cell 3 post fire test

6.2.1   Conclusions from tests

Conclusions were drawn from the two tests. For the full-scale test, the fire in the CLT building lasts for more than one hour, due to the type of material that was ignited for the test, and reaches high temperatures, with a peak of around 1170°C. As the graph shows, the surface temperature of the wall on the other side of the CLT layer, in the adjacent room, remains unaffected for the entire test, proving that CLT is a good thermal insulator even in prolonged high temperatures.

As for the second test, the nitrate fire develops and burns very fast, with a peak temperature of 800° after around 11 minutes. After the nitrate film burns completely, the temperature decreases steadily; due to explosion vents that open with high pressure, the fire develops outside of the vault, without affecting the temperature of the adjacent vaults.

6.3   Shelves

Two different types of shelves were analyzed. The first is mainly used in the European nitrate archives; the cans are divided in stacks of six by six and the shelves are movable, normally made of steel. An example is shown in Figure 38.

Figure 38. Left: schematic of the 6x6 shelf; Right: picture of shelves from Filmarchiv Austria

These shelves do not prevent the spreading of flames hence, in case of fire, the CLT walls are affected. CLT does not stop burning until put out by an artificial system, such as fire sprinklers. To avoid the spreading of fire to adjacent vaults without the utilization of fire suppression systems, each vault needs to be isolated. This is done with compartmentation, which means dividing the structure into isolated compartments. For this to be possible, a completely inflammable material is needed.

Two of the materials that are most indicated to both block fire and insulate from high temperatures are calcium silicate boards and mineral wool. In Figure 39 the thermal conductivity of the two materials are shown, in relation to different temperatures [34] [35].
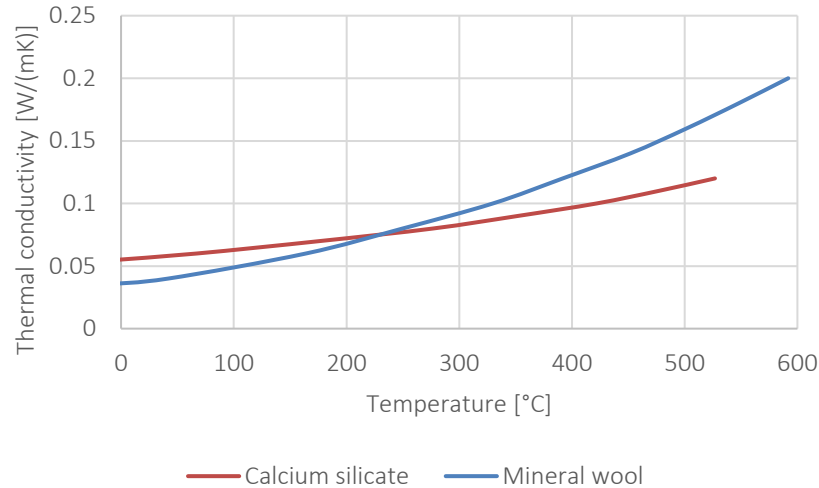
Figure 39. Comparison of relation between thermal conductivity and temperature of calcium silicate and mineral wool.

To isolate the vaults form each other, but still keep the CLT panels exposed toward the vaults, partitions are designed with three different layers: two CLT panels divided by an insulation layer.

The surface temperature of a wall adjacent to a vault on fire was calculated, taking into account the thermal insulation of different layers, for both calcium silicate and mineral wool. Despite the better performance of calcium silicate at higher temperatures, the difference is only 1°C, as shown in the calculations in Appendix 13.4.3. Considering that mineral wool can be used also as thermal insulation of external walls, and that the cost of calcium silicate is double compared to the mineral wool, the latter was chosen.

As for the thicknesses, using either 50 mm or 100 mm gives respectively a surface temperature of 8°C and 5°C as shown in Appendix 13.4.3. Thus, the final design for the vault partitions is: two CLT panels of 60 mm (the minimum allowed, with three timber panels of 20 mm) and a 100 mm rock mineral wool in between, as shown in Figure 40. This design allows the fire to be enclosed in one vault, without spreading to adjacent vaults.
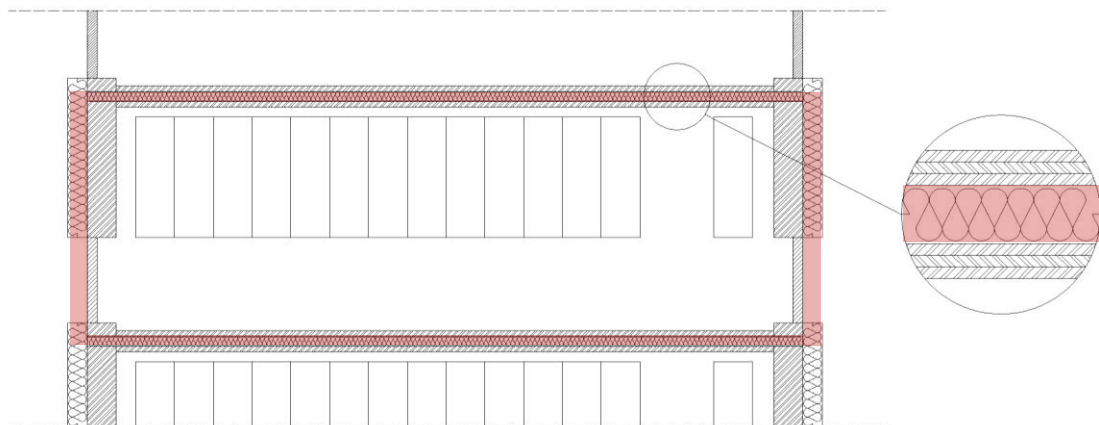

Figure 40. Compartmentation of a vault with rock mineral wool

According to Frangi et al. [37], the charring rate of a panel thickness of 20 mm with a characteristic density of 450 kg/m³ is 0.9 mm/min. In case of fire, the 60 mm CLT panel of the partitions has a fire resistance of more than 1 hour (66 minutes). The main wall, CLT panels of

300 mm, have a fire resistance of more than 5 hours (333 minutes), as required by the standard NFPA 40.

The second types of shelves are designed according to the NFPA 40 standard. In these types of shelves, cubbyholes are created so that cans are divided two by two. The shelves are made of steel-clad insulated material and are sealed up with a temperature-sealing material, so that if a reel burns in one cubbyhole, any adjacent cubbyhole will not reach the ignition temperature.

Figure 41. Left: Schematic of the 2x2 shelf; Right: picture of shelves from MoMA preservation center

Each vault is provided with sprinkler heads (spray-type fixed nozzles, according to NFPA 40), placed on the ceiling. In case of fire, the sprinklers would activate and flood the face of each shelf, cutting off the fire and prevent the spreading to adjacent cubbyholes.
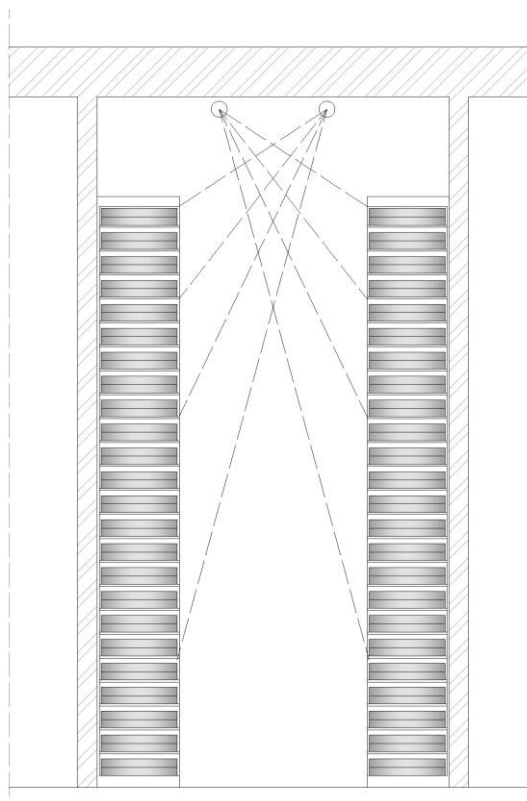


Figure 42. Section of vault with fixed shelves

6.4   Openings

6.4.1   Explosion vents

In accordance with the standard NFPA 40, explosion venting should be provided. Explosion vents are devices used to protect buildings against excessive internal pressure. When a nitrate fire happens, the pressure builds up quickly and, without a pressure relief, it can damage the structure of the building.

The size of explosion vents should be of 0.09 m² for each 1.4 m³ of vault volume and it should be made of completely non-flammable material.

In case of fire, when explosion vents open, the flames spread to the outside, as shown from the fire test from IWM in Section 6.2; for this reason, it is important to redirect the flames as far as possible from the building, so that fire does not reach the adjacent vaults. The façade of the British Film Institute's Master Film Store in Figure 43 can be taken as good example of façade design: in case of fire, the flames are redirected so that roof and façade are not compromised. Moreover, it is fundamental to have a completely non-flammable façade material.
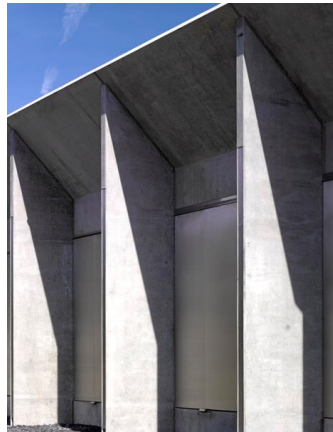
Figure 43. Façade of the BFI's Master Film Store

Since the explosion vents cover a big part of the surface of the façade, thermal insulation needs to be added in order to reduce energy losses and prevent condensation.

6.4.2   Doors

In accordance with the standards NFPA 40, doors should be protected with automatic, self-closing assemblies, and should be made of non-combustible material having fire protection rating of 3 hours. The doors of the archive are fundamental to prevent the spread of flames, smoke, and heat to the rest of the building through the corridor.

The fire resistance of doors is classified with three parameters: fire integrity (E), fire insulation (I), and radiation (W), which are the ability to withstand fire without transferring fire as a result of, respectively, flame or hot gas, heat transfer, and heat radiation by the element or by its unexposed surface to the nearby materials [45].

The standard fire door is built up of two steel skins, generally around 0.8 mm each, edged with rigid rebate and filled with mineral wool with special reinforcement [46].

7 Building energy simulations

The EnergyPlus (EP) base program DesignBuilder was used to create the model of the archive. The goal of the simulation was to estimate the electricity consumption of the archive building and to assess which design strategies can be used to make the building more energy efficient.

For the simulation, the movable shelves are considered and three different scenarios for the archive building are examined: in the first scenario, the collection is divided in 16 vaults, with 2,500 cans for each vault; in the second, the collection is divided in 8 vaults, with 5,000 cans each; in the third, the collection is divided in 4 vaults, with 10,000 cans each. Three simulations with the three scenarios were run. All the models have the same data inputs. The materials used and their thicknesses can be found in Table 4.

Table 4. Materials used in the simulations

Element	Material	Thickness [mm]
Walls	Mineral wool	200
	CLT	300
Partitions	CLT	60
	Mineral wool	100
	CLT	60
Roof	Mineral wool	250
	CLT	300
Floor	Screed	200
	EPS Insulation	300
	Concrete	200
	Gravel	-
Doors	Steel	0.8
	Mineral wool	100
	Steel	0.8
Vents	Steel	3
	EPS	100
	Steel	3

The temperature set point of the vaults is 2°C and the relative humidity is set to be between 20 and 30%, with 35% as an acceptable value. The infiltration rate and ventilation rate are 0.06 ac/h and 0.04 ac/h, respectively. No domestic hot water, equipment, lighting, and human activities are considered since the building is going to be visited only once a year, hence can be neglected.

For the 16-vault scenario, different simulations were run to assess which design strategies and parameters could increase the energy efficiency of the building. The simulation with the initial data was run as a baseline. According to the literature, different parameters were changed, in order to assess their impact on the electricity load of the buildings. In Table 5 the parameters are shown.

Table 5. Parameters for the sensitivity analysis

	Baseline	Improvements
Roof	Single	Double
Emissivity	0.9	0.1
Heat recovery	Off	On

Recirculation	Off	On
Infiltration rate	0.12 ac/h	0.06 ac/h

7.1 Results simulations

The results of the simulations are shown in Figure 44**Error! Reference source not found.**. After assessing that all the design modifications will lead to a reduction in the electricity demand of the building, another simulation was run with all these combined.
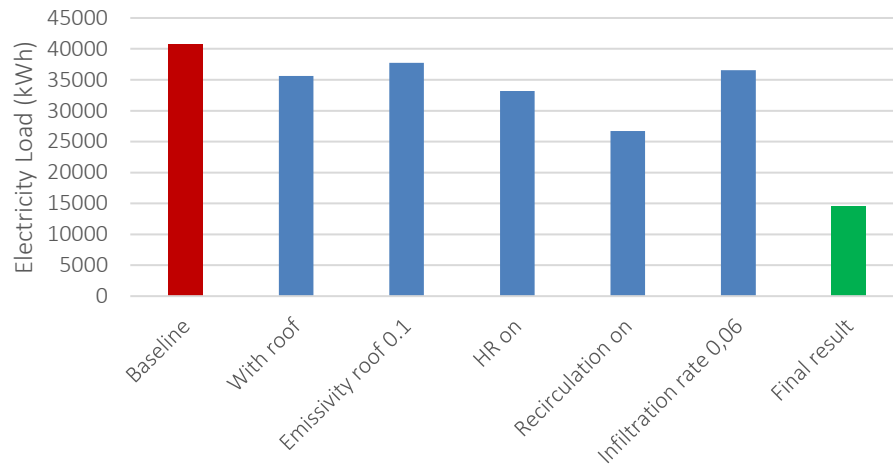

Figure 44. Simulation results

7.1.1 Climatic conditions

The climatic conditions of the vaults according to the model are optimal for the collection, with a constant Relative Humidity of 35% and temperature of 2°C.
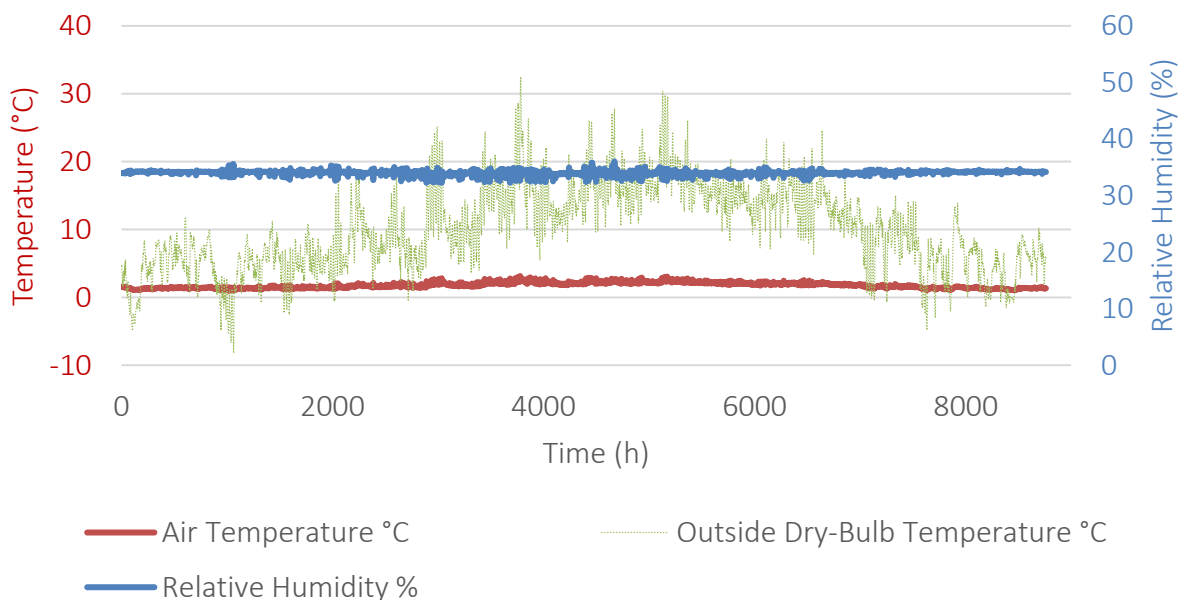
Figure 45. Climatic conditions in the vault

43

7.1.2 Comparison different vault sizes

The improved parameters were used to model the 8-vault and 4-vault archives. Table 6 shows the results.

Table 6. Electricity load for each vault size

	Electricity Load (kWh)	Surface (m²)	Electricity consumption per square meter (kWh/m²)
16 vaults	13,984.58	348.86	40
8 vaults	12,176.40	263.6	46.2
4 vaults	10,859.71	221.5	49

These results were compared to values of the BFI's Master Store and the Filmarchiv Depot, which have an electricity consumption per square meter of 42 kWh/m^2 and 38 kWh/m^2, respectively. Hence, the results from the simulations were considered acceptable.

8 Electricity supply

8.1 PV system

To cover the yearly electricity demand of the archive, the use of photovoltaic panels (PVs)
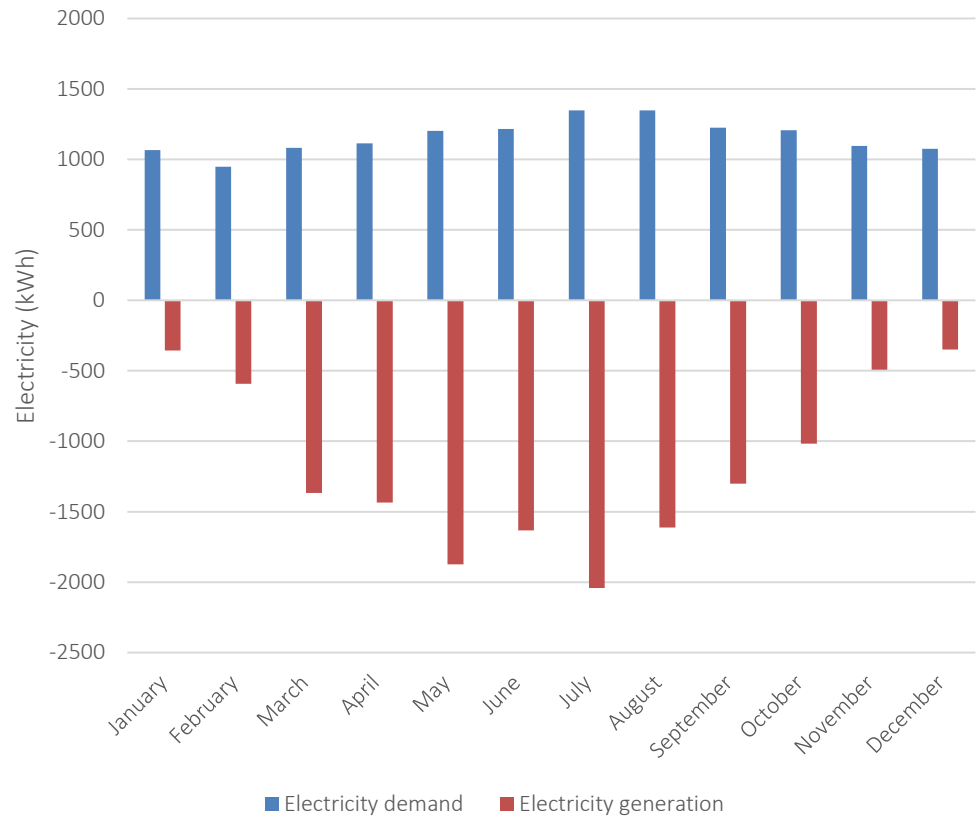
was analyzed.

Figure 46 shows the monthly electricity consumption and the minimum monthly generation needed to cover the yearly demand, produced by 40 PV panels. The electricity demand has a constant baseload given by the ventilation system, with peaks for cooling during the summer months. The electricity generation is lower in winter, when solar irradiance is low, and higher in summer, when values for irradiance are high.
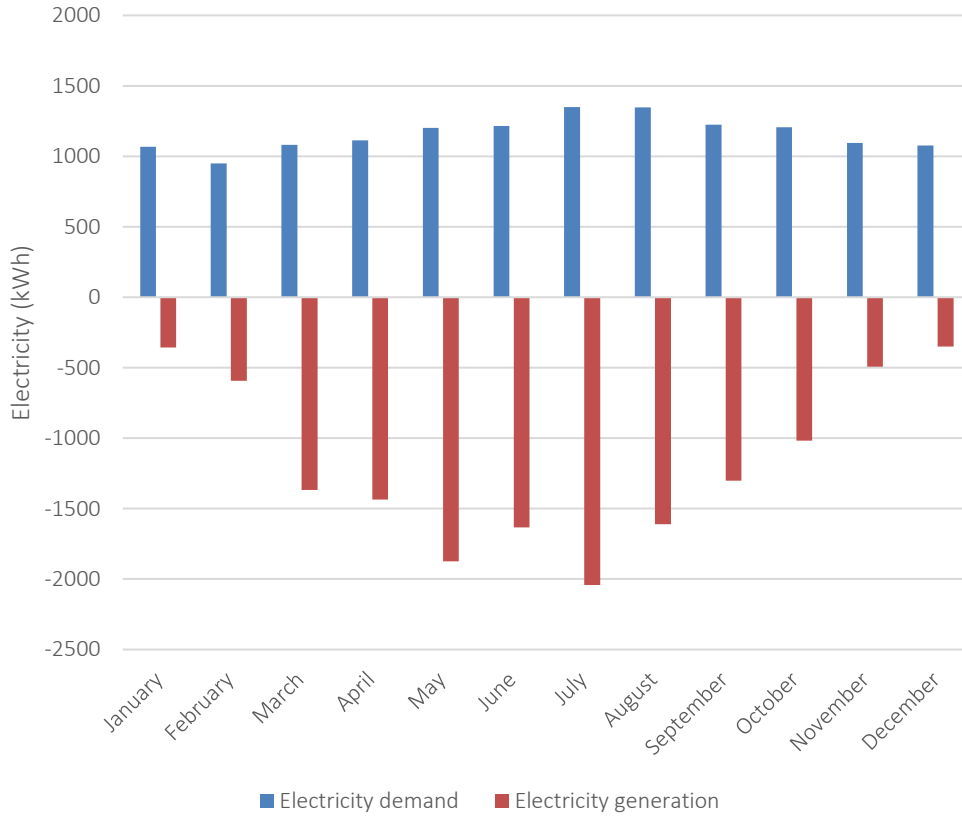
Figure 46. Comparison between monthly electricity demand and electricity generation

When plotting the hourly results (Figure 47), the mismatch between electricity consumption and electricity production is visible. During the day, part of the electricity consumption is covered by the electricity produced by the PV panels; during the night, the electricity production is zero and the electricity needs to be imported from the grid.
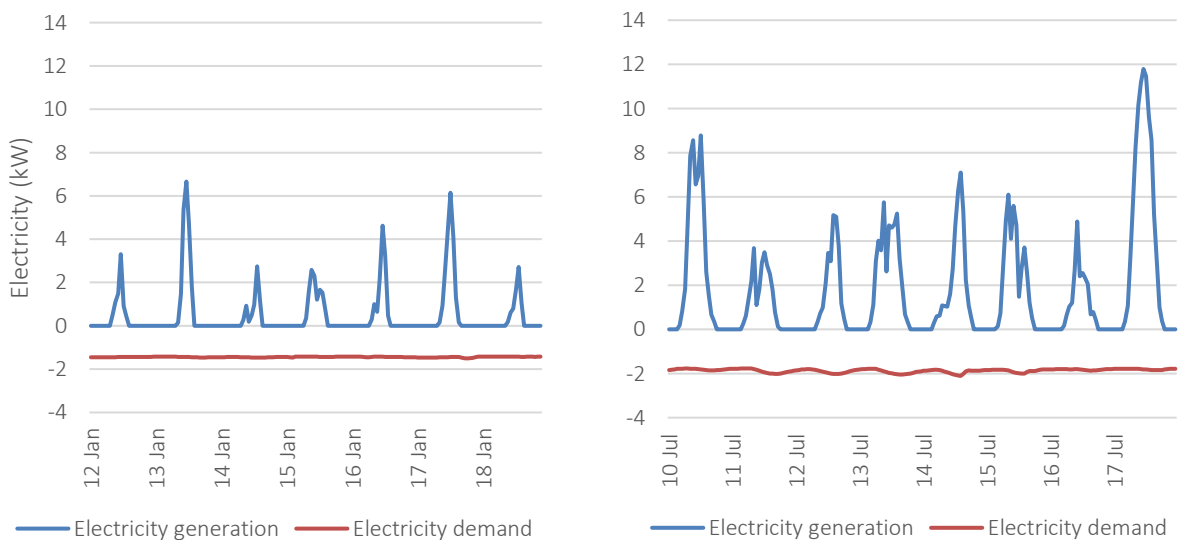
Figure 47. Hourly results for the coldest (left) and warmest (right) weeks of the year

Design Builder was used to model a PV system to simulate the electricity generation on the roof of the archive. Different orientation and a different number of PVs was simulated. The number

of panels analyzed are 40, 50, 60, 70, 80, 90 100, with south and east-west orientation and an inclination of, respectively, 37° and 12°, as advised for the latitude of the Netherlands [47]. The data of the PV panel chosen can be found in Appendix 13.5.1.

8.1.1   Fitting on roof

For the south-facing PVs, assuming a flat roof, the distance between the PV panels was calculated (see Appendix 13.5.3 for calculations).

To avoid self-shadow at any time of the year, the sun elevation of the 21st of December at 9 a.m. the distance between each row of PV panels is 8.85 m Figure 48.
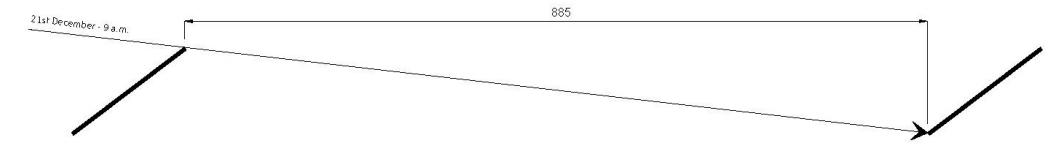
Figure 48. PV panels with 8.85 distance, with sun elevation (7°) on 21st of December at 9 a.m.

If considering the highest demand according to the DesignBuilder simulations, on the 22nd of June, the distance between each row of PV panels is 0.77 m, and a big part of the PV panel surface is shadowed for the most part of the winter (Figure 49).
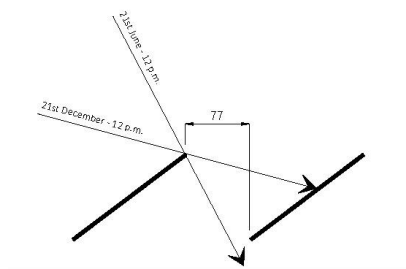

Figure 49. PV panels with 0.77 distance, with sun elevation (15° and 62°) on the 21st of December and 21st of June at 12 p.m.

If a month in between is chosen, for example February or October from 9 a.m. to 3 p.m., the row should be distant 2.70 m (Figure 50). Also in this example, the PVs in the back rows are still partially shadowed. In this way, 112 panels can fit on the roof.
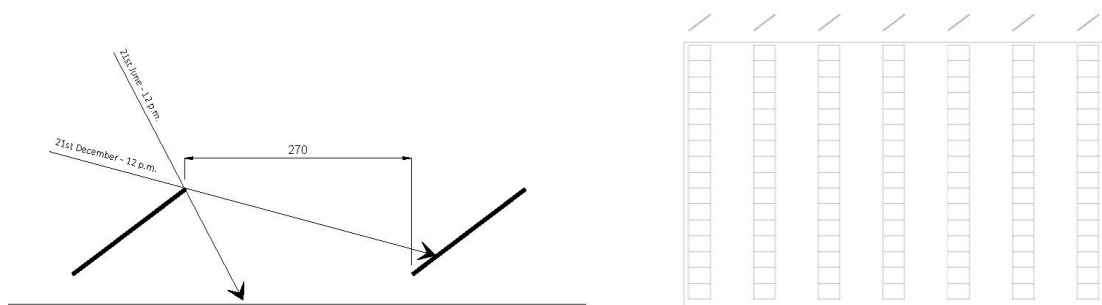

Figure 50. Right: PV panels with 2.70 distance and elevation of sun on the shorter day of the year (21st December, 7°); Left: placement of PVs on roof

To allow all the PV panels to be as efficient as possible, there are two options that can be considered. The first one is to change orientation of the PV panels, placing them toward east and west with an inclination of 12°, as shown in Figure 51.

47

Figure 51. Example of east-west PV panels

The second option is to consider having an inclined rooftop, as the Austrian archive. In this way, the distance between PVs is reduced, more panels can be placed on the roof and self-shadow is minimized.

For the case where PVs are oriented to the south, the distance between rows was calculated with the sun elevation of February-October from 9 a.m. to 3 p.m.; according to the calculations, the rows should be distant 2.70 m. For the three different scenarios with 16 vaults, 8 vaults and 4 vaults, the amount of PV panels that can fit on the roof are 112, 96 and 80, respectively.
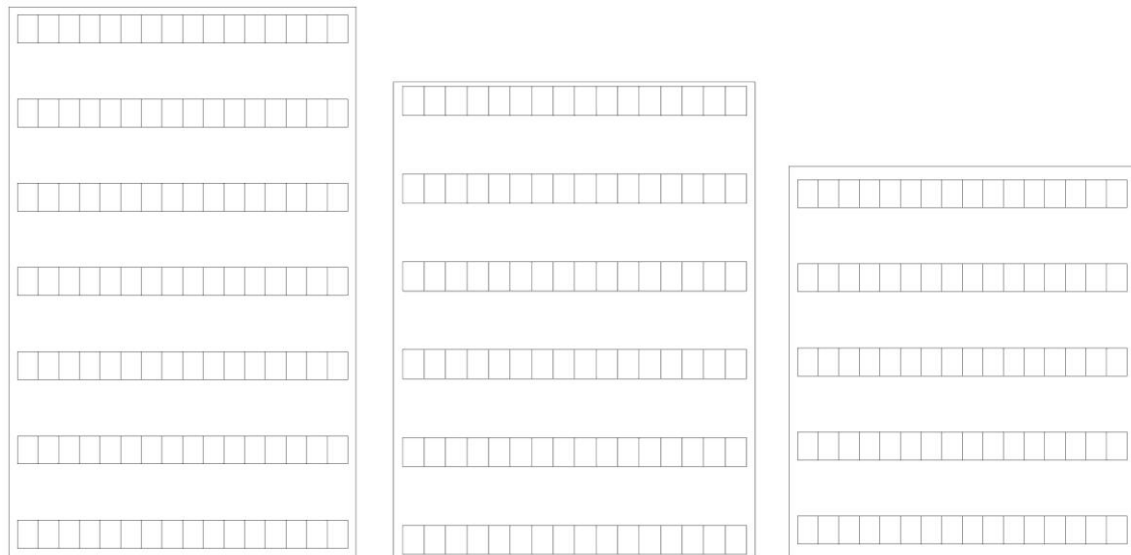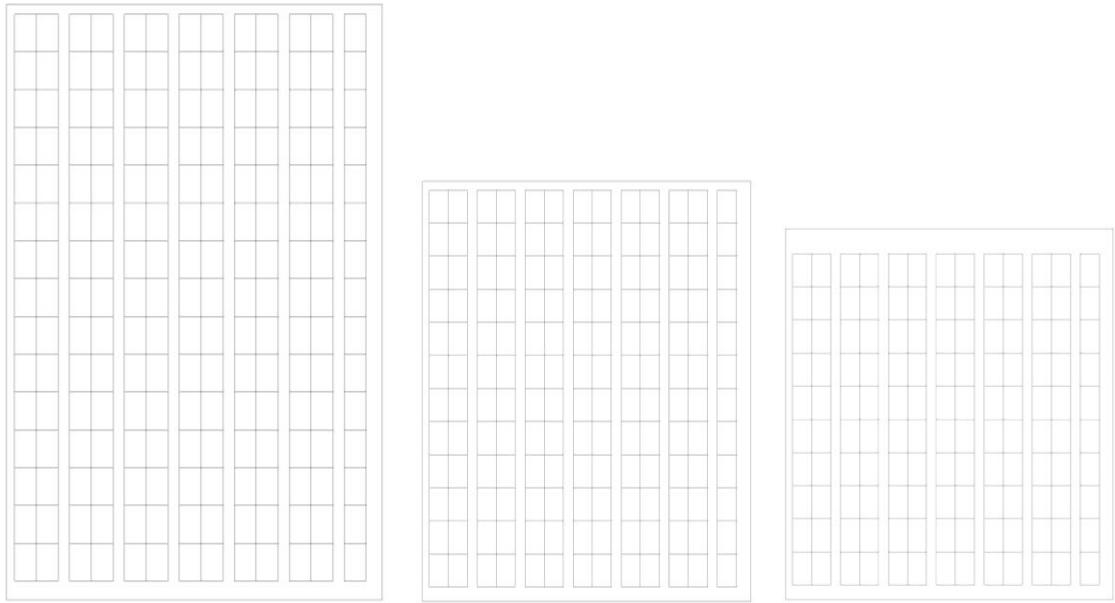

Figure 52. PVs facing south for the three scenarios

In case the PVs are placed with the east-west orientation, 195, 156 and 130 PVs can fit on the roof of the 16-vault, 8-vault, and 4-vault archive, respectively.

Figure 53. PVs facing east-west for the three scenarios

8.2 Energy storage systems

Energy storage systems help offsetting the mismatch between demand and supply and overcome the fluctuating nature of renewable energy sources [48]. Two systems that were analyzed for this research are batteries and ice slurry.

8.2.1 Battery system

Batteries are devices that enable energy from renewable sources, like solar, to be stored and then released at a later moment according to the building's need.

The implementation of batteries was considered to increase the self-consumption on site. For each PV panels number, battery sizes of 30 kWh, 50 kWh and 100 kWh were analyzed.

8.2.1.1. Self-consumption of different combination of PVS and batteries

The results of electricity bought from the grid, sold to the grid, and self-consumed for different combination of PVs number and battery sizes are shown in Figure 54.

The case of PVs without battery shows the highest import from the grid and the lowest self-consumption; nevertheless, if more PVs are installed, less electricity is imported from the grid, more is self-consumed and more is sold to the grid.

As for the case with different size of batteries, the amount of self-consumed electricity is more than the electricity bought from the grid, for each of the combination. The trend is similar: the higher the number of PVs, the lower is the electricity imported from the grid, and the higher is the electricity self-consumed and sold the grid.
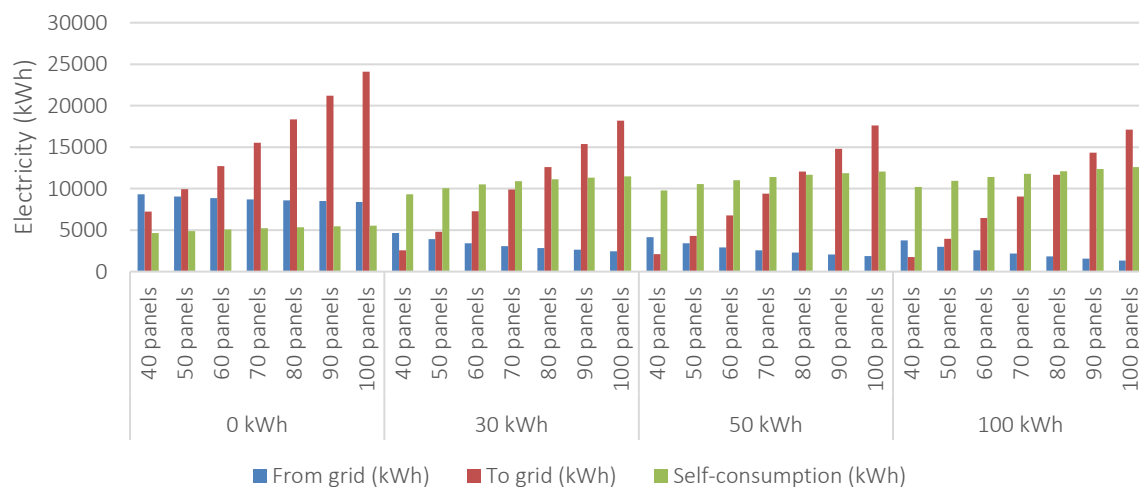

Figure 54. Electricity behavior for different PVs-battery size combination, according to different battery size

When a bigger battery is considered for the same amount of PV panels, the amount of electricity imported from the grid decreases as well as the electricity sold to the grid, but self-consumption increases, as shows Figure 55.
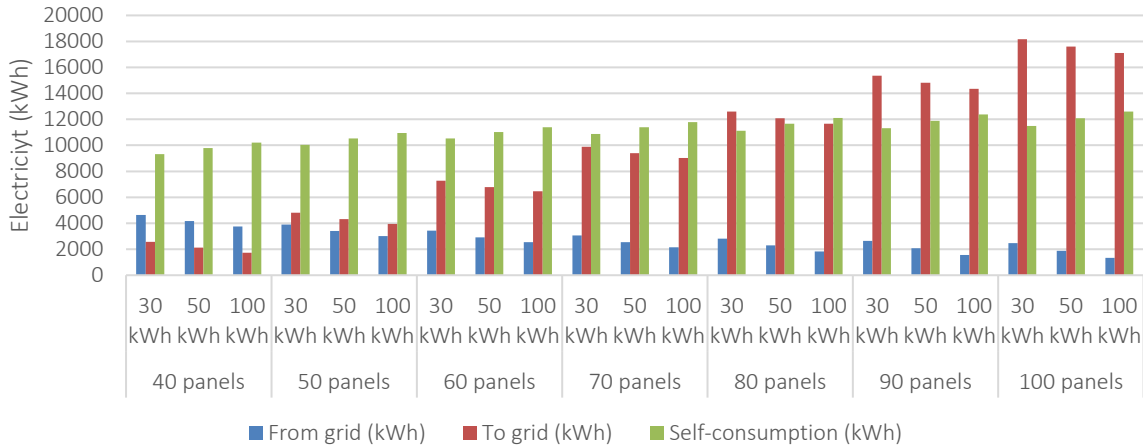
Figure 55. Electricity behavior for different PVs-battery combination, according to different number of panels

The Load Duration Curves (LDC) were plotted with the electricity load of the building without PV panels, with 40 panels, and with 40 panels with different battery sizes, namely 30, 50 and 100 kWh.

The baseload of the LDC curve for the building with no PV panels is around 1.35 kWh. This is due to the fact that the HVAC system runs constantly, to provide optimal climate conditions, both during the day and at night. When PVs are implemented, the operational energy decreases by around one third, as a consequence of self-consumption. If batteries of different sizes are implemented to the PVs, the operational energy further decrease by one third. It can be noticed, nevertheless, that the peak load has a very small reduction when only PVs are implemented, namely 5%. When 30 kWh, 50 kWh and 100 kWh batteries are combined with the PVs, the peak reduction is by 14%, 16% and 20%, respectively.
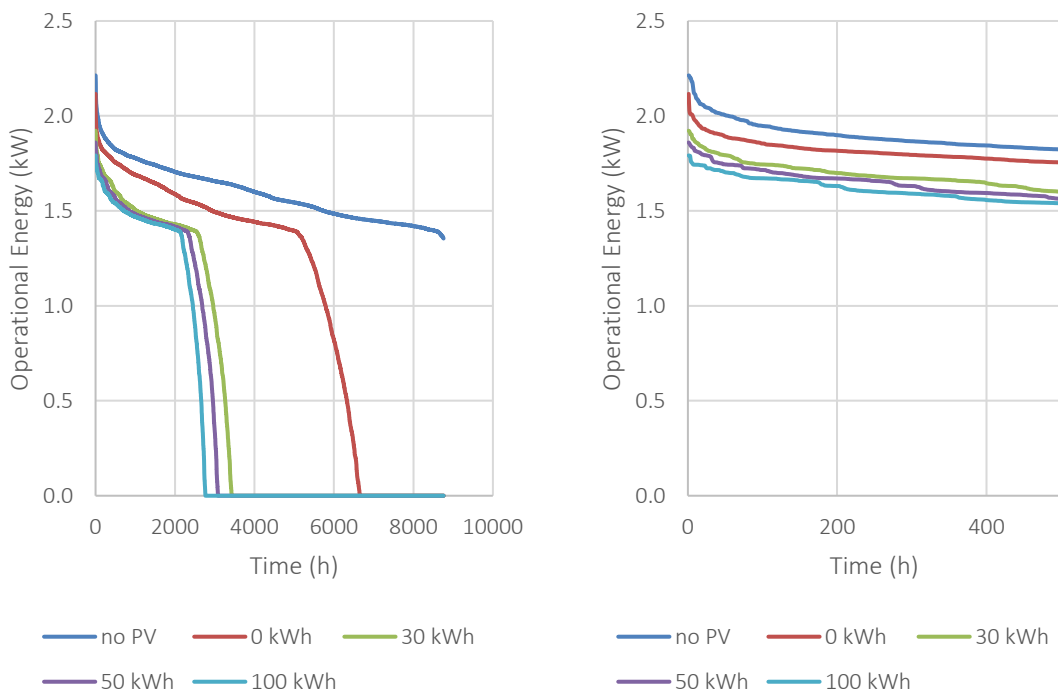

Figure 56. Left: LDC of the electricity load of the archive building, with 40 PVs; Right: peaks of each curve

51

8.2.1.2. Battery State of Charge

The State of Charge (SOC) was analyzed for each combination of PV panels number and battery size. The graphs can be found in Appendix 13.5.4.

Figure 57**Error! Reference source not found.** shows the example for one combination of 40 PV panels with 30 kWh, 50 kWh and 100 kWh batteries. As can be noticed, the 100-kWh battery is oversized, as its SOC range for most of the year, in summer, is between 80 and 100%; as for winter, it does not bring benefits compared to the 30 kWh and the 50 kWh batteries. The 50-kWh battery has the same behavior, with a SOC that, for most of the year, ranges between 60 and 100%.
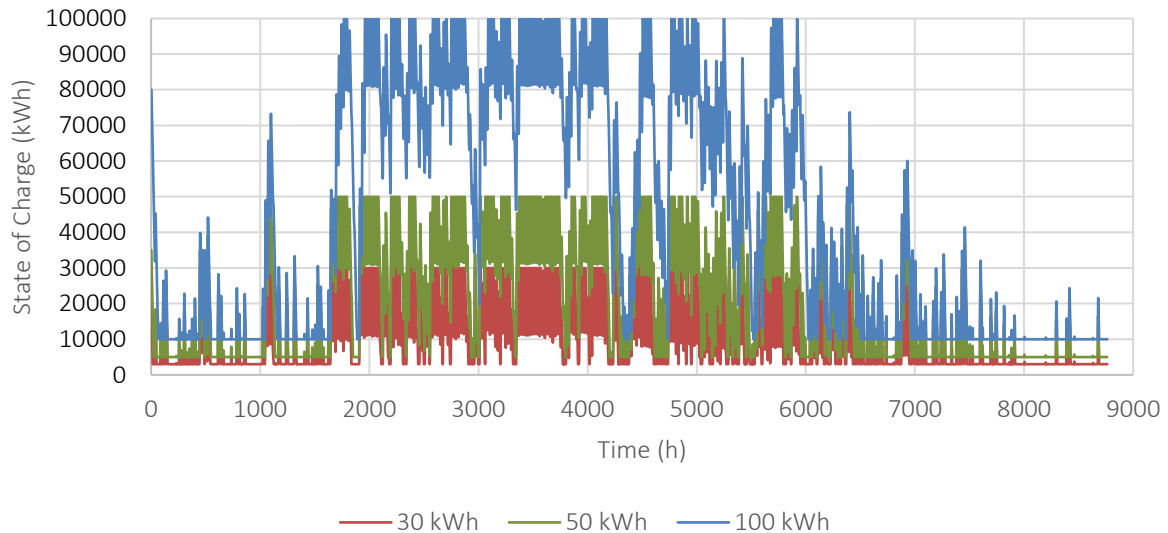

Figure 57. State of charge of 30 kWh, 50 kWh and 100 kWh batteries, 40 PVs

8.2.1.3. Safety battery in case of emergency

The behavior of the building was analyzed in case of a blackout during the warmest period of the year. As Figure 58 shows, the outside temperature has a range between 12°C at night and 27°C during the day. According to the simulation, if the HVAC system would stop working, the temperature of the vault would increase steadily, but for more than two weeks it would stay within the safe threshold of 15°C. On the other hand, RH increases very rapidly, and reaches 100% in around 12 hours.
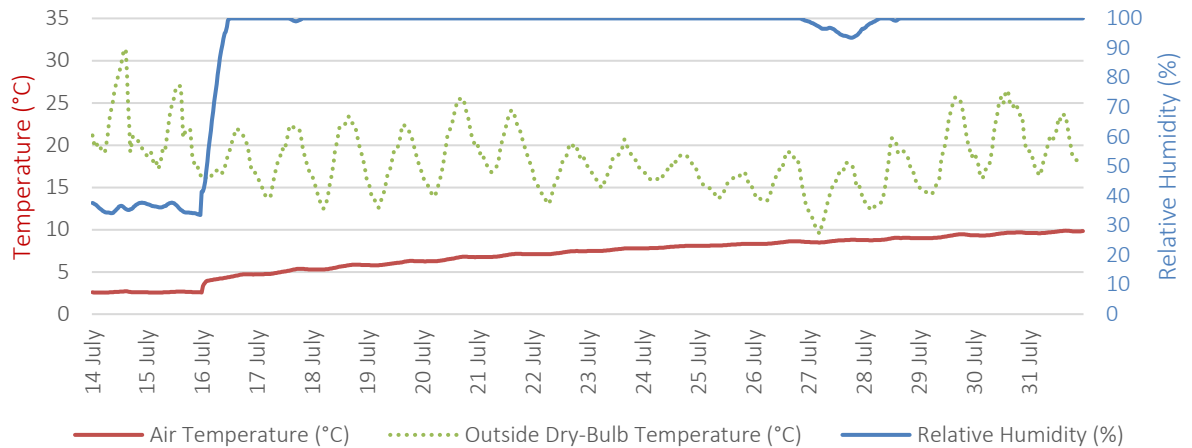
Figure 58. Climatic conditions of the vault in case of blackout

By implementing a safety battery, which always remains completely full and connects only in case of emergency, the collection could remain safe for a longer period.

Figure 59 shows the state of charge of a 30-kWh battery that is fed with 40 PV panels. It can be noticed the distinction between summer and winter: in summer, when solar energy production is high, most of the time the battery is full; on the contrary in winter, when the solar energy production is low, the battery is often empty.
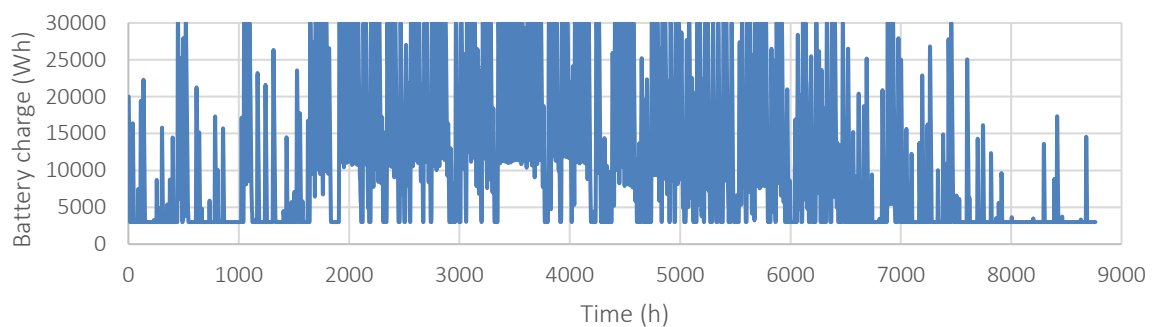

Figure 59. State of charge of 30 kWh battery with a 40-PVs system

Given the difference between seasons, two blackout times were analyzed for the project, one happening in winter, and one happening in summer. Moreover, for each case, the 30-kWh safety battery was implemented in a building with 1) only PV panels (40) and 2) with PV panels (40) and a 30-kWh battery.

In winter, the blackout occurs at 1 a.m. on the 6th of January. Figure 60 shows the state of charge of the batteries in relation to electricity demand and generation. The first peak of electricity generation represents the time of blackout and the time where the safety battery starts functioning.

When the safety battery is implemented to the building with only PV panels, the building can run for around 32 hours without the need of electricity from the grid. When the safety battery is implemented to the building with PVs and battery, it can run for 42 hours, 10 more compared to the previous example.
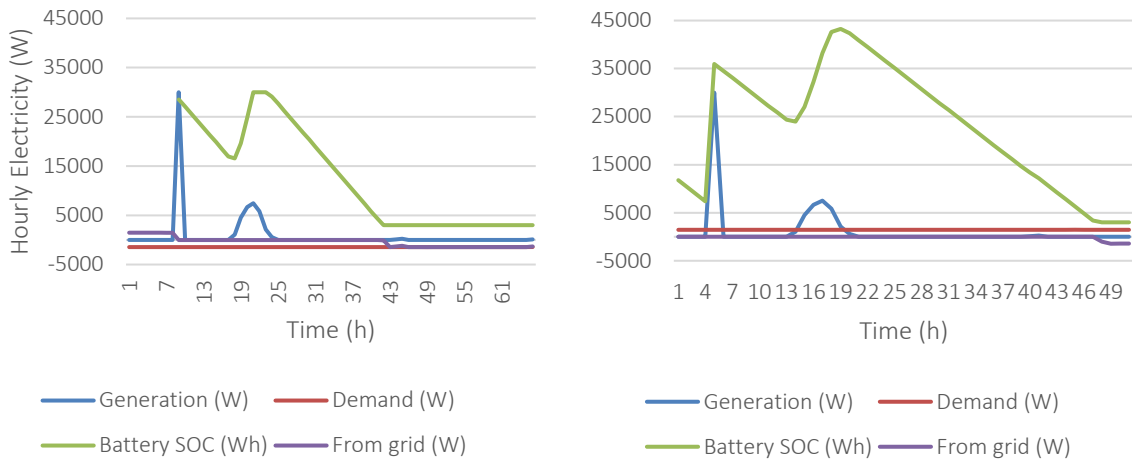
53

Figure 60. Relation between battery state of charge, and electricity generation and demand, during a blackout in winter. On the left, the building runs only with PV panels; in the right, the building has PVs and a 30-kWh battery

In summer the electricity production is high and batteries can gap many hours without electricity, as shown in Figure 57. The blackout occurs at 1 a.m. on the 25th of June. Figure 61 shows the state of charge of the batteries in relation to electricity demand and generation. As the previous case, the first peak of electricity generation represents the time of blackout and the time where the safety battery starts functioning. When the safety battery is implemented to the building with only PV panels, the building can run for around 57 hours without the need of electricity from the grid. When the safety battery is implemented to the building with PVs and battery, it can run for 98 hours, 30 more compared to the previous example.
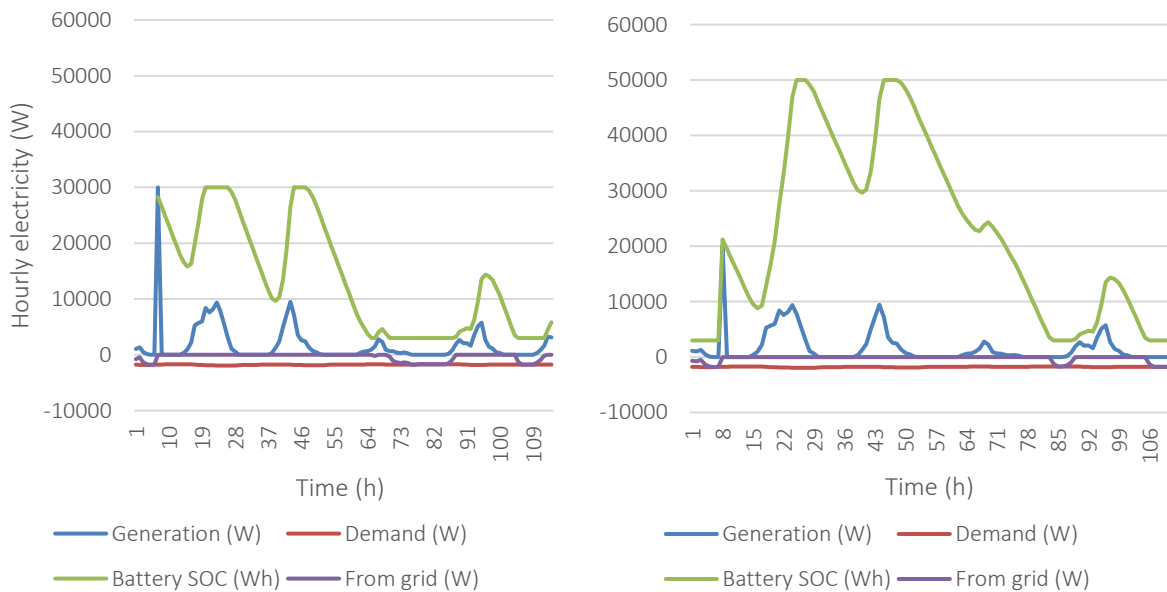

Figure 61. Relation between battery state of charge, and electricity generation and demand, during a blackout in summer. On the left, the building runs only with PV panels; in the right, the building has PVs and a 30-kWh battery

8.3   Ice slurry storage system

Thermal Energy Storage systems (TES) help conserving energy in thermal reservoirs for later usage [49]. Cool energy is stored in form of ice, chilled water, Phase Change Material (PCM) or eutectic solution; ice slurry can be considered as a PCM. The main purpose of using ice slurry is to take advantage of the stored cooling energy in the ice particles when they melt, the so-called latent heat [50]. The composition of ice slurry consists of water with ice crystals, mixed with another fluid such as glycol. Only a fraction of the water is transformed into small ice crystals (around 1 mm); these ensure that the surface area for heat exchanging is very large, comparing with conventional ice storage, and therefore ice instantly melts to meet optimal cooling loads [51].

The applications of ice slurry in air conditioning systems might be beneficial from an energetic point of view when combined with low temperature air distribution systems (temperature of air = 2°C) [52]. The schematic in Figure 62 shows an example of the functioning of an ice slurry system. During the day, the ice slurry generator produces ice slurry and stores it in a tank; at the same time, the chiller provides the cooling load. During the night, a glycol solution passes through the ice slurry tank and through a heat exchanger, interfaced with the existing cooling system of the building. The supply water from the chiller is diverted to the plate heat exchanger and the glycol solution provides the additional drop in temperature required by the load.
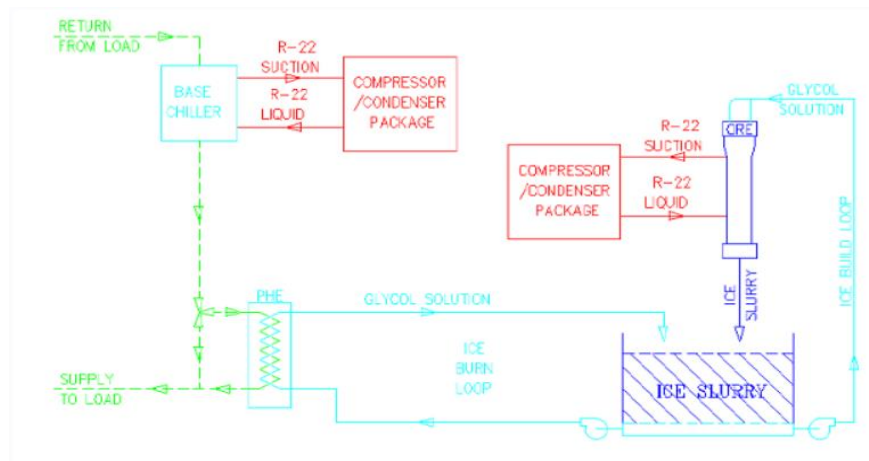

Figure 62. Schematic of ice slurry system cooling [48]

Figure 63 shows the shift in peak of free solar energy, used to produce ice slurry during the day, toward the night, when the melting ice slurry can be used to cover the cooling load.
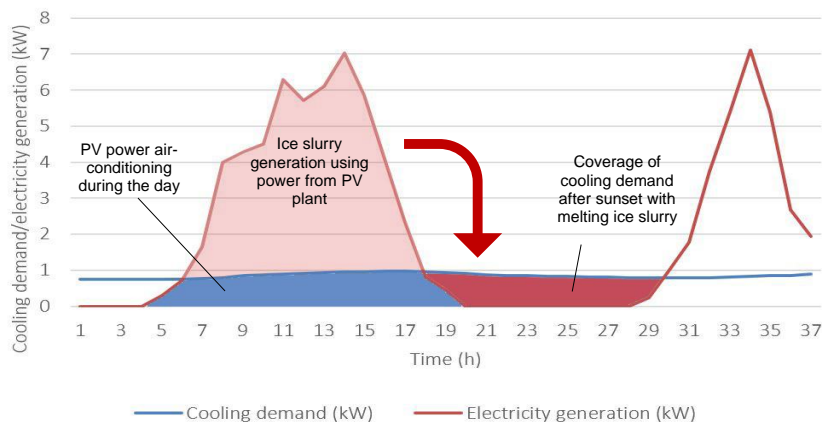

Figure 63. Decoupling of cold generation and cooling demand with the ice slurry system

55

To assess the sensibility of such system for the Eye Filmmuseum, the cooling capacity of ice slurry produced during the day was compared to the electricity from the grid to provide night cooling. The COP of the ice generator was assumed to be 2, according to a study by Liu et al [53]. This was used to calculate the potential cooling energy produced in form of ice slurry from the surplus of the PV panels.
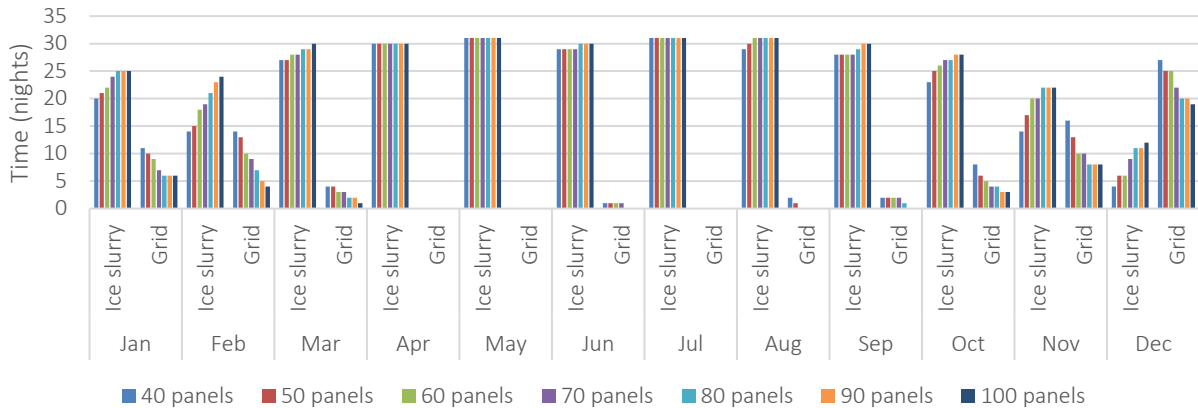

Figure 64. Ice slurry vs electricity grid sensible cooling

The graph shows the number of nights when the sensible cooling load is fully covered by the ice slurry system and how many nights additional electricity from the grid needs to be integrated, for each PV system size. For the central part of the year, April until September, the ice slurry system produces enough cooling capacity during the day to cover for the cooling at night, except for a few days for the cases with fewer PVs. During March and October, the system has still a good performance, with the system covering, on average, 97 and 84% of the days, respectively. For the winter period, November to February, the system is less effective given the low solar irradiance and hence the low electricity production.

The analysis for feasibility of an ice slurry system is only a preliminary study. More research needs to be done concerning charging and discharging cycles and their time, and cost effectiveness.

8.4   Payback period

8.4.1   PVs and battery

The payback period of different combination of PV panels and batteries was calculated. The degradation rate of the PV panels is assumed to be 0.5%, according to the data of the PV chosen.

For the calculation, the Dutch net metering scheme (*salderingregeling*) was taken into account: the Dutch law stipulates that every kWh of electricity that a building feeds back to the grid is worth as much money as what it costs to pay for a kWh consumed from the grid [54]. The current regulation will change from 2025, when the percentage of feed-in energy that is subject to net metering will gradually decrease as shown in Figure 65, until phasing out from 2031 [55].
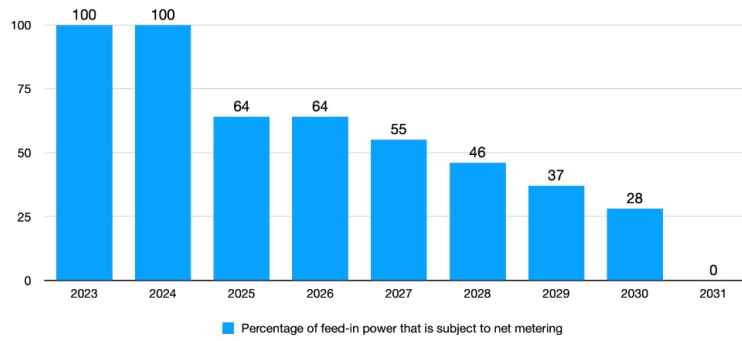
Figure 65. Net metering phase out according to new proposal (postponed from 2023 to 2025)

The price for the PV panels were assumed to be 1 €/Wp. The prices used are in Table 7.

Table 7. Prices for PV panels number

Number of PV panels	Price (€)
20	6200
30	9300
40	12400
50	15500
60	18600
70	21700
80	24800
90	27900
100	31000
150	46500
200	62000

The price of the battery in €/kWh varies according to the size. The bigger the battery, the lower the price in €/kWh. The prices, according to a comparison-advice platform [56] and manufacturers, are shown in Table 8.

Table 8. Prices for battery sizes

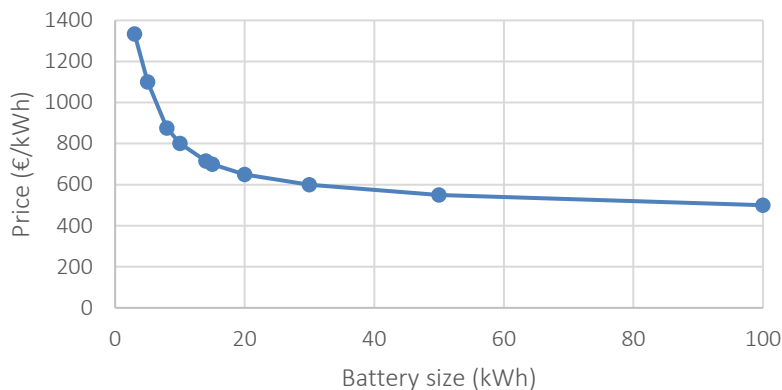| Battery size (kWh)	Price/price range (€)	Price in €/kWh
3	4,000	1,333
5	5,000-6,000	1,100
8	5,000-8,000	875
10	8,000-10,000	800
14	10,000	714
15	9,000-12,000	700
20	12,000-15,000	650

Figure 66. Relation between battery size and price per kWh.

The prices for battery sizes of 30 kWh, 50 kWh and 100 kWh are found by extrapolating from the graph the prices in €/kWh. The electricity prices used in the calculation, taken from Eye's electricity bill, is 0.18 €/kWh, while the compensation for sold electricity is assumed to be 0.10 €/kWh.

Considering the current rise of electricity prices, the payback period for doubled and tripled electricity prices, namely 0.36 €/kWh and 0.54 €/kWh, was assessed. Both PV panels and batteries are assumed to have a lifespan of 25 years.

Figure 67 shows the payback time results. The results show that any number of PV installed without a battery have the same payback period, that is 7 years. For the case with batteries, on average, the bigger the battery, the longer the payback time; for the 100-kWh battery with 40, 50 and 60 PVs, the payback time is more than 25 years. When taking into account only one battery size, if the number of PV panels increases, the payback time is shorter.
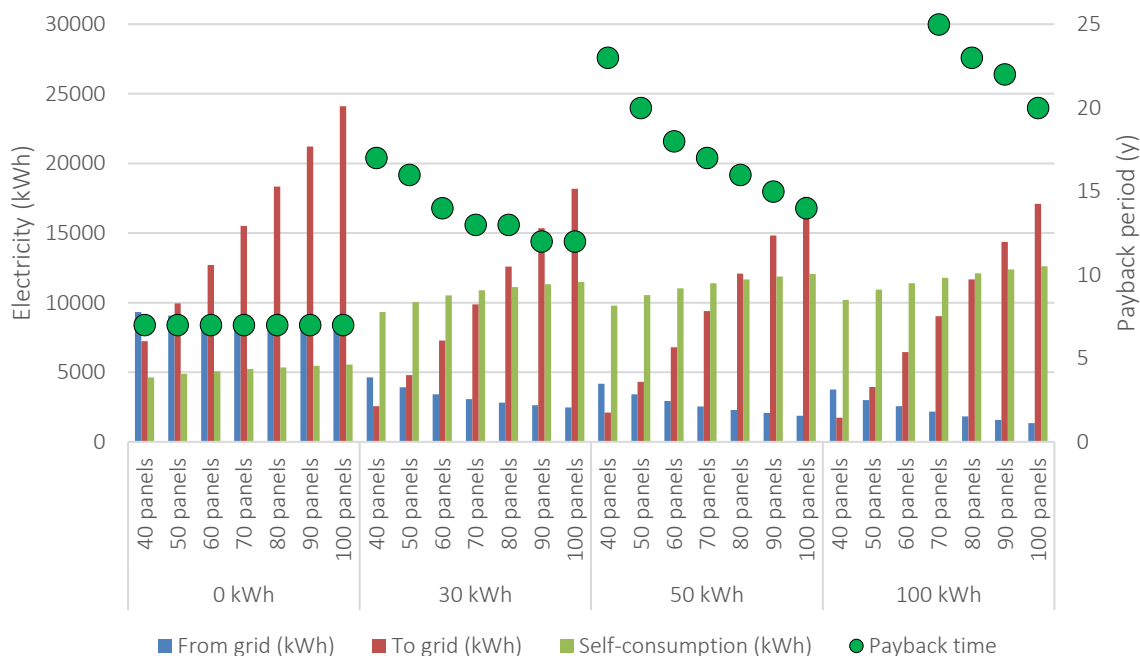

Figure 67. Payback period of PVs and batteries

8.4.1.1. Electricity price increase

As consequence to the current energy crises, the prices of electricity are increasing. The payback time for the PVs and the batteries with double and triple the price, namely 0.36 €/kWh and 0.54 €/kWh, was calculated. The results are depicted in Figure 68**Error! Reference source not found.**. Generally, the highest the electricity price, the lower the payback time. It can be noticed that the payback time decreases exponentially, with a value of 50%, if the electricity increases from 0.18 €/kWh to 0.36 €/kWh, and 30% when electricity increases from 0.36 €/kWh to 0.54 €/kWh. Generally, the highest the electricity prices, the more sensible the implementation of PVs and batteries is.
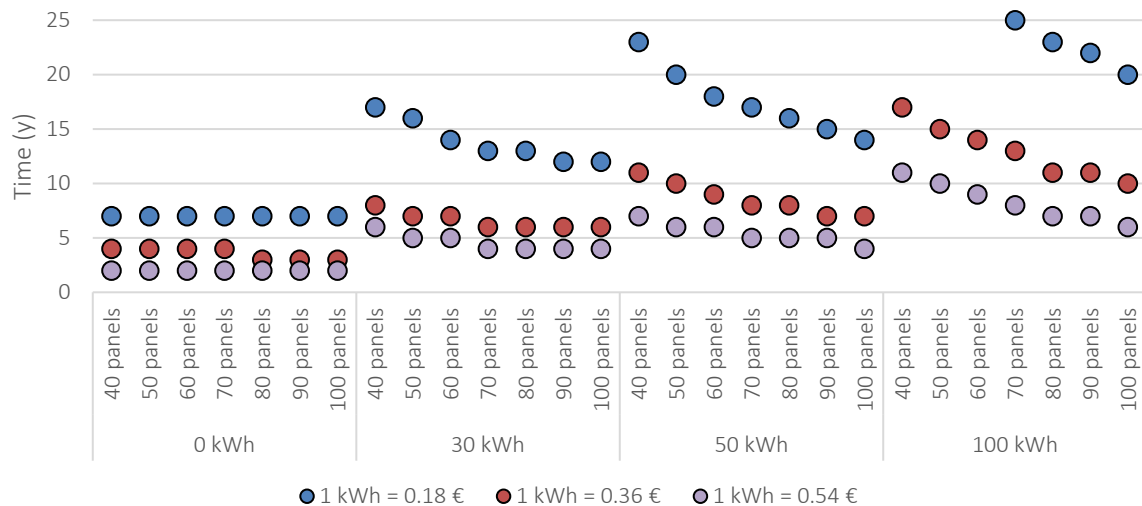

Figure 68. Payback time of PVs and batteries according to different electricity prices

9 Environmental impact

9.1   Life-Cycle Assessment

Life-cycle assessment (LCA) is a tool for analyzing environmental performance of products or processes over their entire life cycle, hence from cradle to grave. This includes raw material extraction, manufacturing, use and reuse, and end-of-life (EOL) disposal and recycling [57].

There are three different phases that can be considered when making a Life Cycle Assessment: cradle-to-grave, the full life cycle assessment from manufacture (cradle) through the use phase, to the disposal phase (grave); cradle-to-gate, the assessment of a partial product life cycle from manufacture (cradle) to the factory (gate), i.e., before it is transported to the consumer; cradle-to-cradle, a specific kind of cradle-to-grave assessment, where the end-of-life disposal step for the product is a recycling process [58].

9.1.1   Environmental Product Declaration (EPD)

Environmental declarations and eco-labels are the main instrument that is used to gather environmental information about a product or service in a reliable, accurate and simplified way [59]. They have the purpose of providing quantified environmental information about the life cycle of a product, facilitating environmental comparison between products that perform the same function [59].

The purpose of an EPD in the construction sector is to provide the basis for assessing buildings and other construction works and to assist in identifying those construction products which cause less stress to the environment considering the whole building life cycle [59]. The standard that is applied to the built environment is the EN 15804, which is the standard for the sustainability of construction works and services. The first version was published in 2012, known as EN 15804+A1, with the name of "Sustainability of construction works – Environmental product declarations – Core rules for the product category of construction products". A second version called EN 15804+A2 was published in 2019, with some changes regarding life cycle, additional environmental indicators, and new content regarding biogenic carbon [60].
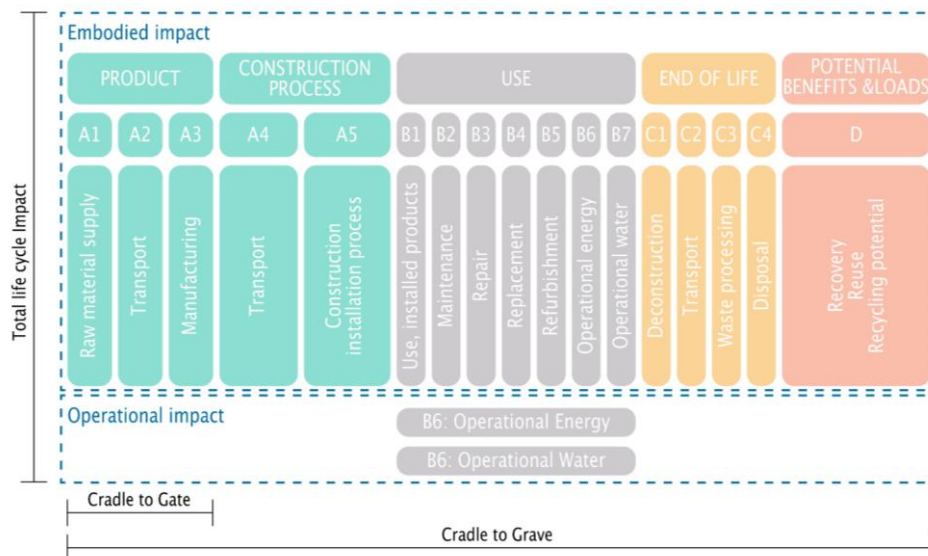

Figure 69. Environmental characteristics in EPD

9.1.2   Goal

The goal of this LCA analysis is to assess the environmental impact of different construction technologies and materials for the same building, namely CLT, concrete and lightweight timber frame, for the cradle-to-gate phase of the building.

So that the value can be compared, the U-value of both walls and roofs were kept the same: 0.11 W/(m²K) for wall and 0.10 W/(m²K) for roof. Calculations can be seen in Appendix 13.6.1.

In Table 9, the material layers for each structure type are shown.

Table 9. Material layers for each structure

	Structure		
	Cross Laminated Timber	**Concrete**	**Lightweight timber frame**
Walls	300 mm CLT 200 mm rock mineral wool	200 mm concrete 300 mm rock mineral wool	10 mm OSB 200 mm mineral wool + studs 100 mm mineral wool 100 mm OSB
Roof	200 mm CLT 250 mm rock mineral wool	200 mm concrete 320 mm rock mineral wool	10 mm OSB 220 mm mineral wool + studs 100 mm mineral wool 100 mm OSB
Partitions	60 mm CLT 100 mm rock mineral wool 60 mm CLT	140 mm concrete	10 mm OSB 200 mm rock mineral wool + studs 10 mm OSB

Floor	200 mm concrete	200 mm concrete	200 mm concrete

Table 10. Walls and partitions for each structure type

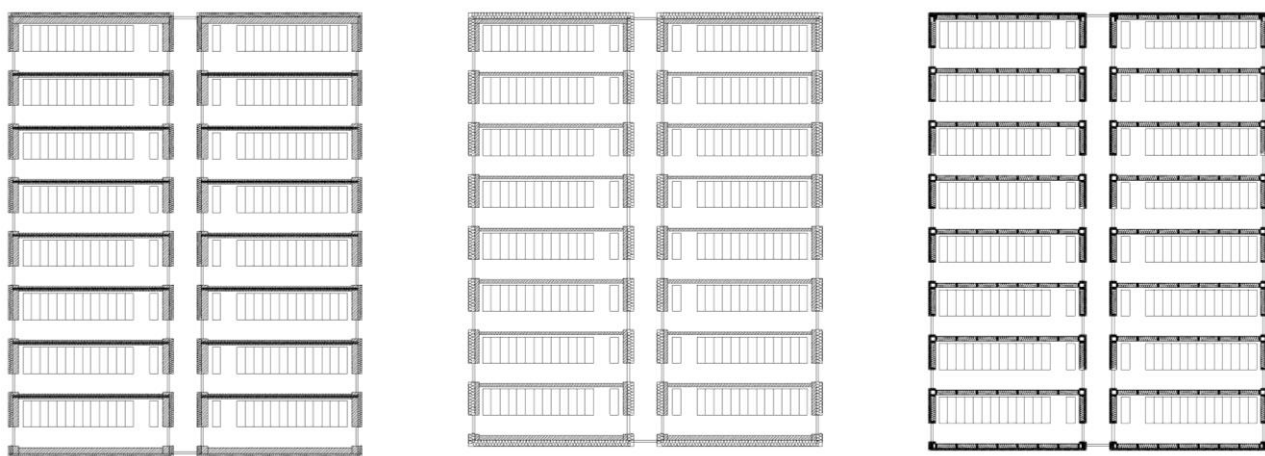|	Cross Laminated Timber	Concrete	Lightweight timber frame
Walls/roof			
Partition			

Figure 70. Plans of 16-vaults archive, with the three different structures.

9.1.3 Impact Categories

The Impact Categories (ICs) represent environmental issues of a certain material or product. An IC groups different emissions into one effect on the environment; the ICs for building materials are generally divided into three groups: environmental impact, waste type and output flows, and resources use. For this study, two impact categories, or indicators, are considered: Global Warming Potential (GWP) and Total use of Non-Renewable Primary Energy Resources (PENRT). The GWP is a measure of how much unit mass of gas contributes to global warming, measured in kg CO_2 equivalents, while the PENRT refers to the sum of all the non-renewable energy required to produce any goods or services, measured in MJ.

9.1.4 Biogenic carbon

Biogenic carbon emissions are those that originate from biological sources, such as plants, trees, and soil; they relate to natural carbon cycle and represent the quantity of CO_2 that are captured in the process of photosynthesis [61]. Bio-based products can contribute to reduce the levels of carbon dioxide in the atmosphere hence lowering the carbon footprint of buildings, by considering biogenic carbon as a "negative emission" [62].

Two approaches can be distinguished when assessing the impact of biogenic carbon and release: in the first, referred as 0/0, it is assumed that the release of CO_2 from a bio-based product at the end of its life is balanced by an equivalent uptake of CO_2 during biomass growth. The

second approach, referred as -1/+1, consists of tracking all biogenic carbon flows over the building life cycle. Here both uptake and release are considered, as well as the transfer of biogenic carbon between the different systems. The uptake of biogenic CO_2 during forest growth is transferred to the building system and reported as a negative emission. At the end of the building life's time, biogenic CO_2 is released, or the carbon content is further transferred to a subsequent product system, in case of recycling.

In both cases a positive emission is reported at the end of life of a product. A risk of misleading results can happen when only cradle-to-gate is considered, given by the positive effect of biogenic CO_2 uptake without reporting the release at the end of life. For this reason, for bio-based products, both methods were taken into account, but only the results of the first approach were used.

9.1.5   System boundaries and functional unit

As stated in previous paragraphs. this analysis covers the life cycle of the different materials from A1 to A3, the so-called "cradle-to-gate". These phases are divided as follows:

   a. A1 – Raw material supply, that includes extraction of materials
   b. A2 – Transport, which is the transportation of materials from the extraction place
   c. A3 – Manufacturing, that is the part where the material is worked to become a final product.

9.1.6   Life Cycle Inventory

The Life Cycle Inventory (LCI) is the phase that involves the compilation and quantification of inputs and outputs for a product throughout its life cycle. The LCI is performed for all the materials: CLT, concrete, wood studs, OSB and mineral wool.

Due to the lack of a common database and the big differences that are encountered between EPDs, even for the same material type, it was decided to choose values from two EPDs for each material, considering the high value and the low value found. Particular attention was paid when choosing the EPDs: for the same material, EPDs from the same year and same country of validity were chosen; moreover, only recent EPDs were taken into account, namely from 2018 onwards.

9.1.6.1. Global Warming Potential (GWP)

On average, the highest impact for Global Warming Potential is given by concrete, followed by the OSB. CLT, wood studs and mineral wool have the lowest values. It can be noticed, nevertheless, that for CLT and concrete the difference between high and low value is high, being around three times and two times, respectively.

Table 11. High and low GWP values for each material

| Material | Database/ company | GWP | | | | Country | Year | EN version |
		GWP total (kg CO_2 eq.)	GWP biogenic (kg CO_2 eq.)	GWP fossil (kg CO_2 eq.)	GWP luluc (kg CO_2 eq.)			
CLT	StoraEnso	-707.35	-762	53.8	0.848	Austria	2020	EN 15804 + A2
	Ökobaudat	-650	-806.4	156.4	ND	Austria	2019	EN 15804 + A2
Concrete	Thomas betonbauteile	461.28	-	-	-	Germany	2020	EN 15804 + A1
	Ökobaudat	234.4	-	-	-	Germany	2021	EN 15804 + A2
Wood studs	EGGER	-752	-706	36.1	0.62	Germany	2021	EN 15804 + A2
	StoraEnso	-698	-733	33.9	0.708	Europe	2020	EN 15804 + A2
OSB	SonaeArauco	-658	-1000	341	2.04	Germany	2022	EN 15804 + A2
	Ökobaudat	-608.8	-986.7	377.9	ND	Germany	2021	EN 15804 + A2
Mineral wool	ROCKWOOL	49.48	-	-	-	Germany	2018	EN 15804 + A1
	Ökobaudat	69.89	-	-	-	Germany	2018	EN 15804 + A2

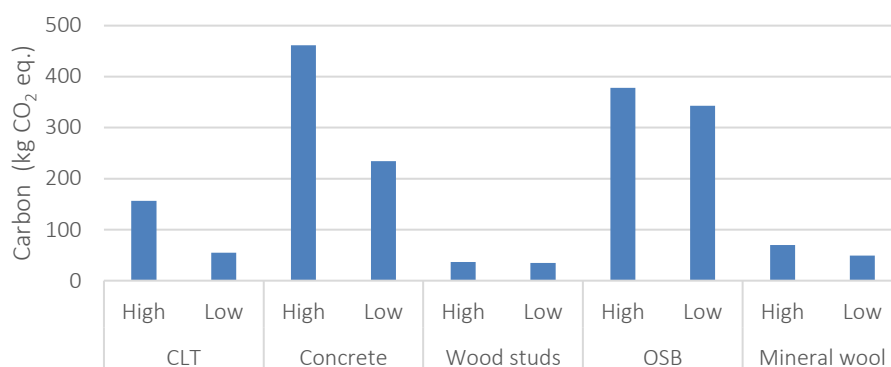*The declared unit for each material is 1 m^3*

Figure 71. High and low GWP for different materials

9.1.6.2. Total use of Non-Renewable Primary Energy Resources (PENRT)

On average, the highest value is given by OSB, followed by concrete and CLT. The lowest values are given by wood studs and mineral wool.

Compared to the values of GWP, the high and low values of PENRT for each material vary enormously; for OSB, for example, the highest value is 13 times bigger than the low value. This is due to the way different companies supply energy when manufacturing a given product.

Table 12. High and low PENRT values for each material

Material	Database/ company	PENRT (MJ)	Country	Year	EN version
CLT	Ökobaudat	2233	Austria	2019	EN 15804 + A2
	StoraEnso	907	Austria	2020	EN 15804 + A2
Concrete	Thomas betonbauteile	3169.71	Germany	2020	EN 15804 + A1
	Ökobaudat	835.6	Germany	2021	EN 15804 + A2
Wood studs	EGGER	694	Germany	2021	EN 15804 + A2
	StoraEnso	129	Europe	2020	EN 15804 + A2
OSB	SonaeArauco	8582	Germany	2022	EN 15804 + A2
	Ökobaudat	643	Germany	2021	EN 15804 + A2
Mineral wool	ROCKWOOL	833.6	Germany	2018	EN 15804 + A1
	Ökobaudat	461.96	Germany	2018	EN 15804 + A2

The declared unit for each material is 1 m^3
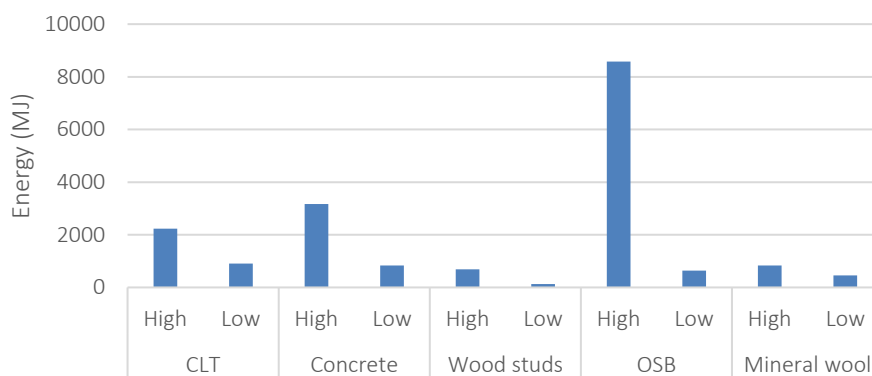
Figure 72. High and low PENRT for different materials

9.1.7   Results

A life cycle assessment was carried out to compare the impact of different structures, CLT, concrete and lightweight timber frame, used for the same building. The parameters considered are Global Warming Potential (GWP) and Total Primary Non-Renewable Energy (PENRT). For each material, a low and a high value were considered, given the differentiation in data found on the Environmental Product Declarations (EPDs). For bio-based materials the biogenic carbon was not taken into account, since the end of life for this research is not considered.

Figure 73 shows the results for GWP. On average, the highest impact is given by the concrete structure, followed by CLT and lightweight timber frame. It can be noticed, nevertheless, that the highest values of the CLT and the lowest values of the concrete have a minimal difference; this means that, taking into account different EPDs, these two structures can be considered to have similar environmental impact. The same results can be noticed with the lowest values for CLT and the highest values of lightweight timber frame.
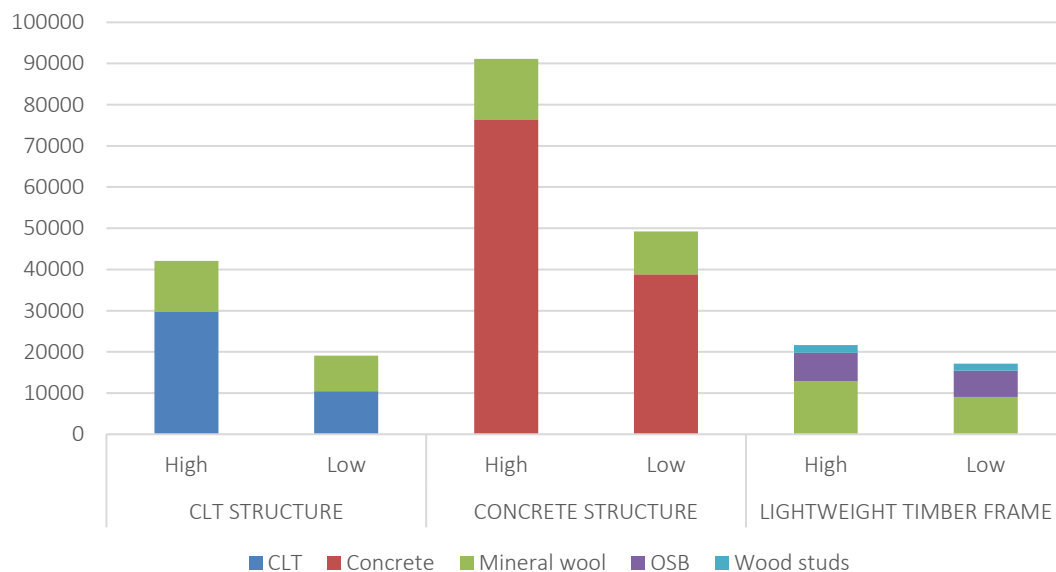
Figure 73. High and low values for GWP of the three different types of structure

As for PENRT, on average the highest impact is given by the concrete structure, followed closely by CLT and finally lightweight timber frame. It can be noticed how the difference between high and low value are almost one third; this is because different manufacturing companies use different energy sources, which can be more or less renewable.
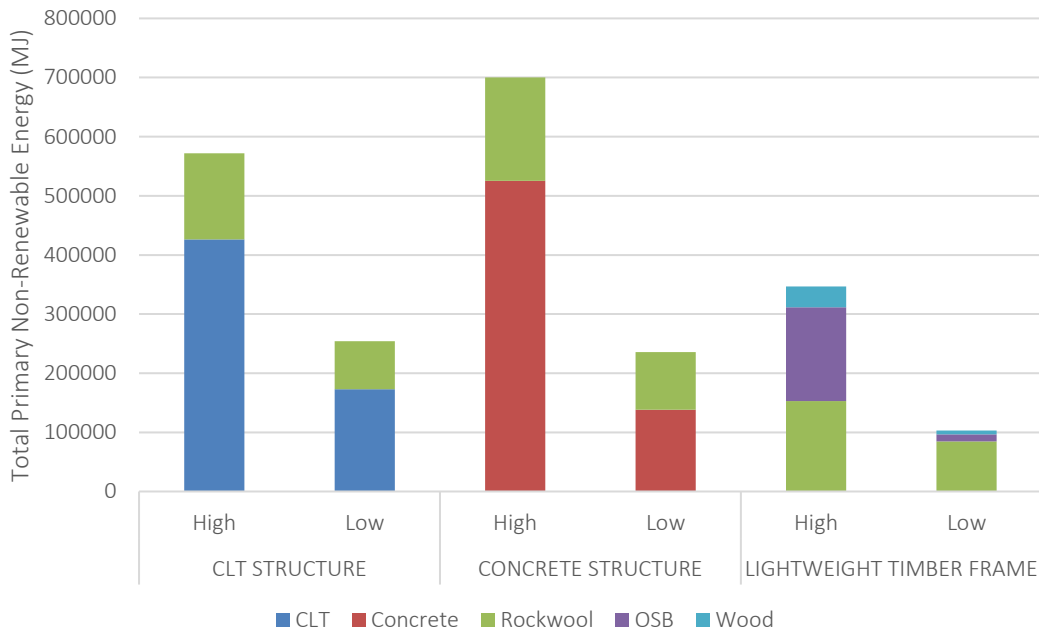
Figure 74. High and low values for PENRT of the three different types of structure

9.2 Carbon payback period

Carbon payback is an estimate on how long a certain element will take to offset the greenhouse gases emitted as a result of its implementation, the embodied carbon, compared to the emissions saved as a result of lower electricity consumption, generated from non-renewable sources, the so-called Operational Carbon (OC).

The OC can be determined by multiplying the operational energy by an Emission Factor (EF). The operational energy is determined by the simulation using DesignBuilder, while the Emission Factor, or greenhouse gas emission intensity, is the volume of emissions of CO_2 that are released to produce a kilowatt hour of electricity (gCO_2e/kWh). The EF is dependent on the grid's source of energy and, for this reason, it fluctuates frequently, due to the changing share of renewable sources of the electricity mix [69]. To simplify the calculations, the average yearly Emission Factor is used; the EF of the Netherlands for year 2020 was 320 gCO_2e/kWh [70].

The carbon payback was calculated for the PV panels and battery system, and for the rock mineral wool insulation according to different thicknesses.

9.2.1 PV panels and battery

The carbon payback period is the period between the initial installation of the PV panels (with battery) and the point in time were the operational carbon saved by self-consumption equals the embodied carbon of the installed PV panels (and battery). To calculate the carbon payback period, values for the embodied carbon of PV panels were researched. The most recent value was found to be 950 kg CO_2/kWp, according to a 2021 research by Müller et al [71].
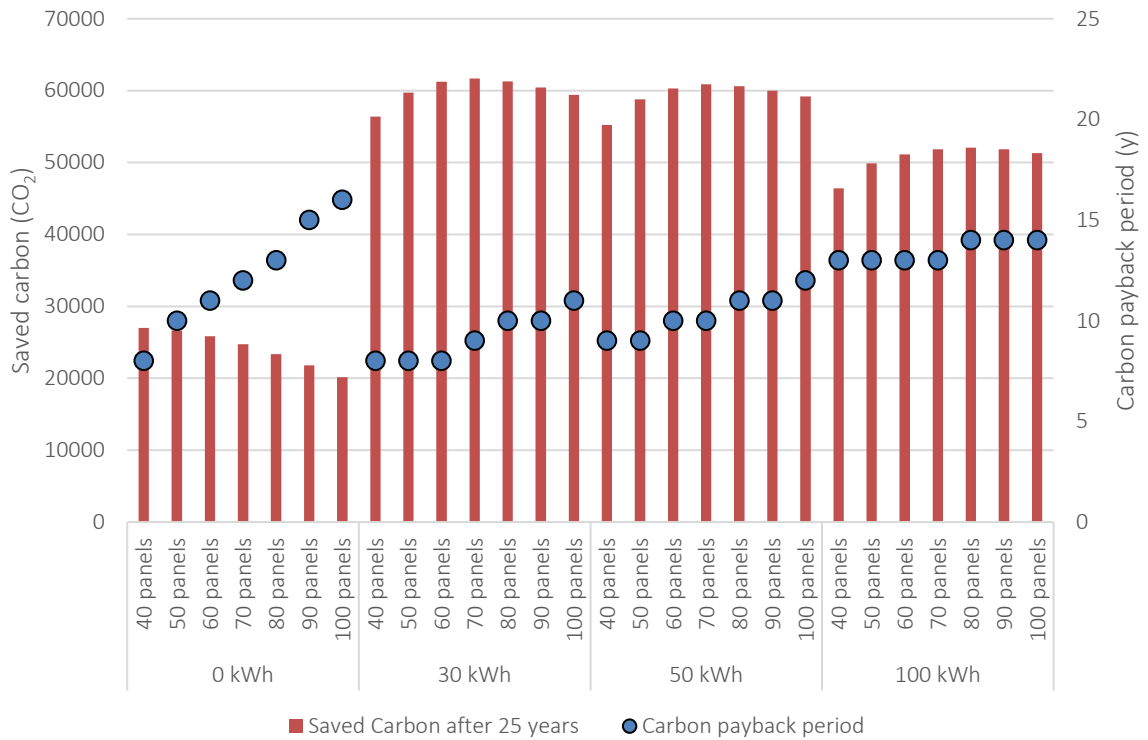
Figure 75. Carbon payback and saved carbon

. Considering 25 years lifespan for both PVs and batteries, all the combinations are viable in terms of carbon payback time. When considering PVs with batteries, smaller batteries give on average a shorter payback time. Considering different number of PVs with the same battery size, the higher the number of PVs, the longer the carbon payback. When considering the carbon saved after 25 years, the PVs have the lowest values; implemented batteries can save up to three times the amount of CO_2. Overall, the best performance is given by smaller batteries, namely 30 and 50 kWh.
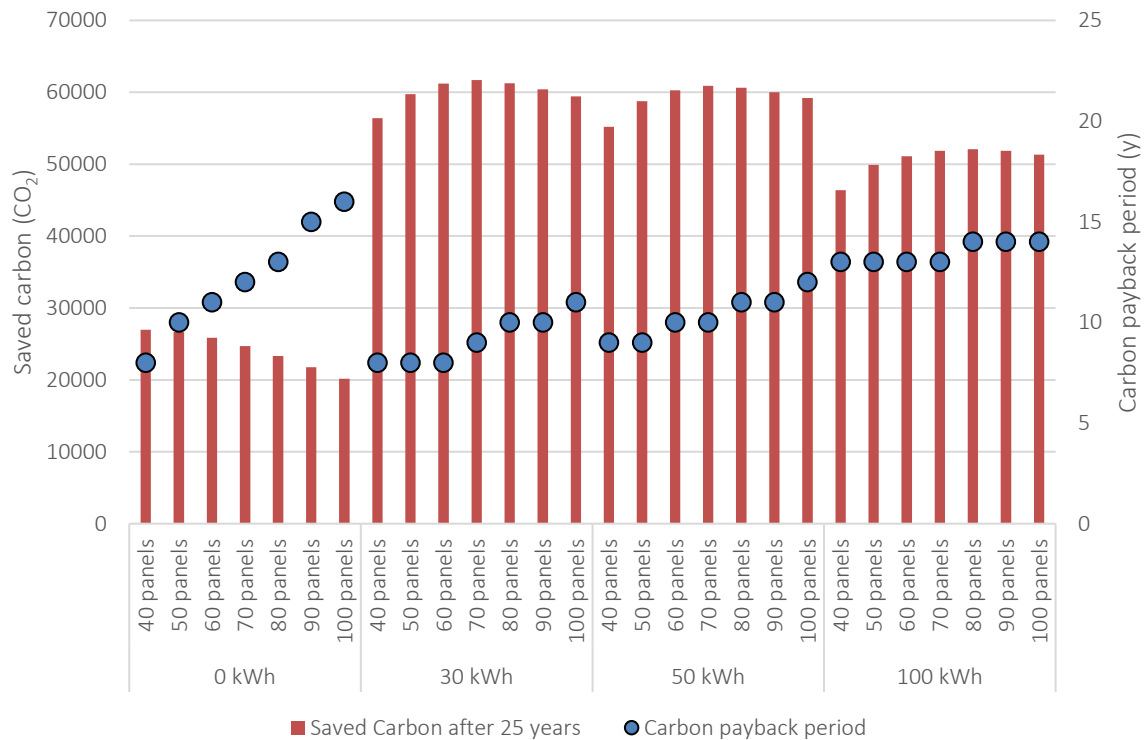
Figure 75. Carbon payback and saved carbon

9.2.2   Insulation thickness

The same concept has been applied to the insulation with different thickness values. The baseline for this analysis is a structure with walls and roof with a maximum U-value of 0.15 W/(m²k). This is given by having an insulation thickness of 150 mm and 200 mm, respectively. To assess the carbon payback of different thicknesses, the insulation of both was increased with a rate of 50 mm, as shown in Table 13 and Table 14. The value for embodied carbon of the insulation, rock mineral wool, was taken as the highest value found in the LCA analysis, namely 69.89 kg CO_2-eq/kWh.

Table 13. Baseline for calculation (in red) with increase of thicknesses and respective U-values, for walls

Insulation		CLT				
Thermal conductivity [W/(m*k)]	Thickness [m]	Thermal conductivity [W/(m*k)]	Thickness [m]	Total thickness [m]	U-value [W/(m²k)]	R-value [(m²k)/W]
0.035	**0.15**	0.11	0.30	0.45	0.139	7.2
0.035	**0.20**	0.11	0.30	0.50	0.116	8.6
0.035	**0.25**	0.11	0.30	0.55	0.100	10.0
0.035	**0.30**	0.11	0.30	0.60	0.087	11.5
0.035	**0.35**	0.11	0.30	0.65	0.078	12.9
0.035	**0.40**	0.11	0.30	0.70	0.070	14.3

Table 14. Baseline for calculation (in red) with increase of thicknesses and respective U-values, for roof

Insulation		CLT				
Thermal conductivity [W/(m*k)]	Thickness [m]	Thermal conductivity [W/(m*k)]	Thickness [m]	Total thickness [m]	U-value [W/(m²k)]	R-value [(m²k)/W]

0.035	**0.20**	0.11	0.24	0.44	0.124	8.1
0.035	**0.25**	0.11	0.24	0.49	0.105	9.5
0.035	**0.30**	0.11	0.24	0.54	0.092	10.9
0.035	**0.35**	0.11	0.24	0.59	0.081	12.4
0.035	**0.40**	0.11	0.24	0.64	0.073	13.8
0.035	**0.45**	0.11	0.24	0.69	0.066	15.2

The differences in electricity load between each thickness and the baseline were calculated, together with the operational carbon, obtained by multiplying the electricity with the Emission Factor, that is 0.32 kg CO_2/kWh. The results are in Table 15.

Table 15. Results of electricity load, saved energy and saved carbon for each insulation thickness

	Thickness insulation wall [m]	Thickness insulation roof [m]	Electricity load [kWh]	Electricity saved compared to baseline (kWh)	Operational carbon saved (CO_2)
Baseline	0.15	0.20	14,705.18	-	-
Option B	0.20	0.25	13,984.58	744,5	238,24
Option C	0.25	0.30	13,387.66	1317,52	421,61
Option D	0.30	0.35	12,939.29	1765,89	565,08
Option E	0.35	0.40	12,546.52	2158,66	690,77
Option F	0.40	0.45	12,264.77	2440,41	780,93

The carbon payback time of the different options are shown in Figure 76. It can be noticed that the payback increases linearly by 3 years for each 50 mm of insulation added, while the electricity load decreases in an exponential curve. Given that the building has a long lifespan, all the options are viable.
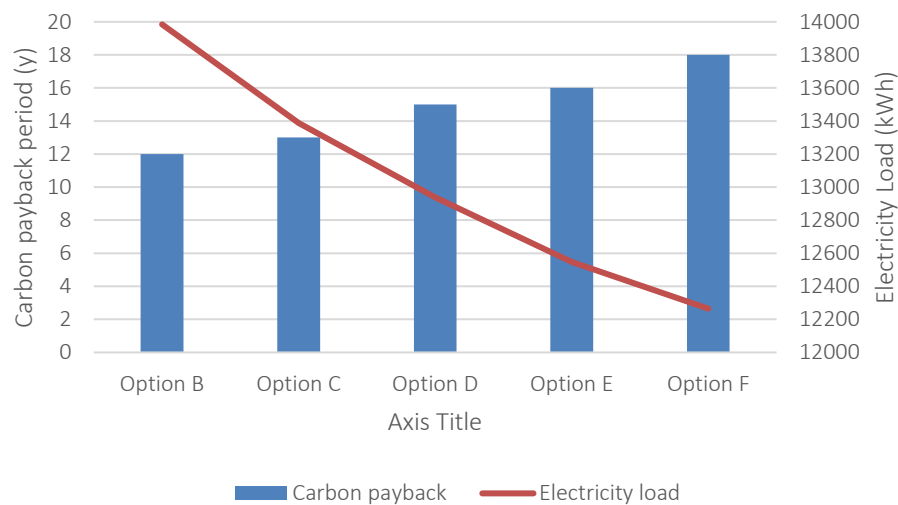
Figure 76. Payback time for different insulation thicknesses

9.3 CO_2 emission reduction scenarios

The Dutch government, in line with the EU goals, wants to reduce the Netherlands' emission of greenhouse gases to almost zero by 2050. The government is working to achieve a low-carbon energy supply by 2050 that will be safe, reliable and affordable; examples of low CO_2 emission energy forms are solar energy, wind energy, biomass, geothermal, and hydropower [72].

As a forecast for future CO_2 emissions, according to the Dutch goals, the Emission Factor is assumed to be 20 g CO_2e/kWh in 2050, comparable to the carbon intensities of countries that already reached 100% renewability [73]. The Emission Factor of the Netherlands for 2020, namely 320 g CO_2/kWh, was used as a starting point, and the EFs for the years in between were extrapolated assuming a linear decrease, as shown in Figure 77.
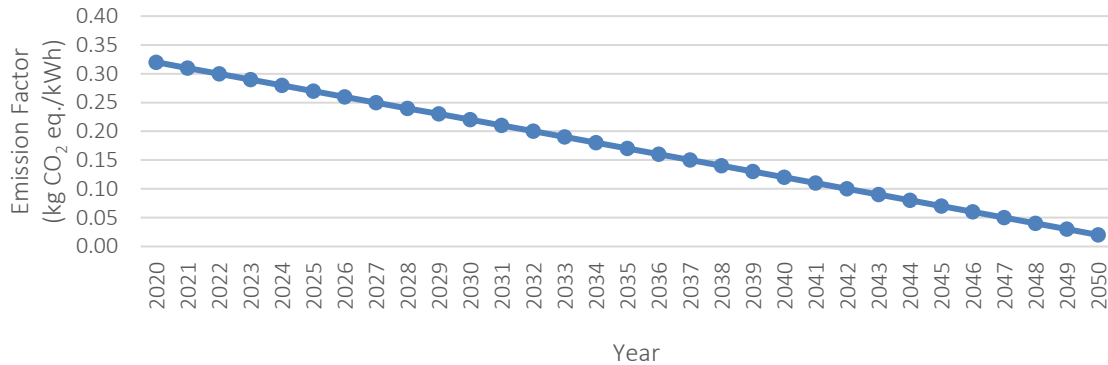

Figure 77. Emission Factors data and prediction for years 2020-2050

The Operational Carbon of the building archive through the years until 2050 was analyzed, for all the PV and battery size combinations. All the plots can be found in Appendix 13.6.2. The archive with 40 panels and 100 kWh battery was chosen as an example (Figure 78), and the Load Duration Curve of the Operational Carbon was plotted for the years 2020, 2030, 2040 and 2050.
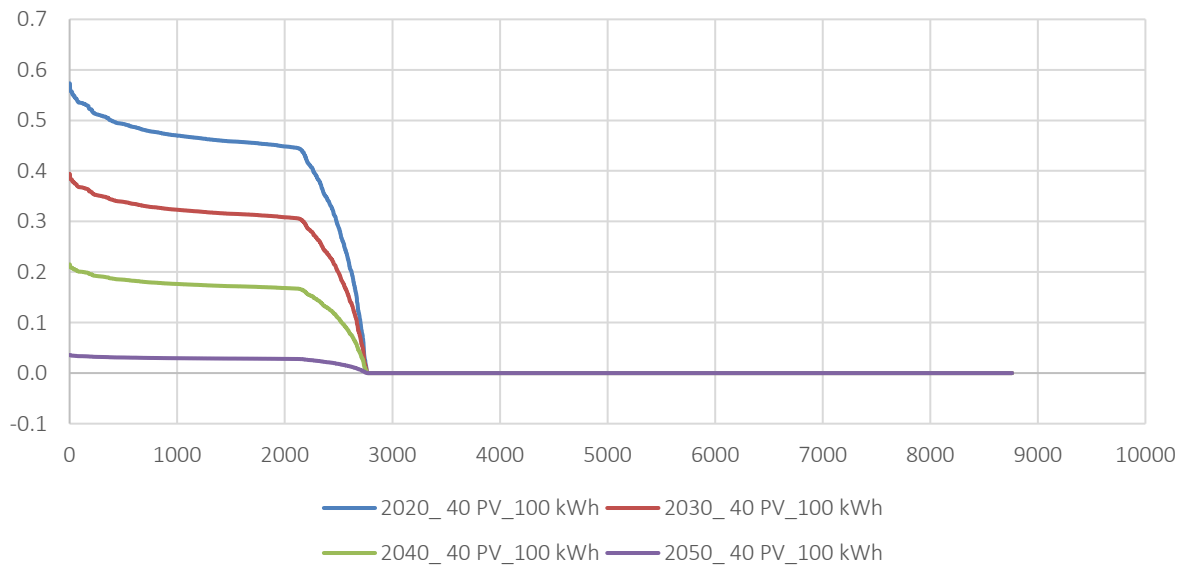
Figure 78. LDCs of the archive OC for different years

As the grid electricity mix gets more and more renewable through the years, according to the 2050 goal, the Operational Carbon reduces according to the projected Emission Factor; this affects the carbon payback results. Figure 79 shows the carbon payback data of 40 PV panels and 100 kWh battery, considering an emission factor of 0.29 kg CO_2/kWh for 2023 and 0.02 kg CO_2/kWh for 2050. It can be noticed that the transition to the grid toward greener energy sources increases the carbon payback period from 12 to 16 years. Choosing lower embodied carbon solutions in the early design phase, will compensate the reduction of carbon through the years given by the transition of the grid toward renewable energy sources.

69
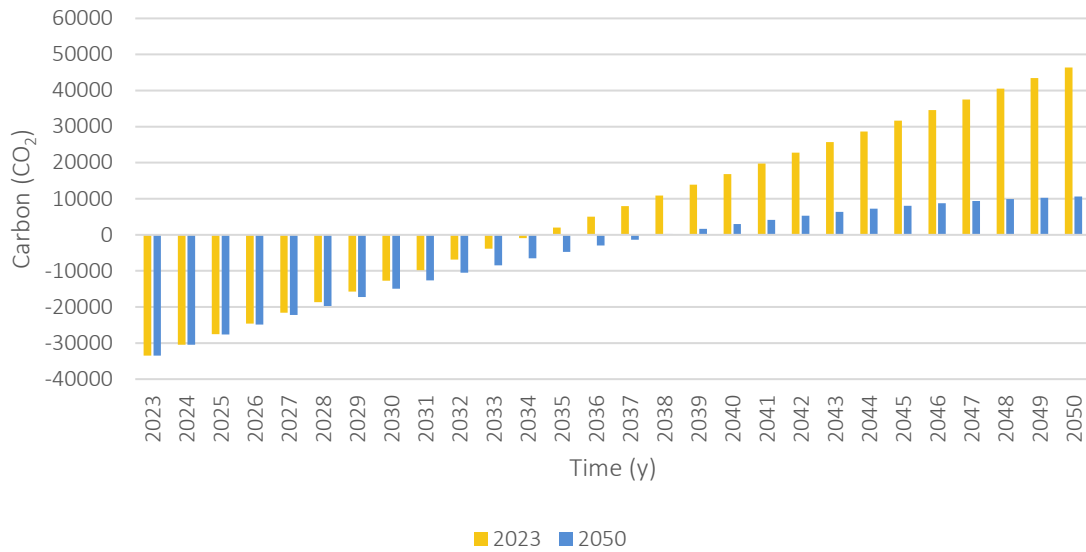
Figure 79. Carbon payback according to 2020 and 2050 emission factor, for 40 panels and 100 kWh battery

Figure 80 shows the carbon payback results for each combination of PV number and battery size. In general, the carbon payback increases for each combination; in the cases with no battery and 100 kWh battery combined with 80, 90 and 100 panels have the bigger differences; the first given by low self-consumption, the latter due to high carbon investment. For the 30 and 50 kWh battery cases, the payback time only increase by one or two years, and can be considered as the best option, where carbon invested is quickly saved, even considering the lower emission factors through the years.
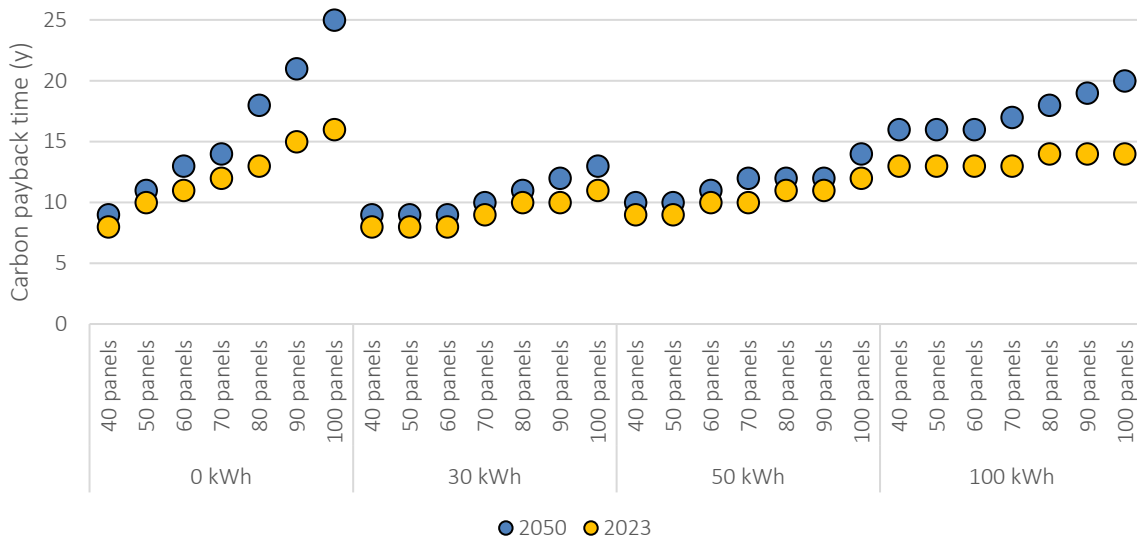
Figure 80. Carbon payback time for each PV number and battery size combination, according to years 2023 and 2050

For the different insulation thicknesses the same concept was applied. The carbon payback time increases when considering the emission factor from 2050. As Figure 81 shows, when choosing a bigger thickness, which means higher carbon investment, the payback time increases exponentially compared to a smaller thickness: option B has a difference of two years, while

70

Option B has a difference of six years, that is 30% more of the carbon payback considering the EF of 2023.
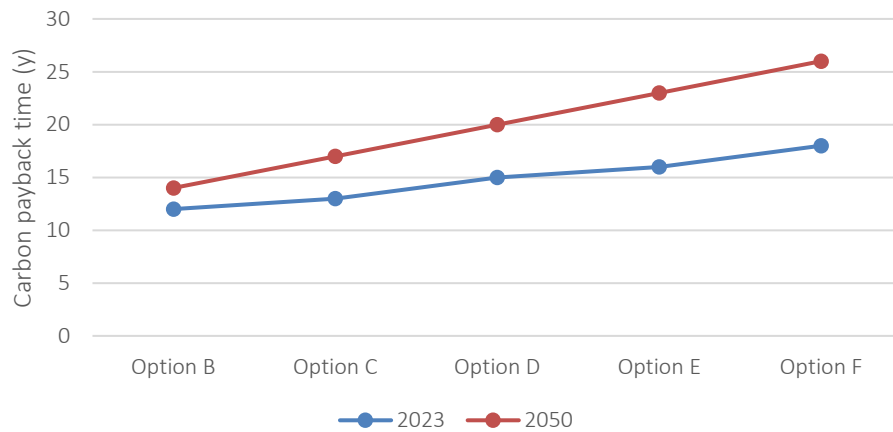
Figure 81. Difference in carbon payback time between 2023 and 2050, for different insulation thicknesses

This analysis shows the importance of choosing low carbon solutions to decrease the carbon payback, taking into account the behavior of the grid according to the 2050 goal.

10   Cost estimation

The construction industry in the Netherlands has seen a significant cost increase in the past years. This is attributed to the rise of raw material prices, higher labor cost and, more recently, the energy crisis. Due to the fluctuating prices, it is difficult to assess the construction cost of the archive building, considering that it might take a few years before it is built. Nevertheless, according to different sources, a range of the possible cost was estimated. Taking as example a construction cost index diagram from Eurostat [74], the costs of a building can be divided as Figure 82 shows.
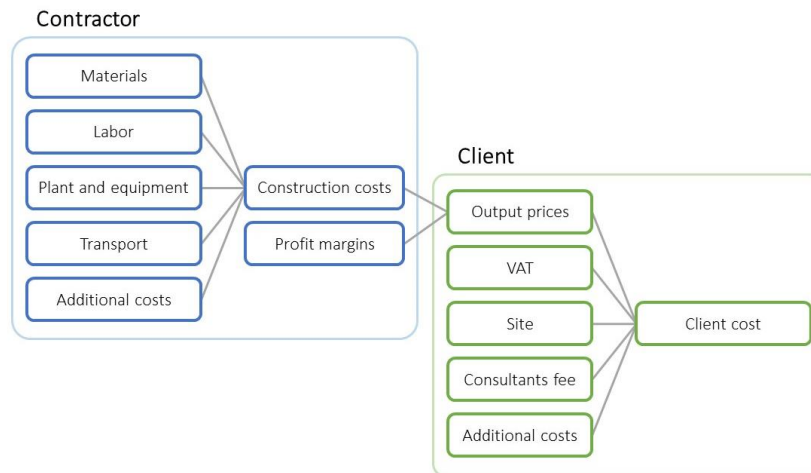
Figure 82. Construction cost index diagram

For the materials, the cost was assessed by calculating the volume of the materials used in the archive building; the prices, which include material cost, manufacturing, and profit were taken by suppliers. The price of other construction elements, for example foundation, were found on Bouwkosten Online, a Dutch database for construction costs [75]. The roofing structure, the office/technical room volume and the cladding material were not considered. Labor, plant and equipment, transport, and additional costs were taken from Bremen Bouwadviseurs [76], which created a tool that assesses a range of construction costs, according to building typology. Since the archive building typology was not included, the section "Museum" was considered. The tool divides the costs in direct, indirect, and additional. The direct costs include the building structure, installations, fixed equipment, and terrain finishing; indirect costs include construction, logistics, and land cost; additional costs include professional fees, such as engineers and architects, taxes, and other finance costs.

Results

The calculation can be found in Appendix 13.7. The cost of the building ranges from around 2,500 €/m² to 5,000 €/m².

Table 16. Cost estimation of the archive building considering different sizes

		Movable shelves			Fixed shelves
		16 vaults	8 vaults	4 vaults	
Cost (€)	High	1,734,132	1,292,951	1,075,044	1,974,070
Cost (€)	Low	907,558	670,122	550,676	1,020,778
Cost (€)	Average	1,320,845	981,537	812,860	1,497,424
Cost per m² (€/m²)	High	4,971	4,906	4,830	8,869
Cost per m² (€/m²)	Low	2,601	2,543	2,474	4,586
Cost per m² (€/m²)	Average	3,786	3,724	3,652	6,728

The costs were compared with the data found regarding the costs of the two nitrate facilities in Austria and in the UK. Both building cost 3,000 €/m²: 750,000 € the first, with a surface of 250 m², and 9 million € the second, with a surface of 3,000 m².

Since these archives were built respectively in 2010 and 2011, the increase in price needs to be considered. Figure 83 and Figure 84 show the Construction Cost Index (CCI) for both Netherlands and Austria. The values are comparable, with an increase of CCI of around 30% in both countries. The range of price to considered is therefore the range from average to high.
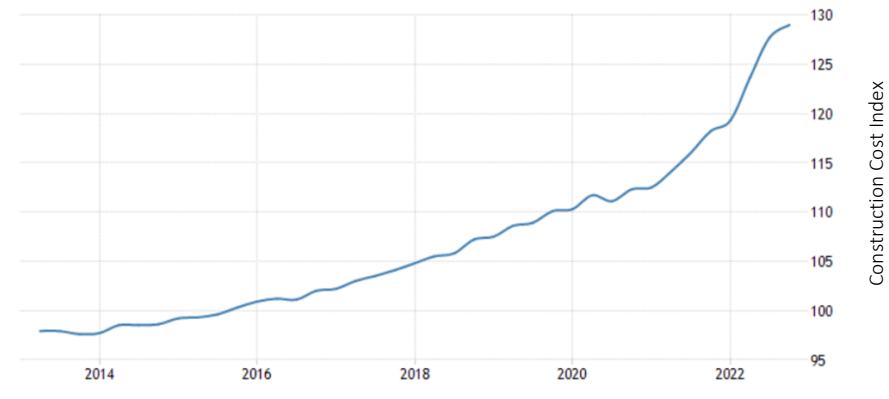
Figure 83. Construction Cost Index – Netherlands [77]
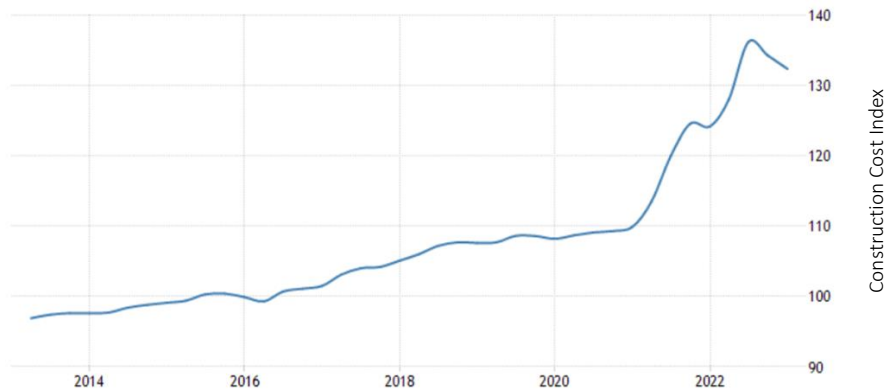
Figure 84. Construction Cost Index – Austria [78]

11 Future scenarios according to simulations

Climate change is one of the biggest global challenges of our time. Studies project that the global temperatures will keep increasing, causing a negative impact on the planet, with more and more extreme events such as heat and cold waves. This will directly affect the built environment causing higher cooling and heating loads in buildings.

The Royal Netherlands Meteorological Institute (KNMI), the Dutch national weather service, carried out a study to assess the behavior of future climate in the Netherlands, regarding temperature, precipitation, sea level and wind [79]. Four different scenarios were analyzed, which are the four combinations of two possible values for the global temperature increase, "Moderate" and "Warm", and two possible changes in the air circulation pattern, "Low value" and "High value", as Figure 85. Four future scenarios according to KNMIFigure 85 shows.

According to the research, between 1951 and 2013 the average temperature of the Netherlands increased by 1.4°C and is projected to exceed 2°C, relative to pre-industrial time, at the end of the 21st Century.

To obtain an impression of the future weather in the country, KNMI used two methods. The first one, they considered regions with similar climate; the second, they considered different months for the same climates.
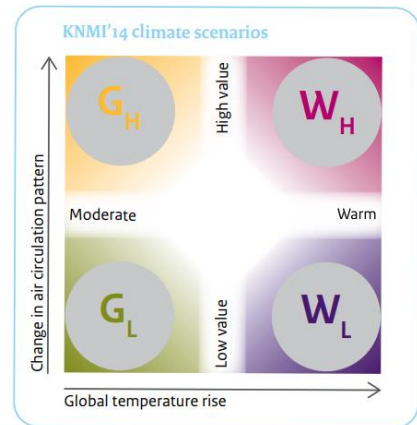
Figure 85. Four future scenarios according to KNMI

11.1 Regions with a similar climate

KNMI highlighted regions for which the present-day climate is similar to the climate of Amsterdam in 2050, according to the four different scenarios. Under the worst scenario, W_H, Amsterdam will have winters in 2050 that are similar to current winters in Nantes or Bordeaux, as depicted in Figure 86.
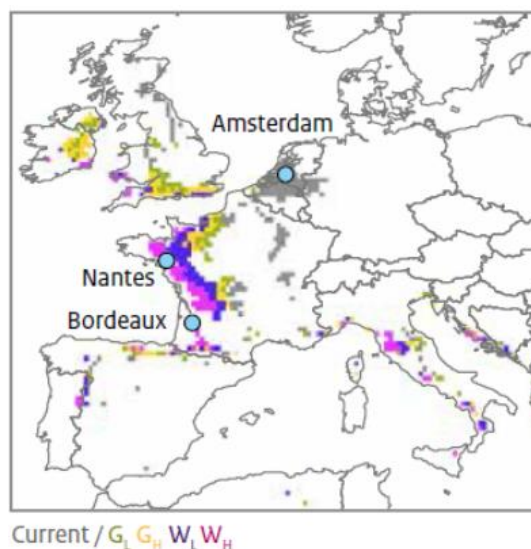

Figure 86. Regions with current winter climate similar to the winter climate of Amsterdam in 2050 under the KNMI scenarios

11.2 Similar months

The second way of addressing future weather conditions is considering neighboring calendar months. January and February in the worst scenario (W_H) around 2050 will resemble the current March month, in terms of temperature (Figure 87). Average monthly temperature of around 18°C, which in the present climate occurs in July, will happen in all three summer months, namely June, July, and August.
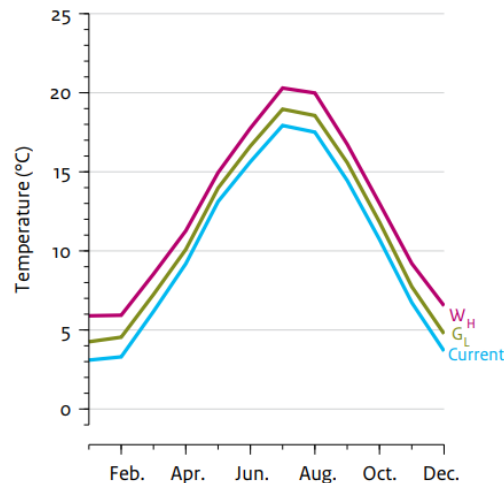

Figure 87. Seasonal cycle of temperature for the current climate and the future climate around 2050, for G_L and W_H scenarios.

11.3 Simulation results

The two methods were used to assess the impact that climate change could have on the nitrate archive in the future. The first method, which uses the warmer climate of a different city, was used for the winter months, namely December to February, while the second method, that uses neighboring months, was used for the summer months, namely June to August.

Simulations of the building archive were run for the months of December, January, and February with three different characteristics. For the first simulation the Dutch data file was used, with the original archive model. Secondly, the weather data file was changed with the one of Bordeaux, to simulate future climate predictions. Finally, the same weather data was kept, and 100 mm of extra insulation were added.

Figure 88**Error! Reference source not found.** shows the results of the simulations. Considering the predicted temperature for 2050, using the climate data from Bordeaux, the electricity load of the building increases, on average, by 10%. If 100 mm of insulation material are added, the projected results, obtained by using the climate of Bordeaux, are on average close to the current situation.
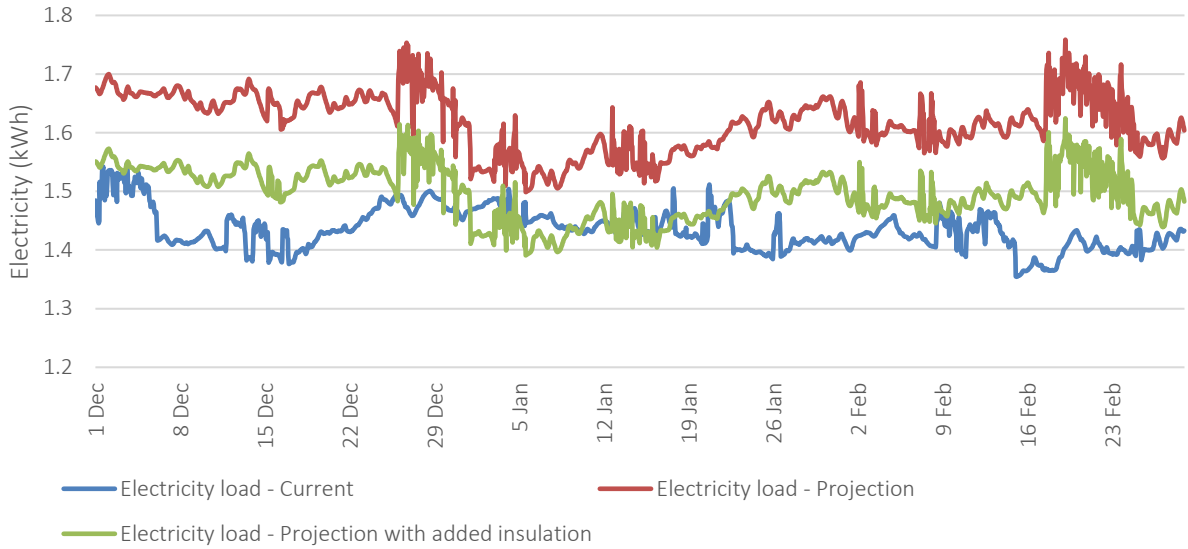
Figure 88. Comparison between electricity loads for current climate, projected climate, and projected climate with added insulation

Moreover, an hourly simulation for the summer months was run, from June until August, and the results of the cooling loads were compared with a second dataset created by using the months of July for three consecutive times, as suggested by the method from KNMI. The results are shown in
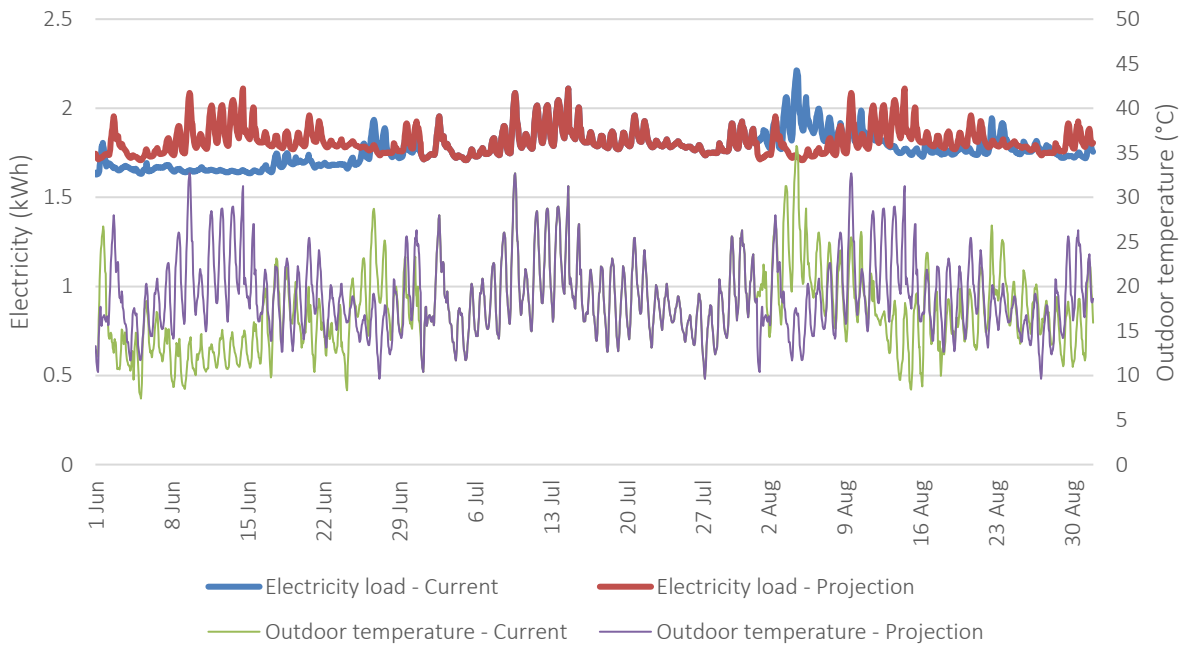

Figure 89. Despite July and August seem to have the same temperatures on average, higher temperatures are shown for June, when comparing the current data with the projected one, which bring to a highest electricity load.
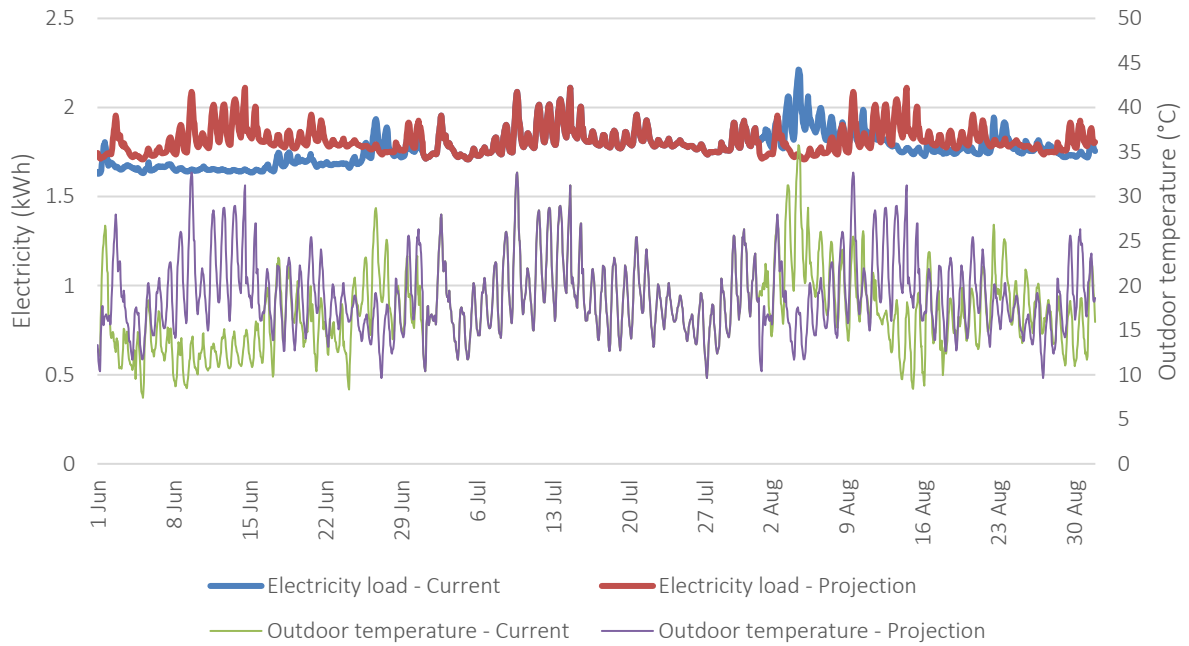
Figure 89. Comparison between current cooling loads and predicted cooling loads, for the summer months

To prevent a higher impact of the nitrate archive in the future, considering the projected increased temperature, a bigger thickness insulation could be considered, for both walls and roof.

12   Design recommendation for a safe and energy-efficient nitrate archive building

The final chapter compiles the information from the previous analysis, taking into account simulation and references, to have a final overview on suggestions for a safe archive building, for the collection and for the environment, that is energy and cost efficient.

The type of shelving chosen has a high impact on the final result of the building. By choosing the movable shelves, different sizes of vaults can be considered. By choosing the fixed shelves, that needs to be face-opened and adjacent to walls, the size of the vaults is more restrained.

For both, the starting point were the cans. There are different sizes of cans, and the most common are of diameter 36 cm and height 4 cm, as shown in Figure 90. These are the reference for the project.
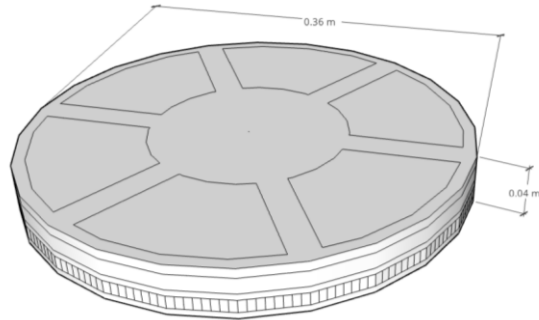
Figure 90. Left: picture of film can with reel; right: sizes of a film can

12.1 Option A

12.1.1 Three different scenarios

Three different scenarios of the same archive are designed, by dividing the collection in different numbers:

Collection is divided by 16, with each vault containing 2,500 cans. The vaults are smaller, which means that more material is used; nevertheless, in case of burning of one of the vaults, less collection will be lost.

Collection is divided by 8, with each vault 5,000 cans.

Collection is divided by 4, with each vault containing 10,000 cans. The vaults are bigger, which means that less material is used; nevertheless, in case of burning of one of the vaults, more collection will be lost.

12.1.2 Shelves size

The sizes of the shelves were designed according to the size of the cans, and the Filmarchiv Austria was taken as an example. The cans are stacked six by six, with 10 stacks per column. The cans have 1.5 cm between each other, and 4 cm were left on top of each stack, so that air can flow through and provide proper ventilation. Each shelf can contain 180 cans and they are designed to be movable, so that space can be saved.

The sizes of the vaults were designed according to the size of the shelves. By changing to the layout of the shelves, two different sizes of chambers can be created. Gaps between the walls and the shelves are considered for better ventilation: 10 cm on the side and 20 cm on the front. The corridor in the vault should be of 960 mm.
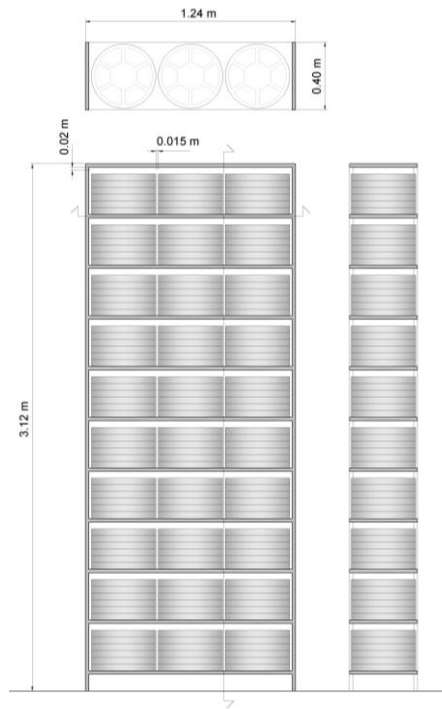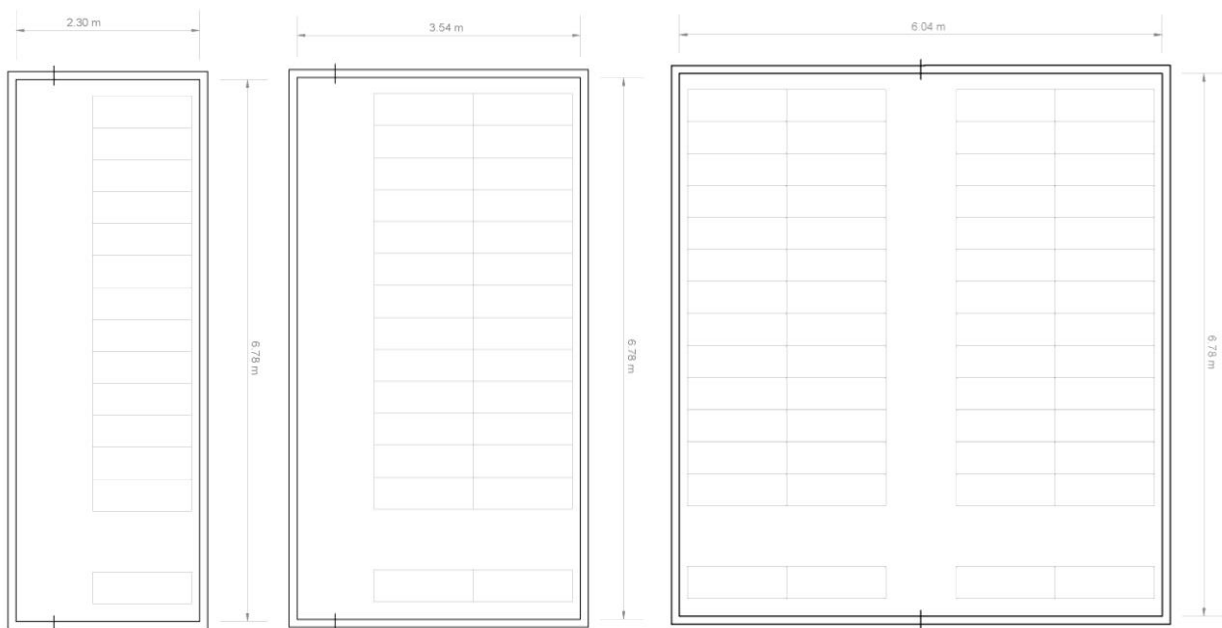
Figure 91. Sizes of shelves

Figure 92. Three vault sizes – 2,500 cans, 5,000 cans and 10,000 cans

12.1.3 Structure

The structure of the archive is made of Cross Laminated Timber walls and roof, concrete floor, and rock mineral wool insulation. The thicknesses are in Table 17.

Element	Material	Thickness [mm]
Walls	Mineral wool	200
	CLT	300
Partitions	CLT	60
	Mineral wool	100
	CLT	60
Roof	Mineral wool	250
	CLT	300
Floor	Concrete	-

WALL ROOF PARTITIONS
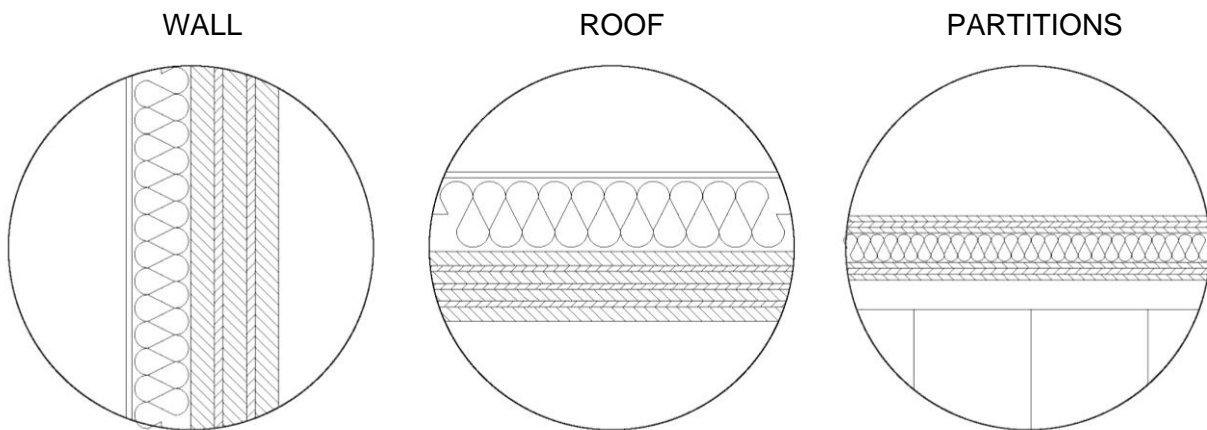
Figure 93. Composition of wall, roof, and partition

According to the simulations, the most energy-efficient shape for each scenario of the archive is shown in Figure 94. The vaults are divided in two sides and can be accessed by a central corridor. Each block is separately isolated.

The office/technical room block is placed on the south of the building, to protect the vaults from direct solar radiation. As the depot of Filmarchiv Austria and the Master Store of BFI showed, it is important for the technical room containing the HVAC system to not be in a room adjacent to the vaults. As shown in the archive in Overveen, in fact, having the technical room next to them increases the temperature, causing high cooling demand and unproper climate conditions for the collection.

Figure 94. Plans of the archive, for 16, 8 and 4 vaults
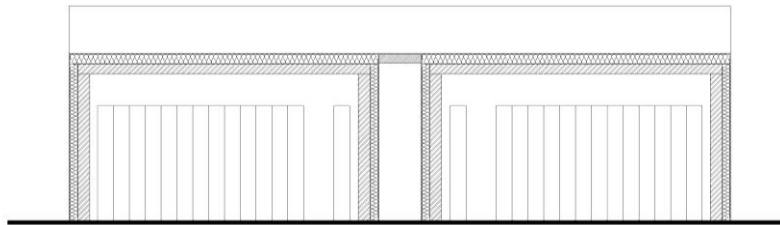
Figure 95. Section of the archive

Table 18. Dimensions of the three different vaults

	Dimensions (m)	Surface (m²)
16 vaults	16.66 x 20.94	348
8 vaults	16.66 x 15.82	263
4 vaults	16.66 x 13.30	221

12.2 Option B

12.2.1 Shelves sizes

The sizes of the shelves were designed according to NFPA 40 and the example from the Celeste Bartos Preservation Center. The cans are stacked two by two, with 30 stacks per column.

The shelves are made of steel-clad insulated material and are sealed up with a temperature-sealing material, so that if a reel burns in one cubbyhole, any adjacent cubbyhole will not reach the ignition temperature.
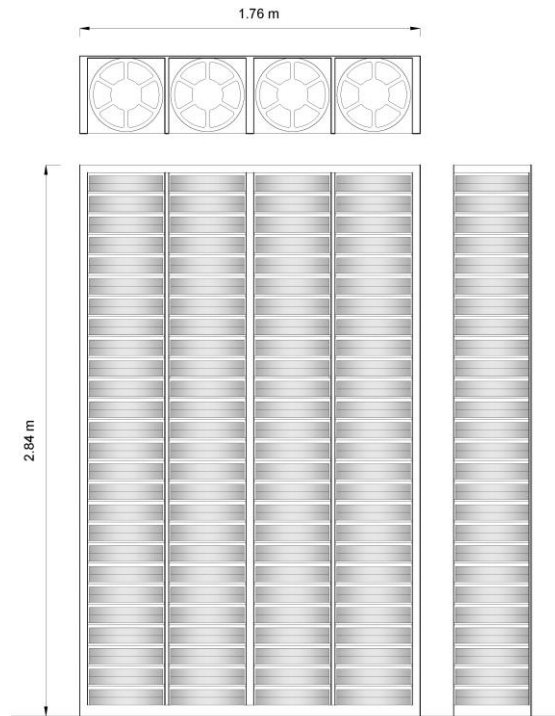
Figure 96. Size of shelf

12.2.2 Structure

The structure for option B has the same materials, but the partitions does not need rock mineral wall insulation in the partitions since, in case of fire, thanks to the shelf design and to the fire sprinklers the flames would not spread to the walls. The thicknesses are in Table 19.Table 17. Materials and thicknesses

Table 19. Materials and thicknesses

Element	Material	Thickness [mm]
Walls	Mineral wool	200
	CLT	300
Partitions	CLT	200
Roof	Mineral wool	250
	CLT	300
Floor	Concrete	-

WALL ROOF PARTITIONS
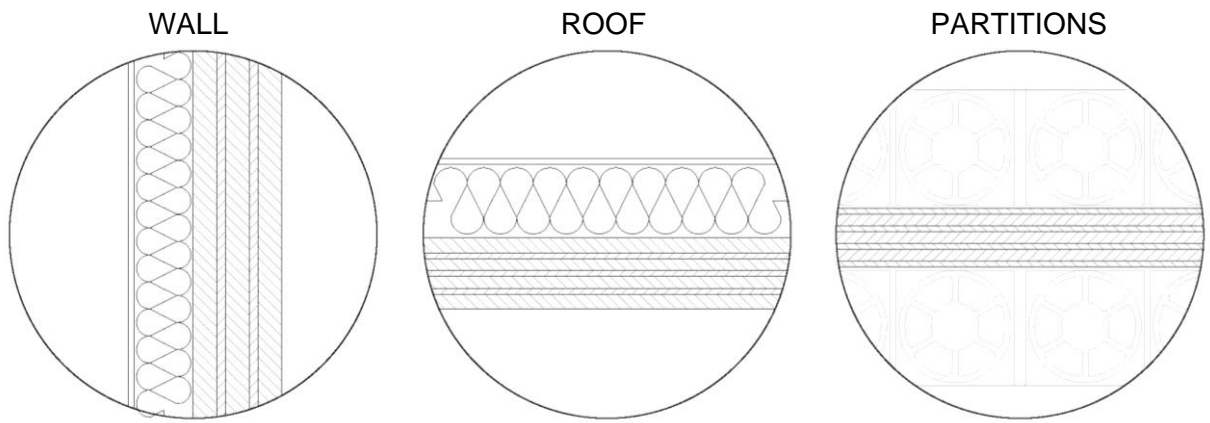
Figure 97. Composition of wall, roof, and partition
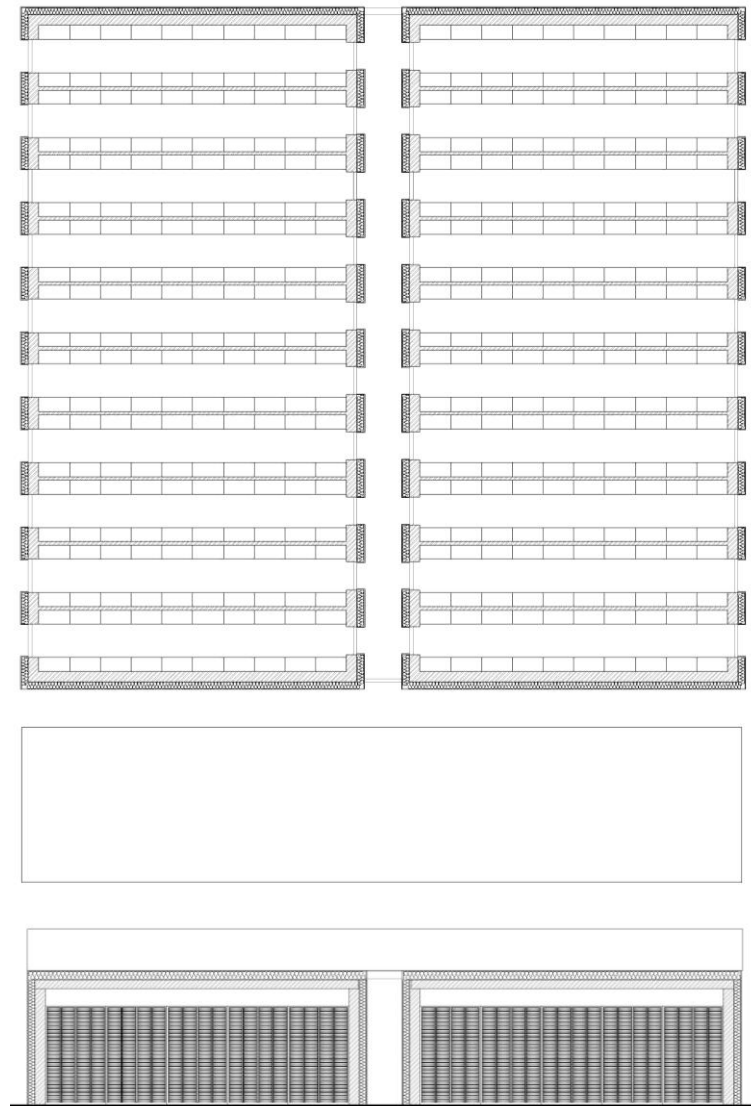
Figure 98. Plant and section

12.3 Fire design

OPTION A

Each vault is a module independent from the others. In case of fire, the explosion vents open for the built-up pressure and CLT burns. Thanks to the properties of CLT and the low thermal conductivity of rock mineral wool, the heat does not transfer to the adjacent vaults; the temperature of these remains low and the rest of the collection is safe.
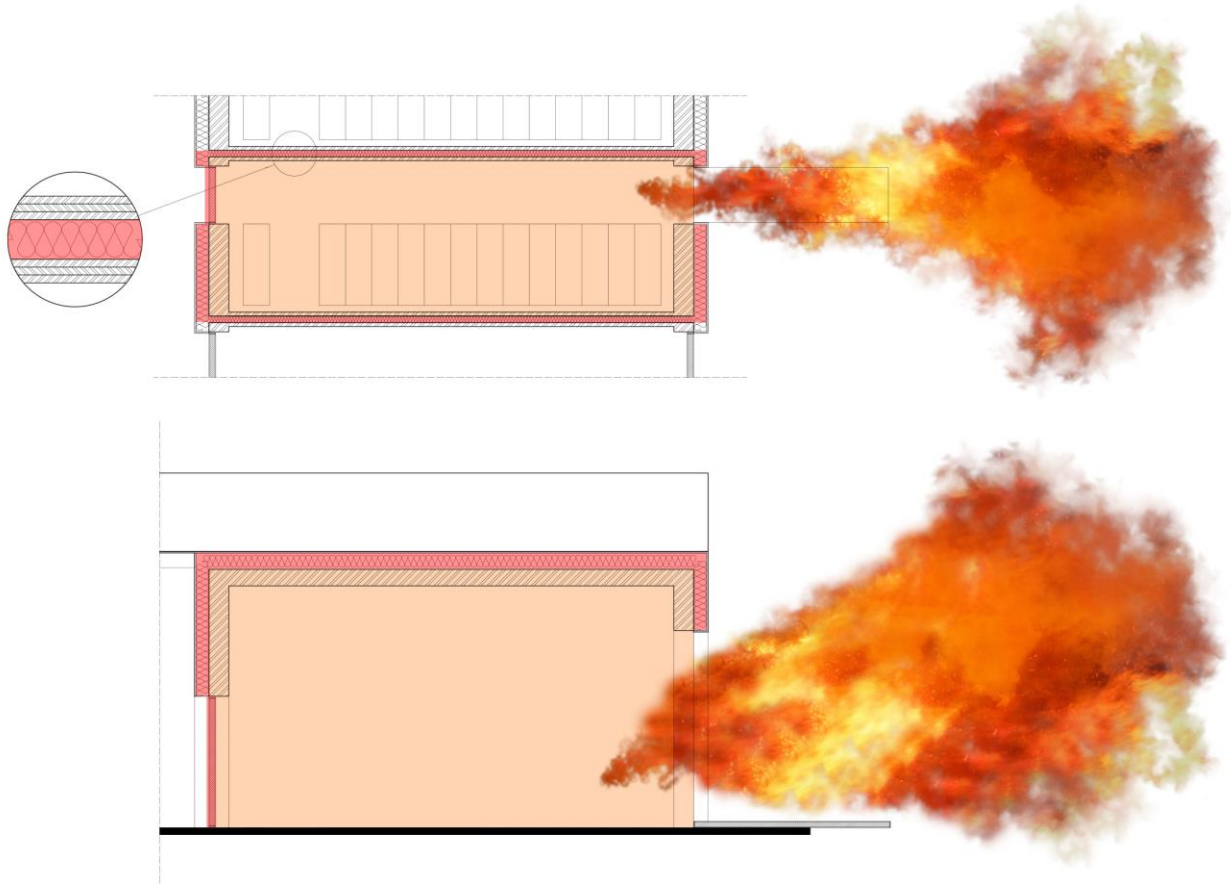

Figure 99. Plan and section of vault during fire

When exposed to fire and after an initial heating phase, timber starts a process of thermal degradation, known as pyrolysis, and it then produces combustible gasses, that results in loss of mass of timber due to evaporation and moisture migration. After this phase, a char layer is formed on the fire-exposed surface. The char layer acts as a natural insulator for the underlying timber, due to its low effective thermal conductivity, and provides thermal protection to the timber beneath the char. This results in a steep in-depth gradient in the uncharred timber and a shallow penetration depth. According to Wiesner at al. [40], thermal penetration depth is typically 25 to 35 mm at any time between 30 to 90 min during standard fire exposure. To isolate the vaults form each other and keep the CLT panels exposed toward the vaults, partitions are designed with three different layers: two CLT panels divided by an insulation layer.

To avoid the spreading of fire to adjacent vaults, in case the CLT layer might fail, each vault needs to be isolated. Thanks to its non-flammability and to its low thermal conductivity at high

temperatures, rock mineral wool is used to create compartments and avoid spread of fire and thermal transfer to the adjacent vaults.
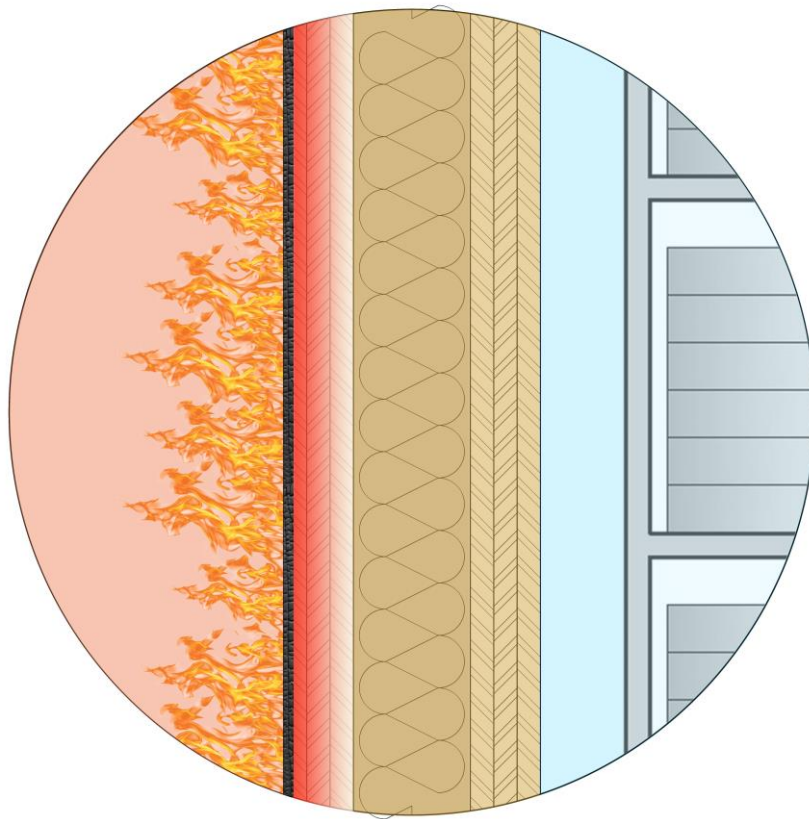
Figure 100. Partitions behavior in case of fire

OPTION B

The building is one whole structure and the partitions do not have insulation. Each vault is provided with sprinkler heads (spray-type fixed nozzles, according to NFPA 40), placed on the ceiling. In case of fire, the sprinklers would activate and flood the face of each shelf, cutting off the fire and prevent the spreading to adjacent cubbyholes.
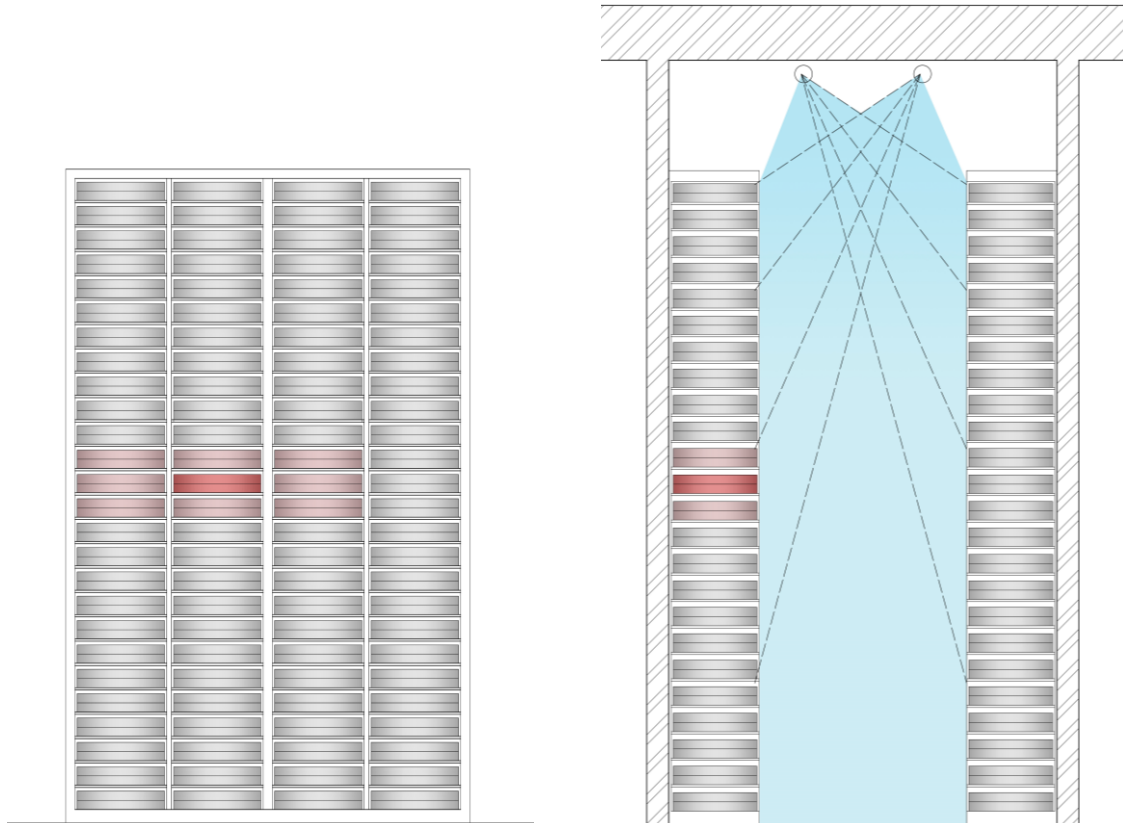
Figure 101. Shelf behavior in case of fire

12.3.1   Openings

Explosion vents needs to be considered as a pressure relief measure in case of fire in one of the vaults. The size of the vents is 0.09 m² of external wall area for each 1.4 m³ of vault volume, according to NFPA 40. When the pre-set opening pressure is exceeded, the vent opens on the three sides. The fourth side is fixed to avoid it flying away.

The door that connects the vaults and the central corridor need to be fire resistant with a protection rating of 3 hours (REI 180), according to NFPA 40. This prevents that fire spreads to the rest of the building archive through the central corridor.

Both vents and door should have a low thermal conductivity (U-value) to avoid heat loss of the building to outdoor and to the unconditioned corridor.

12.3.2 Façade

The façade cladding should be made of non-flammable material, to avoid the fire to spread from the outside to the adjacent vaults. Moreover, the design of the façade can help guiding the flames away from the building without affecting the adjacent vaults. This is showed in two examples of nitrate archive: the British Film Museum's Master Store and the Imperial War Museum's archive in Duxford, UK.

According to tests from the past, the flames that exit the explosion vent during a nitrate fire can have a span of several meters. For this reason, it is important to choose an isolated area, and that the space on the side of the vaults remains always free to avoid damages and casualties.

12.4 Cooling and dehumidification

PASSIVE COOLING

Roof structure - A second roof is placed on top of the building. This prevents solar heat gains from the ceiling and helps lowering the cooling load. According to literature and simulations, it is more effective when ventilated.

Low emissivity and reflective materials - According to literature and simulations, having a reflective and low-emissivity material can help lowering the cooling load of a building. This can be achieved with a cool roof, a conventional roof with a solar reflective material, such as liquid applied coatings, on the exterior surface. The high solar reflectance and thermal emittance of the coating helps the surface to maintain cooler temperatures, compared to conventional roofs under the same conditions. This measure is the easiest to apply since the optical properties can be controlled just by acting on the surface of the roof, generally changing the color or by using high reflective materials. Reflective materials applied to exterior building components can reflect the solar energy year-round, lowering the cooling load of buildings. A cool roof has a great potential to reduce the daily heat gain; decreasing the temperature of opaque components reduces the heat flow onto the building, leading to energy savings in air-conditioned buildings.

ACTIVE COOLING

Both heat pump and air chiller seem to be good for the archive, according to the already-built archives from the Filmarchiv Austria and British Film Institute. Moreover, both archive uses desiccant wheel as a dehumidification system, which appear to be the right solution for such low temperature and RH combined. Using the heat recovery from the cooling system, such as the chiller, can improve the efficiency of the desiccant wheel.

12.5 Ventilation

The ventilation rate can be as low as 0.042 ach, which means that the air in each vault is changed once per day. This allows lower dehumidification and cooling load but is still enough to maintain a safe environment for the collection. For better performance, the outlet should be located near the ceiling and the exhaust near the floor on the opposite wall. The nitrous gases are heavier than air and, evaporating from the decomposing film, accumulate on the floor, where are cleaned by the ventilation system. A CFD simulations could help assessing the optimal position of the vents.

12.6 Infiltration rate

Air tightness of a building structure is an important property that has a big impact on the building's indoor climate, atmosphere, and energy. The infiltration rate should be of a passive house, preferably around 0.06 ach. This prevents heat from entering the building and keeps the cooling loads low.

Initial moisture content in the CLT panels weakens the airtightness of the external wall. 5-layer CLT panel can be considered and used as an air-tight layer in external wall construction as long as its initial low moisture content, about 13%, is maintained during both construction and service life.

12.7 Electricity demand

According to the simulations, three different scenarios (16 vaults, 8 vaults and 4 vaults) can be covered by the electricity production of 40, 35 and 32 PV panels that have a capacity of 12.5kW, 11kW and 9.5 kW, respectively. These were coupled with different battery sizes 30 kWh, 25 kWh and 20 kWh, which give good results as a trade-off between self-consumed energy, yearly electricity bought from the grid and payback period. For each example, the PVs can fit on the flat roof of the archive without causing shelf-shading.

In the following table and graphs, the options of PV system with and without batteries are shown.

Table 20. Option for PVs number and battery size for each scenario

		Battery size (kWh)	Self-consumption (kWh)	Electricity from grid (kWh)	Payback period (years)	Earnings after 25 years	Initial investment (€)
16 vaults	**40 panels**	0	4635	9314	7	24053	12400
		30	9314	4635	17	13499	30400
8 vaults	**35 panels**	0	4038	8103	7	20710	10850
		25	8103	4038	17	11692	26350
4 vaults	**32 panels**	0	3627	7204	7	18631	9920
		20	7171	3660	17	11301	22920
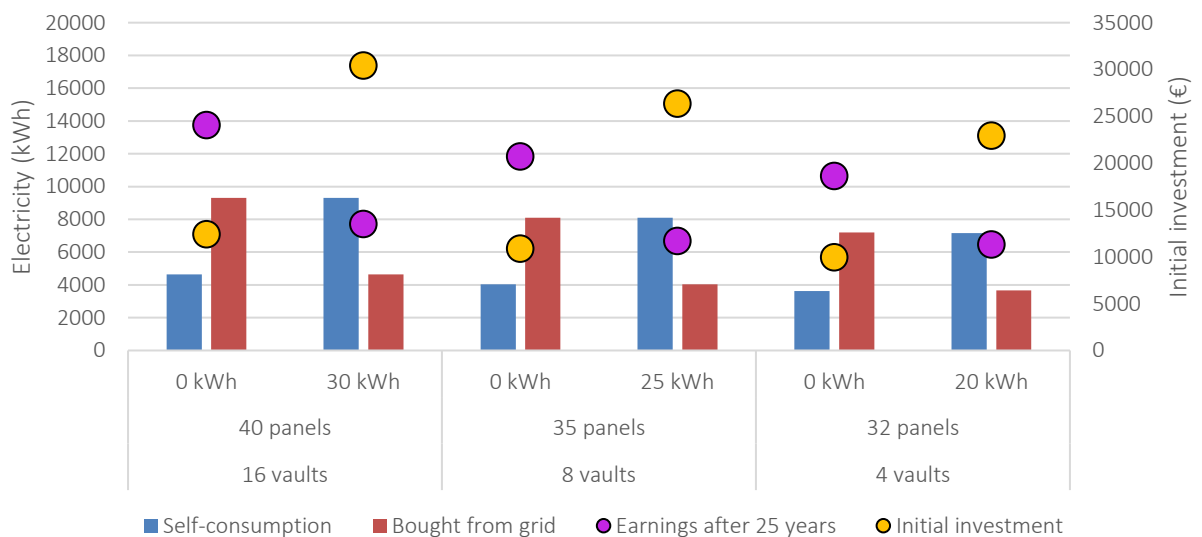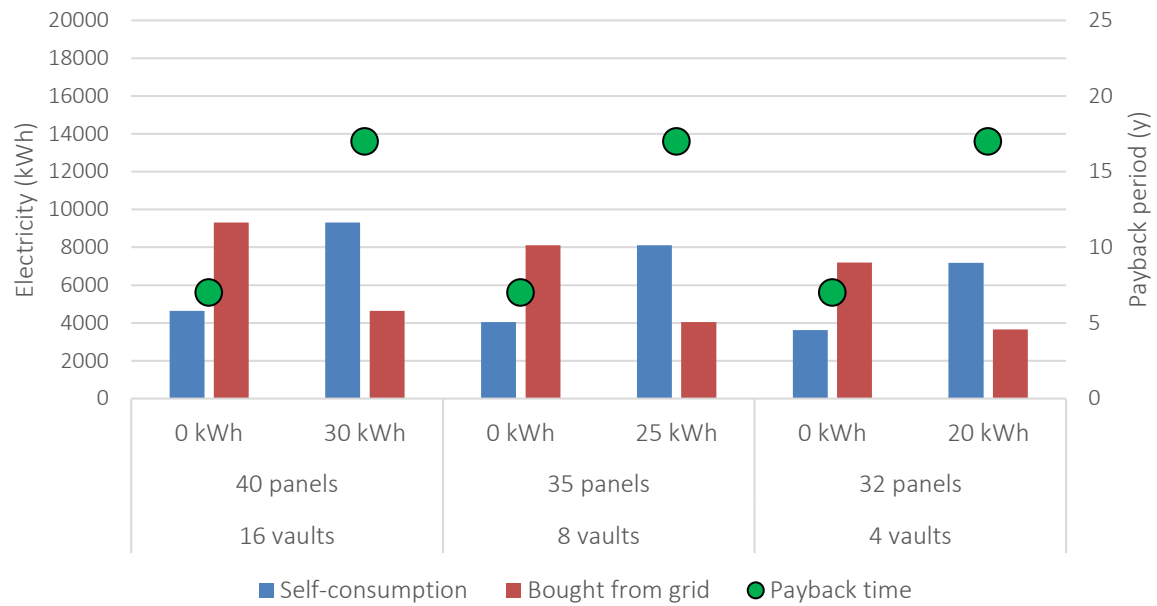
The system with PVs without battery has shorter payback, lower initial investment, and higher earning after 25 years, which is the assumed lifespan of the system.

Nevertheless, when batteries are connected to the PV system, the self-consumption of electricity doubles and, consequently, the electricity that needs to be imported from the grid halves. This has a high impact on the monthly electricity bill.

As shown in the report, adding more PV panels and bigger batteries is possible, to have higher amount of self-produced electricity to sell to the grid and get higher earnings. Nevertheless, this requires a higher initial investment and brings to longer payback period.

These calculations were done with the current electricity price provided by the Eye Filmmuseum (0.18 €/kWh). Considering the current energy crisis and the increase of prices, the results might change. Moreover, the calculations do not include subsidies that the Dutch governments offers.

12.7.1 Emergency battery

The behavior of the building was analyzed in case of a blackout during the warmest period of the year; the outside temperature has a range between 12°C at night and 27°C during the day. According to the simulation, if the HVAC system would stop working, the temperature of the vault would increase steadily, but for more than two weeks it would stay within the safe threshold of 15°C. On the other hand, RH increases very rapidly, and reached 100% in around 24 hours. By implementing a safety battery, which always remains completely full and connects only in case of emergency, the collection could remain safe for a longer period. Given the difference between seasons, two blackout times were analyzed for the project, one happening in winter and one happening in summer.

Table 21. Option for PVs number and battery size for each scenario

		Battery size (kWh)	Emergency battery size (kWh)	Safe hours in summer	Safe hours in winter
16 vaults	**40 panels**	0	20	29	26
		0	30	57	32
		30	20	75	35
		30	30	98	42
8 vaults	**35 panels**	0	20	29	26
		0	30	57	33
		25	20	71	35
		25	30	77	42
4 vaults	**32 panels**	0	20	29	26
		0	30	54	32
		20	20	69	35
		20	30	75	42

The addition of emergency batteries was analyzed for all three scenarios. Two different cases were considered: a building with PVs but no batteries, and a building with PVs and batteries, as shown in Figure 102. The results show that all the combinations give more than 1 full day (24 hours) of safety in case of blackout. The scenarios where batteries are already implemented in the system give better results, especially in the summer, compared with a building with only PVs.
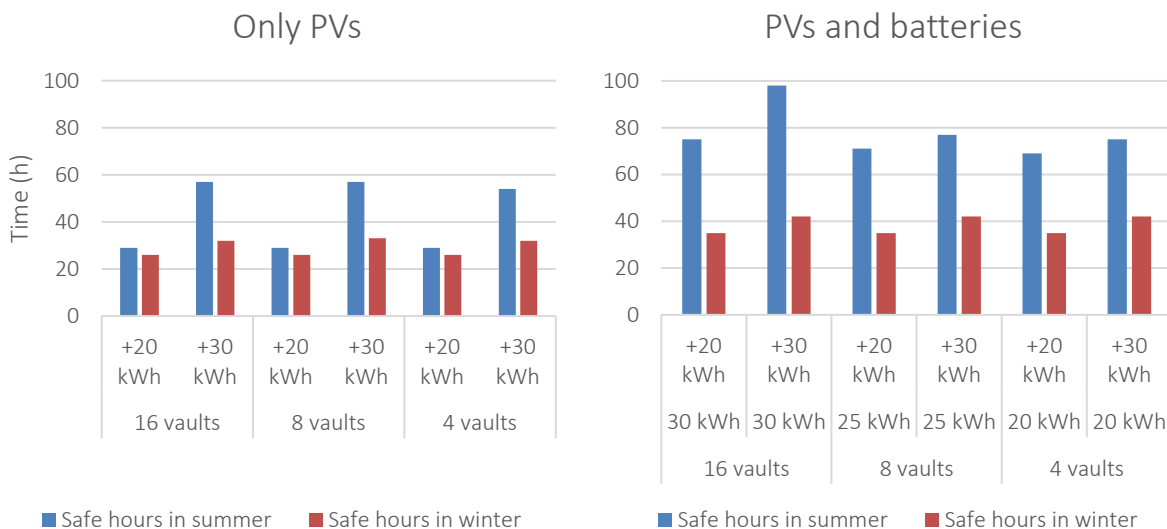
Figure 102. Hours in which the building can run, by implementing the emergency battery during blackout; Left: building with only PVs; Right: building with PVs and fixed batteries

12.7.2 Thermal Energy Storage

Thermal Energy Storage systems (TES) help conserving energy in thermal reservoirs for later usage. The cool energy is stored in form of ice. Ice slurry can be considered as a Phase Change Material (PCM) that acts as a secondary building coolant. The main purpose of using ice slurry is to take advantage of the stored cooling energy in the ice particles when they melt, the so-called latent heat. Using ice slurry coolants in HVAC systems can provide more efficient cooling with substantially lower operational and equipment costs. Ice slurry has been recognized for its significant potential to improve cooling capacity because of its high energy storage density. Ice slurry can be used in the design of the archive to act as a secondary coolant. During the day, once the electricity demand is fully covered by the electricity production of the PVs, the electricity surplus can be used to produce ice slurry which is store in tanks. During the nights the ice slurry melts, and the cooling capacity can be used to cover the cooling load.
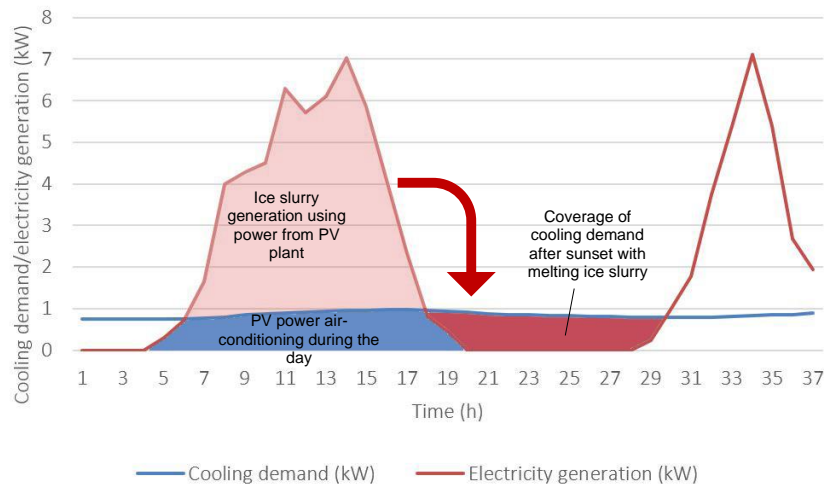
The analysis for feasibility of an ice slurry system is only a preliminary study. More research needs to be done concerning charging and discharging cycles and its time, and cost effectiveness.

12.8 Future scenario

According to researchers, the temperature in the future will increase due to climate change. This will deeply affect the built environment and the electricity demand of buildings.

To prevent the impact of climate change on the archive building, a solution is to add more insulation during design phase. Simulations show that increasing the thickness by 100 mm while using a climate file with projected temperature for 2050, the results for cooling demand are similar to using a current data file and less insulation.

Bibliography

[1] National Park Service, "Appendix M: Management of Cellulose Nitrate and Cellulose Ester Film," p. 39, 1999.

[2] Eastman Kodak Company, "Storage & Handling of Processed Nitrate Film," *Kodak*. https://www.kodak.com/en/motion/page/storage-and-handling-of-processed-nitrate-film/ (accessed Jan. 02, 2023).

[3] Wikipedia, "File:Decomposing Nitrate Film," May 01, 2007. https://commons.wikimedia.org/wiki/File:Decomposing_Nitrate_Film.jpg (accessed Feb. 09, 2023).

[4] N. S. Allen, M. Edge, C. V. Rorie, T. S. Jewitt, and J. H. Appleyard, "The Degradation and Stabilization of Historic Cellulose Acetate/Nitrate Base Motion-picture Film," *The Journal of Photographic Science*, vol. 36, no. 3, pp. 103–106, May 1988, doi: 10.1080/00223638.1988.11736978.

[5] "National Fire Protection Association," *Wikipedia*. Oct. 04, 2022. Accessed: Jan. 02, 2023. [Online]. Available: https://en.wikipedia.org/w/index.php?title=National_Fire_Protection_Association&oldid=1114045245

[6] "1937 Fox vault fire," *Wikipedia*. Nov. 12, 2022. Accessed: Jan. 02, 2023. [Online]. Available: https://en.wikipedia.org/w/index.php?title=1937_Fox_vault_fire&oldid=1121472897

[7] S. Magazine and J. Daley, "Forty Years Ago, 12.6 Million Feet of History Went Up in Smoke," *Smithsonian Magazine*. https://www.smithsonianmag.com/smart-news/forty-years-ago-126-million-feet-history-went-smoke-180970977/ (accessed Jan. 02, 2023).

[8] NFPA - National Fire Protection Association, "International." https://www.nfpa.org/international (accessed Jan. 02, 2023).

[9] International Organization of Standardization, "ISO 10356:1996," *ISO*. https://www.iso.org/standard/18413.html (accessed Jan. 02, 2023).

[10] National Fire Protection Association, *NFPA® 40: standard for the storage and handling of cellulose nitrate film.* 2019.

[11] International Federation of Film Archives, "Journal of Film Preservation - Vol. 99 - 10.2018. The Wooden Vault. A Unique Approach to Nitrate Film Storage at Filmarchiv Austria." https://www.fiafnet.org/pages/Publications/International-Index-Film-Periodicals.html (accessed Jan. 03, 2023).

[12] "BFI Master Film Store | Ongreening." https://ongreening.com/en/Projects/bfi-master-film-store-1110#sustainability (accessed Jan. 03, 2023).

[13] "BFI Master Film Store by Edward Cullinan | Dezeen." https://www.dezeen.com/2011/09/12/bfi-master-film-store-by-edward-cullinan/ (accessed Jan. 03, 2023).

[14] "BFI Acetate & Nitrate Film Stores / Edward Cullinan Architects | ArchDaily." https://www.archdaily.com/166262/bfi-acetate-nitrate-film-stores-edward-cullinan-architects (accessed Jan. 03, 2023).

[15] "BFI's new £12m film storage facility to preserve Britain's reel history | Film | The Guardian." https://www.theguardian.com/film/2011/aug/29/bfi-new-film-storage-facility (accessed Jan. 03, 2023).

[16] P. K. Larsen, M. Ryhl-Svendsen, L. A. Jensen, B. Bøhm, and T. Padfield, "Ten years experience of energy efficient climate control in archives and museum stores," p. 13.

[17] R. Harris, "Cross laminated timber," in *Wood Composites*, Elsevier, 2015, pp. 141–167. doi: 10.1016/B978-1-78242-454-3.00008-1.

[18] M. Dewsbury, *Mass-timber as thermal mass*. 2016.

[19] V. Kukk, A. Bella, J. Kers, and T. Kalamees, "Airtightness of cross-laminated timber envelopes: Influence of moisture content, indoor humidity, orientation, and assembly," *Journal of Building Engineering*, vol. 44, p. 102610, Dec. 2021, doi: 10.1016/j.jobe.2021.102610.

[20] "Cross-laminated timber (CLT) - Wood products | Stora Enso." https://www.storaenso.com/en/products/mass-timber-construction/building-products/clt (accessed Jan. 23, 2023).

[21] KLH Massivholz GmbH, "Cross Laminated Timber - KLH Massivholz GmbH," *KLH Massivholz GmbH*. https://www.klh.at/it/ (accessed Jan. 23, 2023).

[22] M. A. Kamal, "An Overview of Passive Cooling Techniques in Buildings: Design Concepts and Architectural Interventions," *Civil Engineering*, vol. 55, no. 1, p. 15, 2012.

[23] European Standards, "EN 13501-1+A1 - Fire classification of construction products and building elements - Part 1: Classification using test data from reaction to fire," *https://www.en-standard.eu*. https://www.en-standard.eu/ilnas-en-13501-1-a1-fire-classification-of-construction-products-and-building-elements-part-1-classification-using-test-data-from-reaction-to-fire-tests-1/ (accessed Jan. 23, 2023).

[24] knauf insulation, "Safer Fire Resistant Insulation | Knauf Insulation." https://www.knaufinsulation.co.uk/homeowners-hub/fire-protection (accessed Jan. 29, 2023).

[25] ROCKWOOL, "Euroclass System of Products Fire Classification." https://www.rockwool.com/uk/resources-and-tools/building-regulations/fire-regulations/euroclasses/ (accessed Jan. 29, 2023).

[26] P. van den Engel, "Passive buildings – KLIMAPEDIA." https://klimapedia.nl/module/passive-buildings/ (accessed Feb. 13, 2023).

[27] A. van den Dobbelsteen, E. van den Ham, T. Blom, and K. Leemeijer, "1.1.1 Introduction to Zero-Energy Design," *TU Delft OCW*. https://ocw.tudelft.nl/course-lectures/1-1-1-introduction-to-zero-energy-design/ (accessed Feb. 13, 2023).

[28] D. K. Bhamare, M. K. Rathod, and J. Banerjee, "Passive cooling techniques for building and their applicability in different climatic zones—The state of art," p. 24, 2019.

[29] I. Oropeza-Perez and P. A. Østergaard, "Active and passive cooling methods for dwellings: A review," *Renewable and Sustainable Energy Reviews*, vol. 82, pp. 531–544, Feb. 2018, doi: 10.1016/j.rser.2017.09.059.

[30] N. Gupta and G. N. Tiwari, "Review of passive heating/cooling systems of buildings," *Energy Sci Eng*, vol. 4, no. 5, pp. 305–333, Oct. 2016, doi: 10.1002/ese3.129.

[31] A. Almusaed and A. Almss, "Improvement of Thermal Insulation by Environmental Means," in *Effective Thermal Insulation - The Operative Factor of a Passive Building Model*, A. Almusaed, Ed. InTech, 2012. doi: 10.5772/35744.

[32] I. Hernández-Pérez, G. Álvarez, J. Xamán, I. Zavala-Guillén, J. Arce, and E. Simá, "Thermal performance of reflective materials applied to exterior building components—A review," *Energy and Buildings*, vol. 80, pp. 81–105, Sep. 2014, doi: 10.1016/j.enbuild.2014.05.008.

[33] J. Pillai, "DEHUMIDIFICATION STRATEGIES AND THEIR APPLICABILITY BASED ON CLIMATE AND BUILDING TYPOLOGY," p. 8, 2018.

[34] P. di Milano, "Desiccant dehumidification and cooling," p. 7.

[35] Image Permanence Institute, "IPI's Guide to Sustainable Preservation Practices for Managing Storage Environments." https://store.imagepermanenceinstitute.org/sustainable-preservation-practices-guidebook (accessed Jan. 23, 2023).

[36] "Performance of the bio-based materials," in *Performance of Bio-based Building Materials*, Elsevier, 2017, pp. 249–333. doi: 10.1016/B978-0-08-100982-6.00005-7.

[37] A. Frangi, M. Fontana, E. Hugi, and R. Jübstl, "Experimental analysis of cross-laminated timber panels in fire," *Fire Safety Journal*, vol. 44, no. 8, pp. 1078–1087, Nov. 2009, doi: 10.1016/j.firesaf.2009.07.007.

[38] B. A.-L. Östman, "Fire performance of wood products and timber structures," *International Wood Products Journal*, vol. 8, no. 2, pp. 74–79, Apr. 2017, doi: 10.1080/20426445.2017.1320851.

[39] S. A. Lineham, D. Thomson, A. I. Bartlett, L. A. Bisby, and R. M. Hadden, "Structural response of fire-exposed cross-laminated timber beams under sustained loads," *Fire Safety Journal*, vol. 85, pp. 23–34, Oct. 2016, doi: 10.1016/j.firesaf.2016.08.002.

[40] F. Wiesner *et al.*, "Structural capacity in fire of laminated timber elements in compartments with exposed timber surfaces," *Engineering Structures*, vol. 179, pp. 284–295, Jan. 2019, doi: 10.1016/j.engstruct.2018.10.084.

[41] S. van der Westhuyzen, R. Walls, and N. de Koker, "Fire tests of South African cross-laminated timber wall panels: fire ratings, charring rates, and delamination," *J. S. Afr. Inst. Civ. Eng.*, vol. 62, no. 1, 2020, doi: 10.17159/2309-8775/2020/v62n1a4.

[42] A. Frangi, "Natural Full-Scale Fire Test on a 3 Storey XLam Timber Building," 2008.

[43] EingineeringToolbox, "Calcium Silicate Insulation." https://www.engineeringtoolbox.com/calcium-silicate-insulation-k-values-d_1171.html (accessed Jan. 25, 2023).

[44] EingineeringToolbox, "Mineral Wool Insulation." https://www.engineeringtoolbox.com/mineral-wool-insulation-k-values-d_815.html (accessed Jan. 25, 2023).

[45] D. Izydorczyk, B. Sędłak, B. Papis, and P. Turkowski, "Doors with Specific Fire Resistance Class," *Procedia Engineering*, vol. 172, pp. 417–425, 2017, doi: 10.1016/j.proeng.2017.02.010.

[46] DFM Europe, "Steel fire resistant doors and non fire resistant doors," *DFM Europe | Fire Resistant Doors & Sliding Gates*. https://www.dfm-europe.eu/products/steel-fire-resistant-doors-and-non-fire-resistant-doors/ (accessed Jan. 25, 2023).

[47] B. van Aken, A. Binani, K. Cesar, and K. Cesar, "Towards nature inclusive east-west orientated solar parks".

[48] I. Dincer and D. Erdemir, "Heat Storage Methods," in *Heat Storage Systems for Buildings*, Elsevier, 2021, pp. 37–90. doi: 10.1016/B978-0-12-823572-0.00010-2.

[49] Y. H. Yau and B. Rismanchi, "A review on cool thermal storage technologies and operating strategies," *Renewable and Sustainable Energy Reviews*, vol. 16, no. 1, pp. 787–797, Jan. 2012, doi: 10.1016/j.rser.2011.09.004.

[50] C. Hägg, "Ice Slurry as Secondary Fluid in Refrigeration Systems. Fundamentals and Applications in Supermarkets".

[51] G.F. Hundy, A.R. Trott, and T.C. Welch, "Chapter 12 - Distributed Cooling and Heating," *Refrigeration, Air Conditioning and Heat Pumps (Fifth Edition)*, pp. 199–207, 2016, doi: 10.1016/B978-0-08-100647-4.00012-7.

[52] M. Kauffeld, M. J. Wang, V. Goldstein, and K. E. Kasza, "Ice slurry applications," *International Journal of Refrigeration*, vol. 33, no. 8, pp. 1491–1505, Dec. 2010, doi: 10.1016/j.ijrefrig.2010.07.018.

[53] X. Liu, Y. Li, K. Zhuang, R. Fu, S. Lin, and X. Li, "Performance Study and Efficiency Improvement of Ice Slurry Production by Scraped-Surface Method," *Applied Sciences*, vol. 9, no. 1, p. 74, Dec. 2018, doi: 10.3390/app9010074.

[54] Business.gov.nl, "Make your company more sustainable with solar energy," *business.gov.nl*. https://business.gov.nl/running-your-business/environmental-impact/energy/make-your-company-more-sustainable-with-solar-energy/ (accessed Jan. 29, 2023).

[55] zonnenfabriek, "Changes in the net metering law postponed until 2025 - Zonnefabriek." https://www.zonnefabriek.nl/en/news/changes-in-the-net-metering-law-postponed-until-2025/ (accessed Jan. 29, 2023).

[56] "Thuisbatterij prijs: € 4.000 à 10.000 [Update 2023]," *Thuisbatterij-expert.nl*. https://www.thuisbatterij-expert.nl/prijs (accessed Jan. 17, 2023).

[57] M. A. Curran, "Life Cycle Assessment," in *Kirk-Othmer Encyclopedia of Chemical Technology*, John Wiley & Sons, Ltd, 2016, pp. 1–28. doi: 10.1002/0471238961.lifeguin.a01.pub2.

[58] I. Muralikrishna and V. Manickam, "Life Cycle Assessment," 2017, pp. 57–75. doi: 10.1016/B978-0-12-811989-1.00005-1.

[59] M. D. Bovea, V. Ibáñez-Forés, and I. Agustí-Juan, "Environmental product declaration (EPD) labelling of construction and building materials," in *Eco-efficient Construction and Building Materials*, Elsevier, 2014, pp. 125–150. doi: 10.1533/9780857097729.1.125.

[60] "EN 15804 - EPD," *Ecomatters - Sustainability*. https://www.ecomatters.nl/services/lca-epd/environmental-product-declaration/en-15804/ (accessed Jan. 26, 2023).

[61] Z.M. Harris, S. Milner, and G. Taylor, "Chapter 5 - Biogenic Carbon—Capture and Sequestration | Elsevier Enhanced Reader." https://reader.elsevier.com/reader/sd/pii/B9780081010365000057?token=5B7688B705841E8E43CAB29BE7ACB178F170204A46B11CD5B4EDBD30A63FB782540E55C3D5A71859070FFA462B9E86C6&originRegion=eu-west-1&originCreation=20230130101652 (accessed Jan. 30, 2023).

[62] "Biogenic Carbon," *One Click LCA Help Centre*, Nov. 08, 2022. https://oneclicklca.zendesk.com/hc/en-us/articles/360015036640-Biogenic-Carbon (accessed Jan. 30, 2023).

[63] Storaenso, *Storaenso - Environmental Product Declaration*. Accessed: Jan. 26, 2023. [Online]. Available: https://www.storaenso.com

[64] Bundesministerium für Wohnen Stadtentwicklung und Bauwesen, "ÖKOBAUDAT - Sustainable Construction Information Portal." https://www.oekobaudat.de/en.html (accessed Jan. 26, 2023).

[65] Thomas Betonbauteile, "EPD beton - Thomas Betonbauteile," *thomas gruppe*. https://www.thomas-gruppe.de/betonbauteile/ (accessed Jan. 26, 2023).

[66] EGGER More From Wood, "EPD - EGGER." https://www.egger.com/nl/?country=NL (accessed Jan. 26, 2023).

[67] Sonae Arauco, "EPD - AGEPAN OSB 3 Ecoboard," *Sonae Arauco*. https://www.sonaearauco.com/enagepan-system/agepan-osb-3-ecoboard_1724.html (accessed Jan. 26, 2023).

[68] ROCKWOOL, "ROCKWOOL stone wool insulation." https://www.rockwool.com/group/ (accessed Jan. 26, 2023).

[69] S. Hamels *et al.*, "The use of primary energy factors and CO2 intensities for electricity in the European context - A systematic methodological review and critical evaluation of the contemporary literature," *Renewable and Sustainable Energy Reviews*, vol. 146, p. 111182, Aug. 2021, doi: 10.1016/j.rser.2021.111182.

[70] "Netherlands: power sector carbon intensity 2000-2021," *Statista*. https://www.statista.com/statistics/1290441/carbon-intensity-power-sector-netherlands/ (accessed Jan. 17, 2023).

[71] A. Müller, L. Friedrich, C. Reichel, S. Herceg, M. Mittag, and D. H. Neuhaus, "A comparative life cycle assessment of silicon PV modules: Impact of module design, manufacturing location and inventory," *Solar Energy Materials and Solar Cells*, vol. 230, p. 111277, Sep. 2021, doi: 10.1016/j.solmat.2021.111277.

[72] Ministerie van Algemene, "Central government encourages sustainable energy - Renewable energy - Government.nl," Jul. 26, 2017. https://www.government.nl/topics/renewable-energy/central-government-encourages-sustainable-energy (accessed Jan. 17, 2023).

[73] "Live 24/7 CO_2 emissions of electricity consumption." http://electricitymap.tmrow.co (accessed Feb. 06, 2023).

[74] Eurostat, "Construction producer price and construction cost indices overview." https://ec.europa.eu/eurostat/statistics-explained/index.php?title=Construction_producer_price_and_construction_cost_indices_overview (accessed Feb. 12, 2023).

[75] Bouwkosten Online, "Archidat richtprijzen voor de bouw." https://bouwkosten.bouwformatie.nl/?gclid=CjwKCAiAxP2eBhBiEiwA5puhNZf6agvWjfU3duriqbQiwuB5kncXl3XbjpuFr8YOZiB8lmpITcJ9sBoC_EAQAvD_BwE (accessed Feb. 15, 2023).

[76] Bremen Bouwadviseur, "Cost indicators for construction, installation and operation," Jun. 01, 2022. https://bremenba.nl/kostenkengetallen/ (accessed Feb. 13, 2023).

[77] TradingEconomics, "Netherlands - Construction cost index - 2000-2022 Historical." https://tradingeconomics.com/netherlands/construction-cost-idx-eurostat-data.html (accessed Feb. 13, 2023).

[78] TradingEconomics, "Austria - Construction cost index - 1990-2022 Historical." https://tradingeconomics.com/austria/construction-cost-idx-eurostat-data.html (accessed Feb. 13, 2023).

[79] Koninklijk Nederlands Meteorologisch Instituut, "Climate scenarios - KNMI Projects," Jan. 28, 2020. https://www.knmiprojects.nl/projects/climate-scenarios (accessed Feb. 07, 2023).

[80] H. and T. S. HTflux, "HTflux - Heat transfer resistance." https://www.htflux.com/en/documentation/boundary-conditions/surface-resistance-heat-transfer-coefficient/ (accessed Jan. 23, 2023).

13   Appendices

13.1 Climatic conditions of the vaults of the archive in Overveen
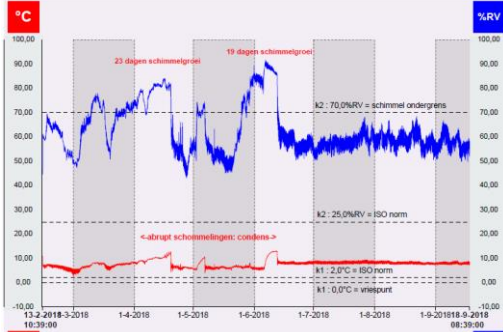
Figure 103. Temperature and RH in vault 1
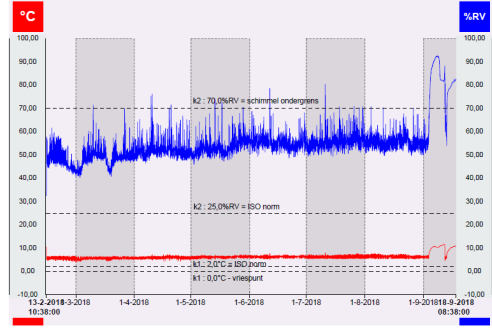
Figure 104. Temperature and RH is vault 2
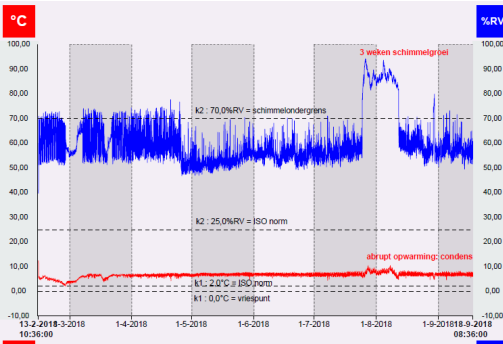
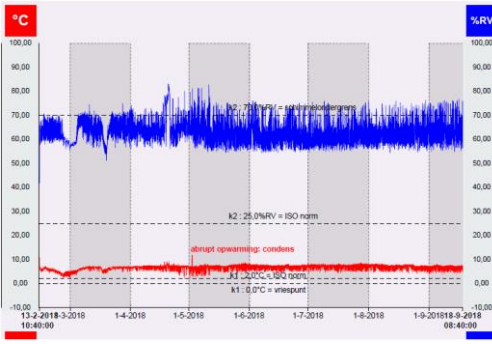*Figure 105. Temperature and RH in vault 3*

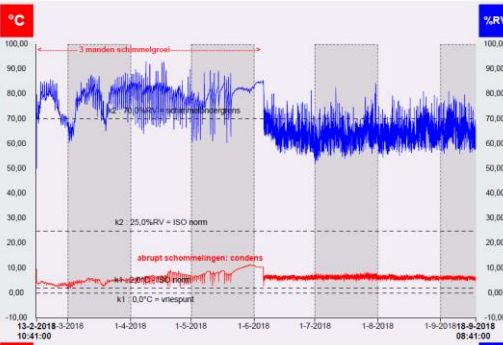*Figure 106. Temperature and RH in vault 4*
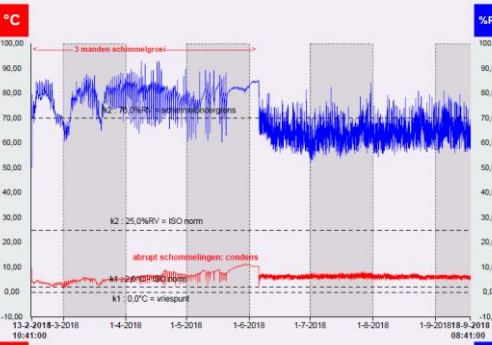

Figure 107. Temperature and RH in vault 5

Figure 108. Temperature and RH in vault 6

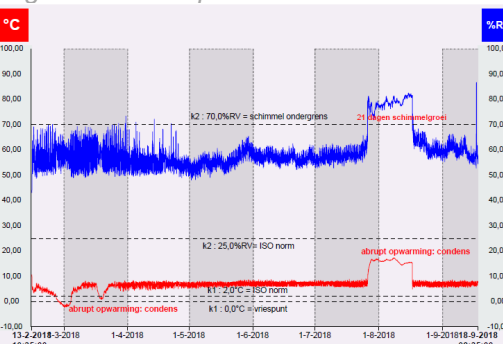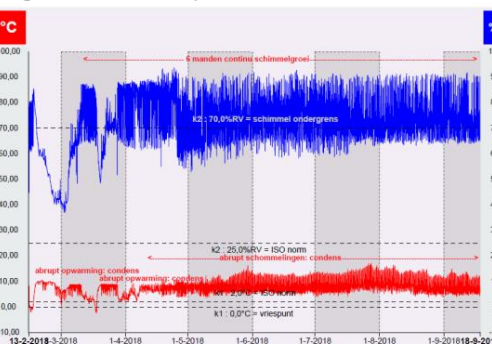*Figure 109. Temperature and RH in vault 7*

Figure 110. Temperature and RH in vault 8

13.2 Overview of nitrate vault in the world

Name	Number of cans	Cans on shelves	Cans division/vault	Fire system	Sustainable features	Notes
Det Danske Filminstitut	24 000					Underground, old bunker
British Film Institute	460 000*	Stacked 6 by 6	30 vaults (6000 cans each)	Early detection and warning system	Ventilation + heat recovery, innovative cooling system, shading system, Highly efficient façade, sustainable urban drainage system, green roof, no light pollution	*Has both nitrate and acetate cans
Imperial War Museum	100 000		11 storage units			
National film and sound archive Australia	15 000	Individual space for each can	Different vaults. Each vault contains 1000 to 2000 cans			
Austria Film Archive	70 000	Stacked 6 by 6	3 different chambers		Massive timber, passive cooling (cladding)	
Library and Archives Canada	5575		22 vaults		Green roof, well-insulated walls (lower energy consumption),	Also photographs (600 000)
George Eastman	27 000	Stacked 2 by 2	12 vaults (2184 cans each)			
New Zealand Film Archive		Stacked 8 by 8	One vault			
Library of Congress Packard Campus	145 000	Stacked 2 by 2	124 vaults	Water sprinkler system	Green roof - filters runoff pollution and conserves water	*It was a Cold War bunker. **It's part of a bigger building
MOMAT	1152	Individual space, in cabinets	3 rooms			There are 3 different archives, the nitrate collection is in Archive III
Swedish Film Institute			20 compartments		The roof is clad with a light-toned metal roofing materials, so the heat build-up in the roof space will be limited.	1500 kg for compartment. Pressure relief "chimneys". Walls and roofs are made entirely of non-combustible materials
UCLA Library	150 000	Stacked 6 by 6	120 vaults			
Celeste Bartos Film Preservation Center	70 000	Individual space (cubbyhole)	34 vaults (2x1000, 1x2000)	each vault has 16 sprinkler heads overhead, that would completely flood the face of the cabinets further cooling them and cutting them off		

Name	Country	Year	Material	Size (m2)	Temperature (°C)	Relative Humidity (%)	Air exchange	HVAC system
Det Danske Filminstitut	Denmark	2007		1160	-5	30		Air-cooled chiller with water recirculation Dehumidification: desiccant wheel
British Film Institute	UK	2011	Concrete	3000	-5	35		
Imperial War Museum	UK	2009	Concrete	1285				
National film and sound archive Australia	Australia		Concrete					
Austria Film Archive	Austria	2010	Timber		0-2	35	Every 24 hours	Heat pump with 4 counter current air flow. Dehumidification: desiccant wheel containing silica crystals
Library and Archives Canada	Canada		Concrete		< -2	20-30		
George Eastman	USA		Concrete		40 °F (4.44°C)	30	Every 20 minutes	
New Zealand Film Archive	New Zealand	2014		100	15	40		
Library of Congress Packard Campus	USA	1969*	Concrete	5510**	39 °F (3.88°C)	30		
MOMAT	Japan		Concrete	45	2 +/-2	35 +/-5		
Swedish Film Institute	Sweden	2006	Concrete		-5 +/-2	22.5 +/-2.5		
UCLA Library	USA	2007	Concrete		33 °F (0.55°C)	32		
Celeste Bartos Film Preservation Center	USA	1996	Concrete		35 °F (1.66°C)			

13.3 Design

13.3.1 Thicknesses

WALL

| Insulation | | CLT | | | | | | | | |
Thermal conduct. [W(m*K)]	Thickn. [m]	Thermal conduct. [W(m*K)]	Thickn. [m]	Rsi [(m²K)/W]	R ins. [(m²K)/W]	R CLT [(m²K)/W]	Rse [(m²K)/W]	Total R [(m²K)/W]	Total thickn. [m]	U-value [W/(m*K)]
0,035	0,15	0,11	0,30	0,13	4,29	2,73	0,04	7,2	0,45	0,139
0,035	0,20	0,11	0,30	0,13	5,71	2,73	0,04	8,6	0,50	0,116
0,035	0,25	0,11	0,30	0,13	7,14	2,73	0,04	10,0	0,55	0,100
0,035	0,30	0,11	0,30	0,13	8,57	2,73	0,04	11,5	0,60	0,087
0,035	0,35	0,11	0,30	0,13	10,00	2,73	0,04	12,9	0,65	0,078
0,035	0,40	0,11	0,30	0,13	11,43	2,73	0,04	14,3	0,70	0,070

*Rsi and Rse are respectively internal and external surface resistances [80]

ROOF

| Insulation | | CLT | | | | | | | | |
Thermal conduct. [W(m*K)]	Thickn. [m]	Thermal conduct. [W(m*K)]	Thickn. [m]	Rsi [(m²K)/W]	R ins. [(m²K)/W]	R CLT [(m²K)/W]	Rse [(m²K)/W]	Total R [(m²K)/W]	Total thickn. [m]	U-value [W/(m*K)]
0,035	0,20	0,11	0,24	0,10	5,71	2,18	0,04	8,04	0,44	0,124
0,035	0,25	0,11	0,24	0,10	7,14	2,18	0,04	9,46	0,49	0,106
0,035	0,30	0,11	0,24	0,10	8,57	2,18	0,04	10,89	0,54	0,092
0,035	0,35	0,11	0,24	0,10	10,00	2,18	0,04	12,32	0,59	0,081
0,035	0,40	0,11	0,24	0,10	11,43	2,18	0,04	13,75	0,64	0,073
0,035	0,45	0,11	0,24	0,10	12,86	2,18	0,04	15,18	0,69	0,066

*Rsi and Rse are respectively internal and external surface resistances [80]
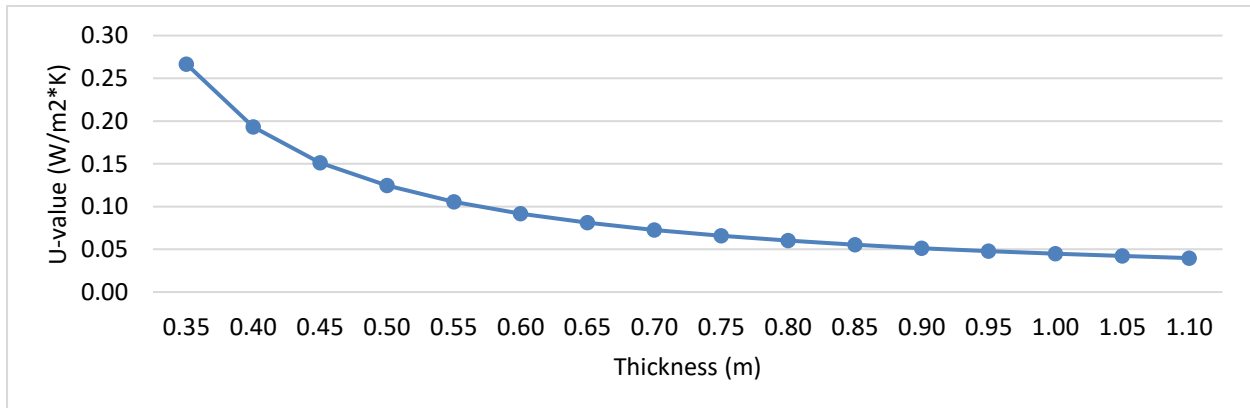
13.4 Fire Safety

13.4.1 Fire classification

Classification French Standard NF		Classification European Standard Euroclasses: NF EN 13501-1					
		FIRE CLASSIFICATION STANDARDS		s = smoke : Smoke production		d = drop : Chute de gouttes et de débris	
-	-	A1	Incombustible	-	-	-	-
M0	Non-combustible materials	A2	Virtually Incombustible	S1	Low smoke production	D0	No flaming droplets or particles
M1	Non-flammable combustible materials	A2	Virtually Incombustible	S1	Low smoke production	D1	Droplets or flaming particles persisting for less than 10 seconds
		A2		S2	Average production of smoke	D0	No flaming droplets or particles
		A2		S3	Significant smoke production	D1	Droplets or flaming particles persisting for less than 10 seconds
		B	Resists prolonged attack by flames or an isolated object while limiting the spread of the flame	S1	Low smoke production	D0	No flaming droplets or particles
				S2	Average production of smoke	D1	Droplets or flaming particles persisting for less than 10 seconds
				S3	Significant smoke production		
M2	Flammable materials with low flammability	C	Withstands a brief attack of flames or a single fiery object while limiting the spread of the flame	S1	Low smoke production	D0	No flaming droplets or particles
				S2	Average production of smoke	D1	Droplets or flaming particles persisting for less than 10 seconds
				S3	Significant smoke production		
M3	Medium flammable combustible materials	D	Withstands a brief attack of small flames while limiting the spread of flame and an isolated arden object	S1	Low smoke production	D0	No flaming droplets or particles
M4 (not dripping)	Combustible materials Highly flammable	D	Resists a brief attack of small flames while limiting the spread of the flame and a fiery isolated object	S2	Average production of smoke	D1	Droplets or flaming particles persisting for less than 10 seconds
		D		S3	Significant smoke production		
M4	Combustible materials Highly flammable	E	Resists a small flaming attack by limiting the spread of the flame			D2	Droplets or flaming particles persisting for more than 10 seconds
		F	No performance determined				

13.4.2 Results IWM fire test

CELL 2 – CANS TEMPERATURES	CELL 2 – WALL TEMPERATURES
Figure 111. Can temperature in cell 2	*Figure 112. Walls temperature in cell 2*
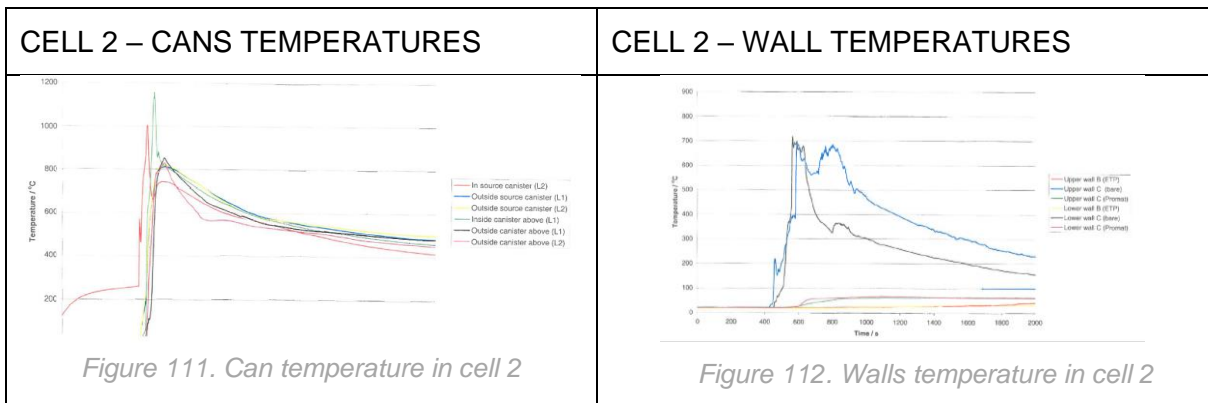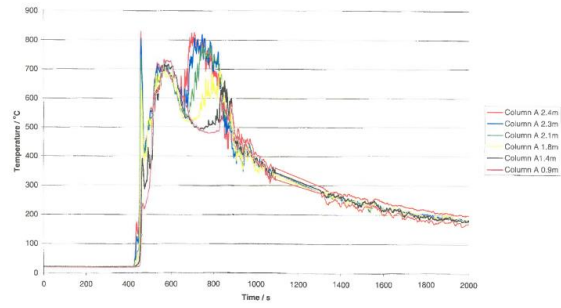
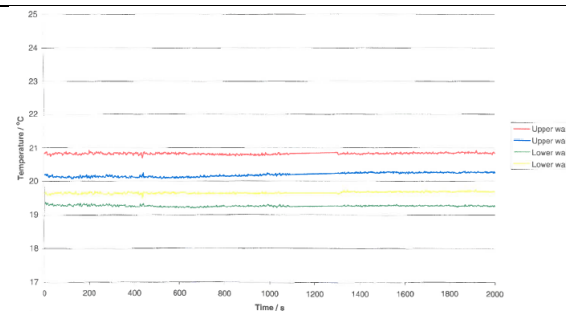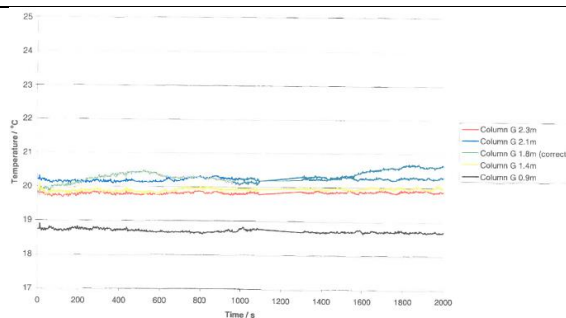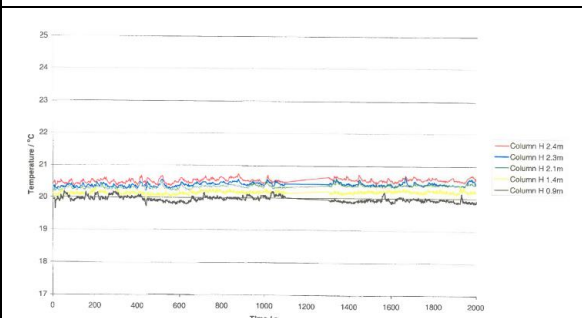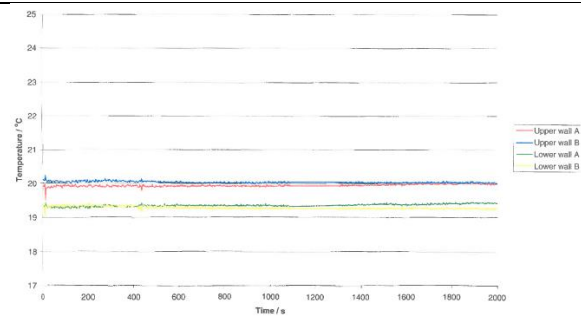| CELL 2 – THERMOCOUPLES COLUMNS	
 Figure 113. Temperature according to thermocouple column - Cell 2 Column A	 *Figure 114. Temperature according to thermocouple column – Cell 2 Column B*
 Figure 115. Temperature according to thermocouple column – Cell 2 Column C	 *Figure 116. Temperature according to thermocouple column – Cell 2 Column D*
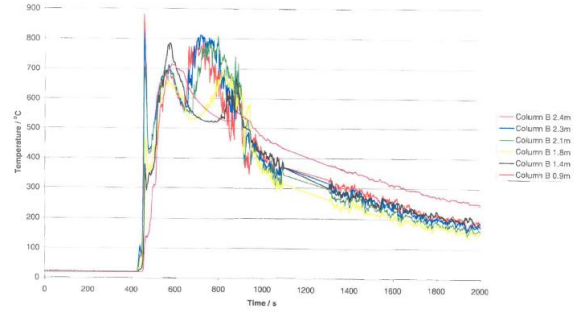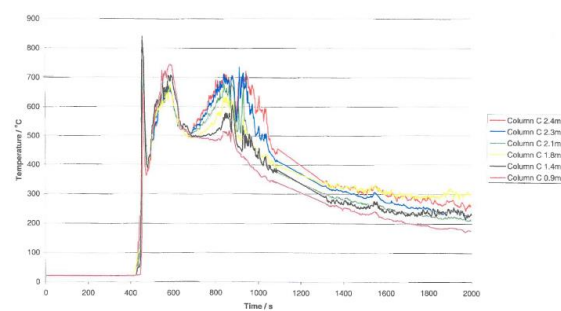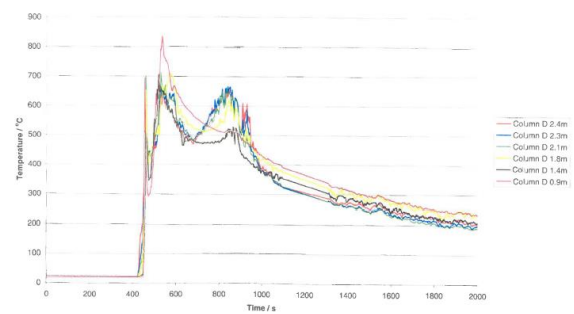
CELL 1 AND 3 - CANS
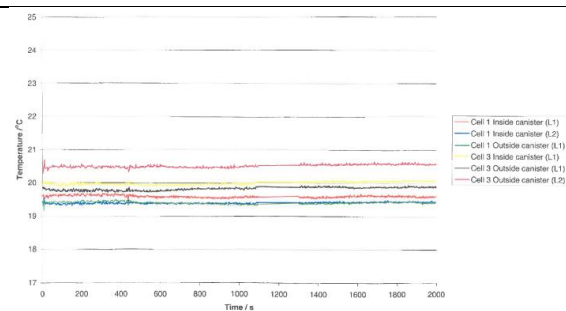
Figure 117. Adjoining cells can temperature

CELL 3 – THERMOCOUPLES COLUMNS	
 Figure 118. Temperature according to thermocouple column – Cell 1 Column E	 *Figure 119. Temperature according to thermocouple column – Cell 1 Column F*
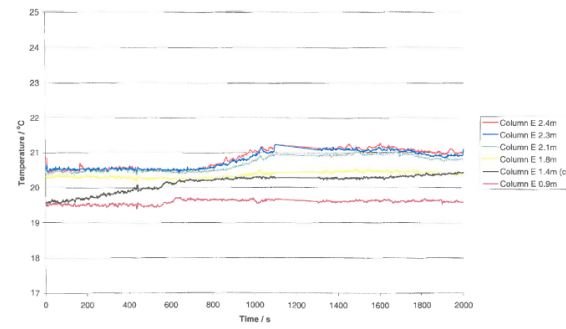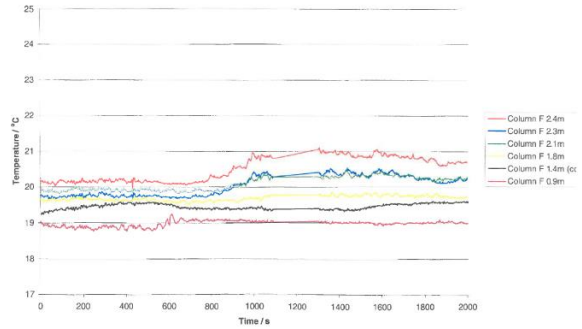
CELL 3 - WALL	
 Figure 120. Temperature according to thermocouple column – Cell 3 walls	

CELL 1 – THERMOCOUPLES COLUMNS	
 Figure 121. Temperature according to thermocouple column – Cell 1 Column G	 *Figure 122. Temperature according to thermocouple column – Cell 1 Column H*

CELL 1 - WALL

Figure 123. Temperature according to thermocouple column – Cell 1 wall

CORRIDOR – THERMOCOUPLES COLUMNS	
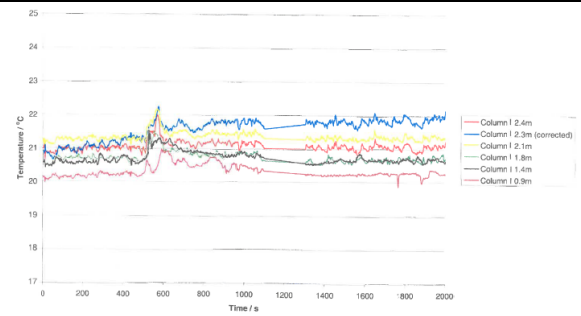
Figure 124. Temperature according to thermocouple column – Corridor Column I
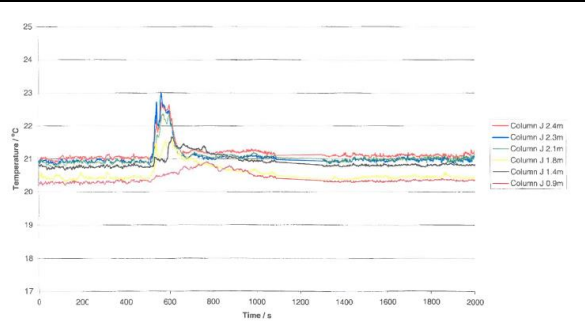
Figure 125. Temperature according to thermocouple column – Corridor Column J

13.4.3   Calculation heat transfer

Surface temperature formula: $T_{se} = \frac{T_e}{R_{tot}}(T_i - T_e)$

Where:

- T_{se} = surface temperature
- T_e = external temperature
- T_i = Internal temperature
- R_{tot} = Total resistance

Resistance formula: Thickness/conductivity
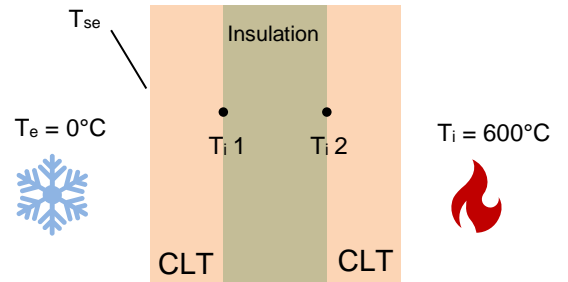
	Temperature [°C]
T_{sc} (T surface vault)	?
T_e (T vault)	0
T_i (T fire room)	600

CLT				Calcium silicate				CLT			
Thickn. [m]	Conduct. [W/(m*K)]	Resist. [(m*K)/W]	T_i 1 [°C]	Thickn. [m]	Conduct. [W/(m*K)]	Resist. [(m*K)/W]	T_i 2 [°C]	Thickn. [m]	Conduct. [W/(m*K)]	Resist. [(m*K)/W]	T_{sc} [°C]
0.06	0.11	0.55	115	0.10	0.143	0.70	18	0.06	0.12	0.50	4

	Temperature [°C]
T_{sc} (T surface vault)	?
T_e (T vault)	0
T_i (T fire room)	600

CLT				Rock mineral wool				CLT			
Thickn. [m]	Conduct. [W/(m*K)]	Resist. [(m*K)/W]	T_i 1 [°C]	Thickn. [m]	Conduct. [W/(m*K)]	Resist. [(m*K)/W]	T_i 2 [°C]	Thickn. [m]	Conduct. [W/(m*K)]	Resist. [(m*K)/W]	T_{sc} [°C]
0.06	0.11	0.55	115	0.10	0.205	0.49	24	0.06	0.12	0.50	5

CLT				Rock mineral wool				CLT			
Thickn. [m]	Conduct. [W/(m*K)]	Resist. [(m*K)/W]	T_i 1 [°C]	Thickn. [m]	Conduct. [W/(m*K)]	Resist. [(m*K)/W]	T_i 2 [°C]	Thickn. [m]	Conduct. [W/(m*K)]	Resist. [(m*K)/W]	T_{sc} [°C]
0.06	0.11	0.55	115	0.05	0.205	0.24	40	0.06	0.12	0.50	8

13.5 Electricity supply

13.5.1 PV panels data sheet

Technische datasheet
Vision 60 M style

◯ SOLARWATT ®

PRODUCT

high power PERC zonnecellen

Vision 60 M style

Glas-glas zonnepaneel

Strak design met de hoogste opbrengsten

Dankzij jarenlange ervaring, toepassing van de beste componenten en een volautomatisch productieproces, leveren de Solarwatt glas-glas modules de hoogste opbrengst op lange termijn. Onze visie op kwaliteit resulteert in robuuste en zeer weerbare zonnepanelen.

De krachtige PERC-zonnecellen zijn in het glas-glascomposiet ingebed en daardoor vrijwel onverwoestbaar, dus optimaal beschermd tegen alle weersinvloeden en mechanische belasting. Solarwatt kan daarom 30 jaar garantie bieden op prestaties en productkwaliteit.

De Solarwatt Volledige Dekking verzekering is gratis en inbegrepen voor 5 jaar. De verzekering biedt een topdekking tegen onvoorziene situaties. Ook een verminderde opbrengst door een defect of tegenvallende prestaties vallen onder de verzekering. De verzekering is tegen een aantrekkelijk tarief te verlengen naar 10 jaar.

CE ◇ ▣ ♡ **BBA**

PRODUCTEIGENSCHAPPEN

- ammoniakbestendig
- zoutnevelbestendig
- bestand tegen extreme hagelbuien
- brandveiligheidsklasse A (conf. IEC 61730)
- LeTID gecertificeerd
- 100 % plussortering
- 100 % PID-bescherming
- optioneel: niet-schittering

MADE IN GERMANY · **SINCE 1993**

100% GROENE ENERGIE · IN DE FABRIEK EN DE KANTOREN

Aan deze informatie kunnen geen ontleend.
Technische wijzigingen voorbehouden.
AZ-TDB-PMS-1109 | Dit informatieblad voldoet aan eisen
IEC 61215-1-1 | REV 026 | 05/2021 | NL

SOLARWATT SERVICE

Volledige Dekking Verzekering
Inbegrepen (tot 1000 kWp*).

Service uit Nederland
Directe en snelle serviceafhandeling door onze Nederlandstalige serviceafdeling.

30 jaar productgarantie
Volgens „speciale garantievoorwaarden voor Solarwatt zonnepanelen van de glas-glas-generatie".

30 jaar vermogensgarantie
Op 87 % van het nominale vermogen volgens „speciale garantievoorwaarden voor Solarwatt zonnepanelen van de glas-glas-generatie".

* Er zijn landspecifieke verschillen van toepassing.

Solarwatt BV | Het Eek 7 | 4004 LM TIEL | Nederland
T +31-344-767-002 | info.benelux@solarwatt.com | solarwatt.nl

Solarwatt GmbH | Maria-Reiche-Str. 2a | 01109 Dresden | Germany
DIN EN ISO 9001, 14001, 45001, 50001

Technische datasheet
Vision 60M style

SOLARWATT®

AFMETINGEN
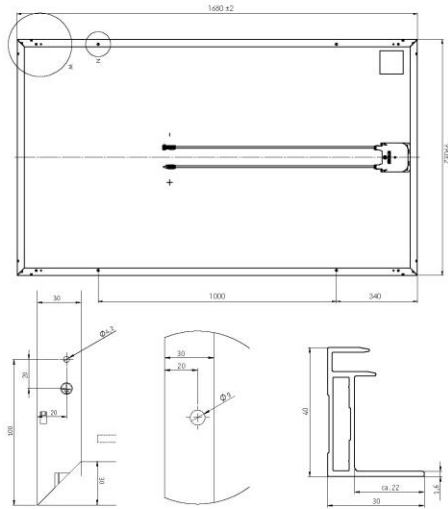
Potentiaalvereffening   Detail montagegat   Frameprofiel

Kwalificaties	IEC 61215 (incl. LeTID) | IEC 61730 | IEC 61701 | IEC 62804 | IEC 62716 | MCS 005

ALGEMENE GEGEVENS

Moduletechnologie	Glas-glas laminaat; zwart aluminium frame
Dekmateriaal	Gehard zonneglas met anti-reflecterende coating, 2 mm
Inkapseling	Zonnecellen in polymeerinkapseling, transparant
Materiaal achterzijde	Gehard zonneglas, 2 mm
Transparant oppervlak	ca. 9,8 %
Zonnecellen	60 monokristallijne PERC hoogrendementscellen
Afmetingen van de cellen	157 x 157 mm
L x B x D / Gewicht	$1.680^{\pm 2}$ x $990^{\pm 2}$ x $40^{\pm 0,3}$ mm / ong. 22,8 kg
Aansluittechniek	Kabel 2 x 1,1 m / 4 mm² Stäubli Electrical MC4-connectors
Bypass-dioden	3
Max. systeemspanning	1.000 V
IP klasse	IP67
Toepassingsklasse	II (conform IEC 61140)
Brandklasse	A (conform IEC 61730/UL 790), E (conform EN 13501-1), B_{ROOF} (t1) (conform EN 13501-5)
Mechanische belastingen volgens IEC 61215	Trekbelasting tot 2.400 Pa (testbelasting 3.600 Pa) Drukbelasting tot 5.400 Pa (testbelasting 8.100 Pa)
Vrijgegeven belastingen conform montage-handleiding	Zie de specificaties in de installatiehandleiding en garantievoorwaarden.

Niet-schittering optie*: Reflectie-eigenschappen bij lage instralingshoeken en vol zonlicht (volgens BRDF): Lv10°=19.000 cd/m² * Beschikbaar op aanvraag voor locaties met hoge eisen aan geen schittering/niet verblindend, prijzen verschillen

VERMOGEN BIJ STC

Onder standaard testcondities STC: Instralingsintensiteit 1.000 W/m² | spectrale verdeling AM 1,5 | temperatuur 25 ± 2°C | volgens EN 60904-3

Nominaal vermogen P_{max}	310 Wp	315 Wp
Spanning V_{mp}	33,0 V	33,2 V
Stroom I_{mp}	9,52 A	9,56 A
Nullastspanning V_{OC}	41,0 V	41,1 V
Kortsluitstroom I_{SC}	9,99 A	10,03 A
Module-efficiëntie	18,8 %	19,1 %

Meettolerantie: P_{max} ±5 %; V_{OC} ±10 %; Isc ±10 %, I_{MP} ±10 %

Terugstroombelastbaarheid I_R: 20 A, bij panelen met een externe voeding is een stringzekering van ≤ 20 A vereist.

VERMOGEN BIJ NMOT EN ZWAKKE LICHTOMSTANDIGHEDEN

NMOT (Nominal Module Operating Temperature): Instralingsintensiteit 800 W/m², spectrale verdeling AM 1,5, temperatuur 20 °C
Zwakke lichtomstandigheden: Instralingsintensiteit 200 W/m², temperatuur 25 °C, windsnelheid 1m/s, werking bij belasting

Nominaal vermogen $P_{max @NMOT}$	230 W	234 W
Nominaal vermogen $P_{max @200 W/m^3}$	61,8 W	62,8 W

Meettolerantie: P_{max} ±5 %; V_{OC} ±10 %; I_{SC} ±10 %, I_{MP} ±10 %.

Het rendement wordt verminderd bij instraling van 1000W/m² tot 200W/m² (bij 25 °C): 4 ± 2% (relatief) / −0,6 ± 0,3% (absoluut).

THERMISCHE EIGENSCHAPPEN

Bedrijfstemperatuur	-40 ... +85 °C
Omgevingstemperatuur	-40 ... +45 °C
Temperatuurcoëfficiënt P_{max}	-0,38 %/K
Temperatuurcoëfficiënt V_{OC}	-0,31 %/K
Temperatuurcoëfficiënt I_{SC}	0,05 %/K
NMOT	44 °C

I-V CURVE (PRESTATIEKLASSE 315 WP)

Stroomspanningskarakteristiek bij verschillende temperaturen en instraling.
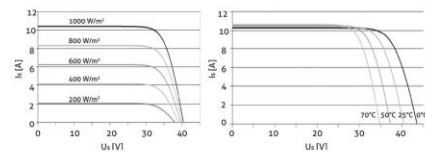
VERZENDING EN TRANSPORT

Module/ Palett	36
Verpackkingsafmetingen/ Palett L x B x D	1.700 x 1.010 x 1.640 mm
Bruto gewicht	859 kg
Paletts per truck	15
Panelen per truck	540

13.5.2 Table with electricity values

16 VAULTS

Battery Size (kWh)	Panels number	From grid (kWh)	To grid (kWh)	Self-consumption (kWh)	Payback time
0 kWh	40 panels	9314	7232	4635	7
	50 panels	9062	9938	4887	7
	60 panels	8867	12701	5082	7
	70 panels	8713	15515	5236	7
	80 panels	8594	18348	5355	7
	90 panels	8495	21204	5454	7
	100 panels	8406	24100	5543	7
30 kWh	40 panels	4635	2570	9314	17
	50 panels	3911	4804	10037	16
	60 panels	3423	7273	10526	14
	70 panels	3065	9885	10884	13
	80 panels	2824	12595	11125	13
	90 panels	2633	15359	11316	12
	100 panels	2467	18178	11482	12
50 kWh	40 panels	4166	2114	9783	23
	50 panels	3415	4320	10534	20
	60 panels	2925	6789	11024	18
	70 panels	2551	9384	11397	17
	80 panels	2289	12073	11660	16
	90 panels	2072	14811	11877	15
	100 panels	1878	17603	12071	14
100 kWh	40 panels	3750	1738	10199	30
	50 panels	3007	3953	10942	30
	60 panels	2553	6457	11396	30
	70 panels	2162	9034	11787	25
	80 panels	1838	11662	12111	23
	90 panels	1571	14350	12378	22
	100 panels	1340	17105	12609	20
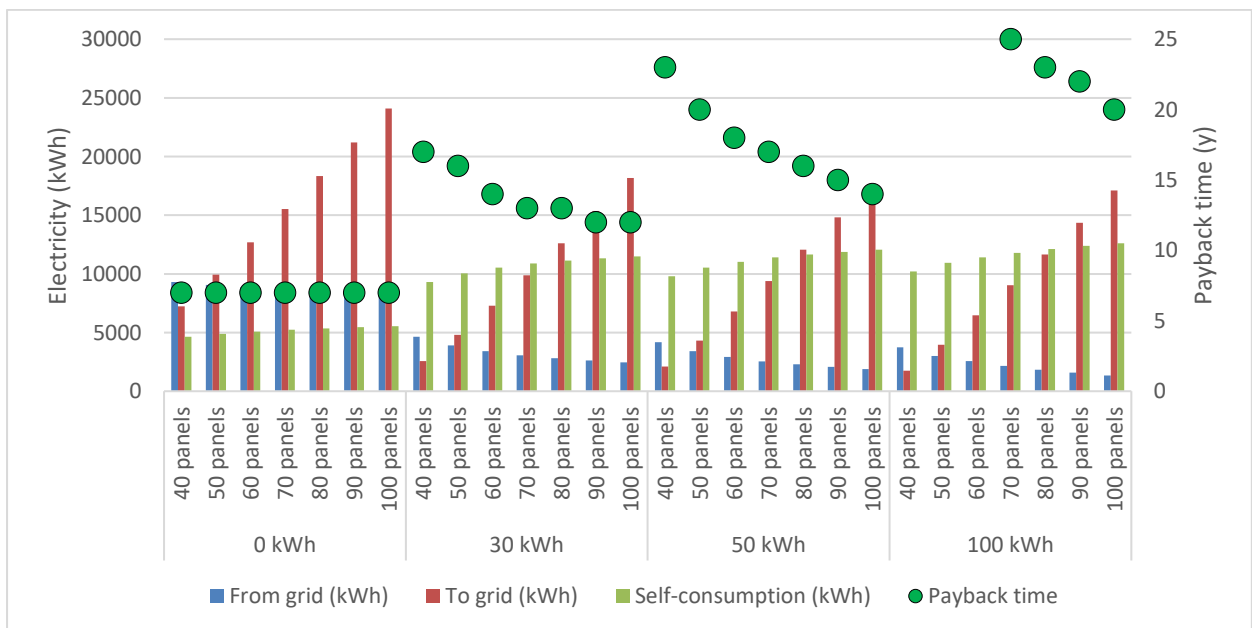
13.5.3 Calculations PV distance

Size PV

- Width 1680 mm
- Length 990 mm
- Height 40 mm

Inclination α = 37°

$$Height\ difference = \sin(\alpha) * module\ width$$
$$Height\ difference = \sin(37°) * 1680\ mm$$
$$Height\ difference = 1011.05\ mm$$

FEBRUARY

20th February, 9am-3pm
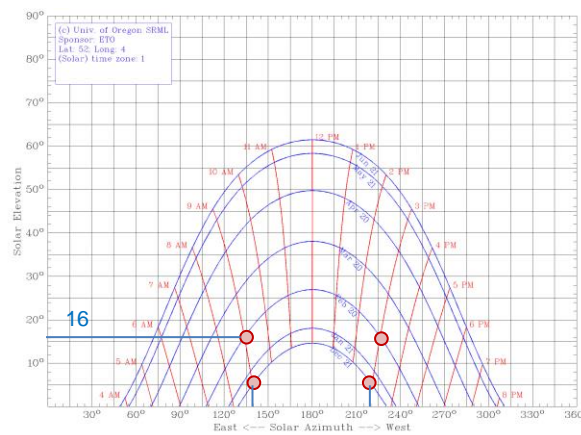
Solar elevation β (according to graph) = 16°

$$Module\ row\ spacing = height\ difference/\tan(\beta)$$
$$Module\ row\ spacing = 1011.05/\tan(36°)$$
$$Module\ row\ spacing = 3525.95\ mm$$

Azimuth correction angle γ (according to graph) = 180°-140° = 40°

$$Minimum\ module\ row\ spacing = Module\ row\ spacing/\tan(\gamma)$$
$$Minimum\ module\ row\ spacing = 3525.95/\tan(40°)$$
$$Minimum\ module\ row\ spacing = 2.70\ m$$
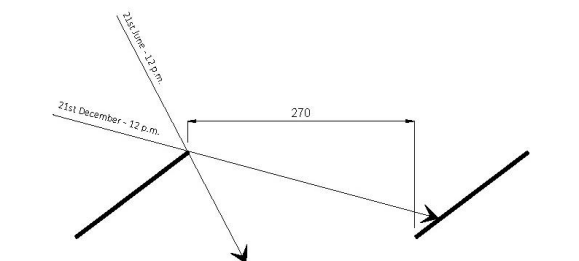
Figure 126. PV panels with 2.70 distance and elevation of sun on the shorter day of the year (21st December, 15°)

JUNE

21st June, 9am-3pm
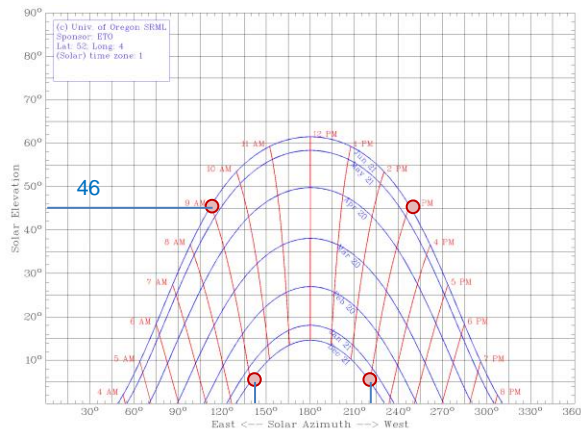
Solar elevation *β* (according to graph) = 46°

$$Module\ row\ spacing = height\ difference/\tan(\beta)$$

$$Module\ row\ spacing = 1011.05/\tan(46°)$$

$$Module\ row\ spacing = 1011.05\ mm$$

Azimuth correction angle *γ* (according to graph) = 180°-140° = 40°

$$Minimum\ module\ row\ spacing = Module\ row\ spacing/\tan(\gamma)$$

$$Minimum\ module\ row\ spacing = 1011.05/\tan(40°)$$

$$Minimum\ module\ row\ spacing = 0.7745\ m$$
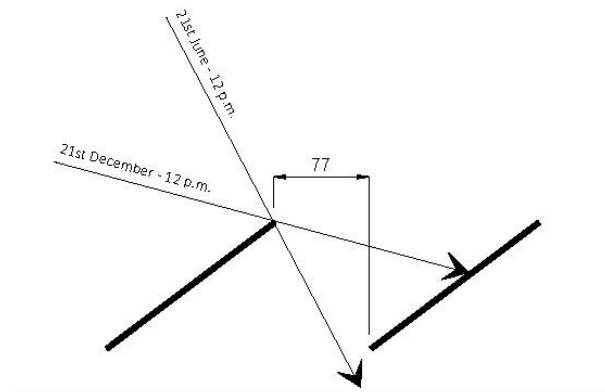
Figure 127. PV panels with 0.77 distance, with sun elevation (15° and 62°) on the 21st of December and 21st of June at 12 p.m.

DECEMBER

21st December, 9am-3pm
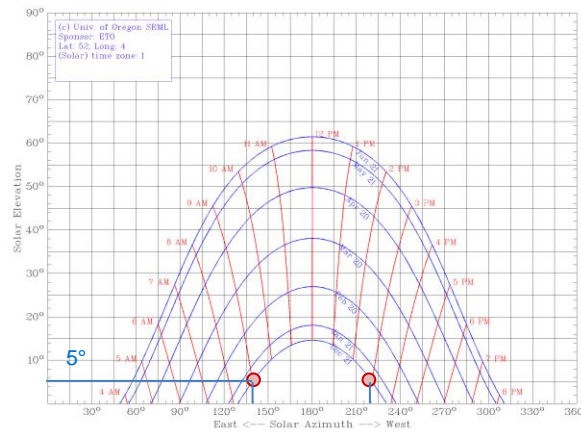
Solar elevation β (according to graph) = 5°

$$Module\ row\ spacing = height\ difference/\tan{(\beta)}$$

$$Module\ row\ spacing = 1011.05/\tan(46°)$$

$$Module\ row\ spacing = 11556.35\ mm$$

Azimuth correction angle γ (according to graph) = 180°-140° = 40°

$$Minimum\ module\ row\ spacing = Module\ row\ spacing/\tan{(\gamma)}$$

$$Minimum\ module\ row\ spacing = 11556.35/\tan(40°)$$

$$Minimum\ module\ row\ spacing = 8.8527\ m$$
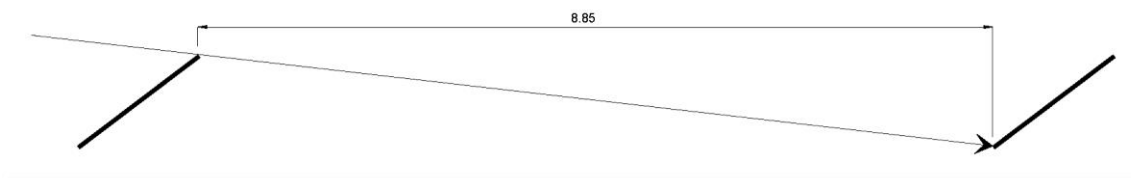
Figure 128. PV panels with 8.85 distance and elevation of sun on the shorter day of the year (21st December, 15°)

13.5.4 State of Charge of the batteries for each case – 16 vaults building

40 panels – 30 kWh
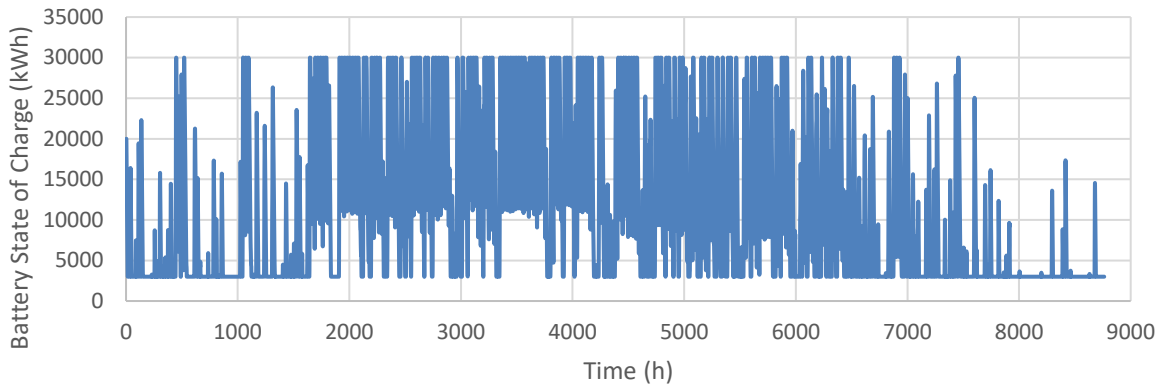
40 panels – 50 kWh

40 panels – 100 kWh

113
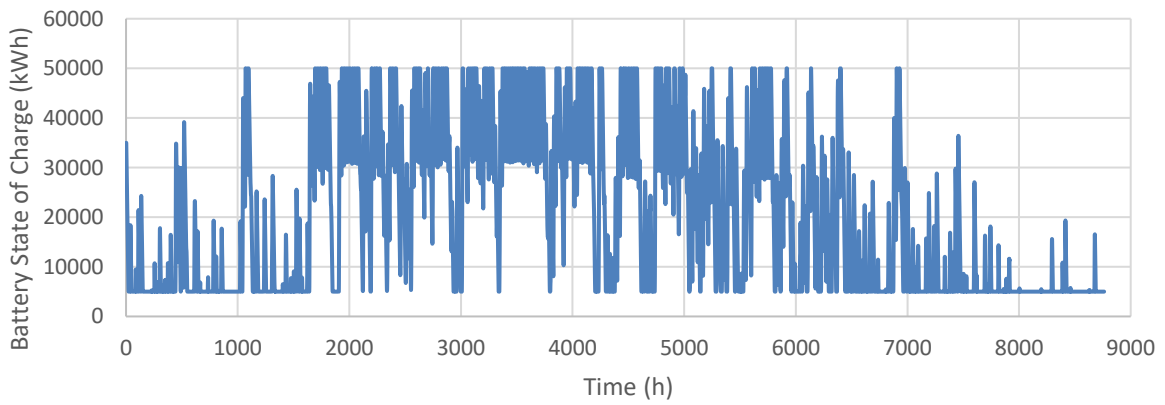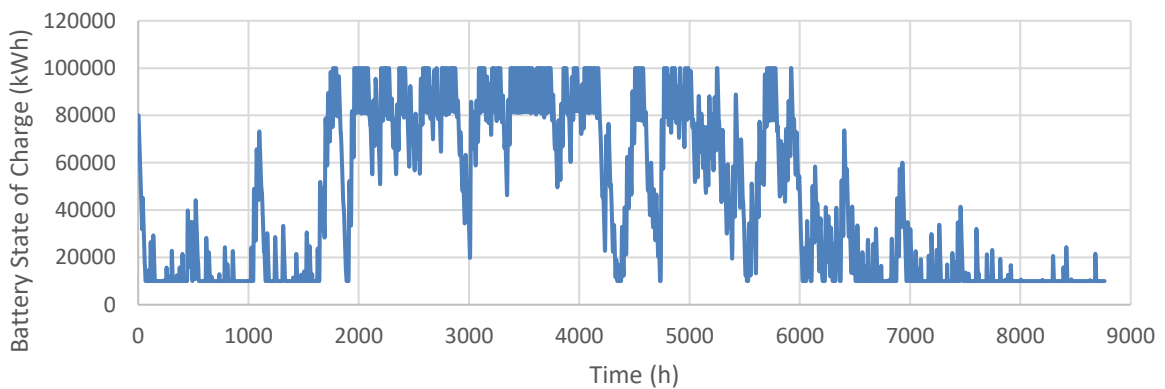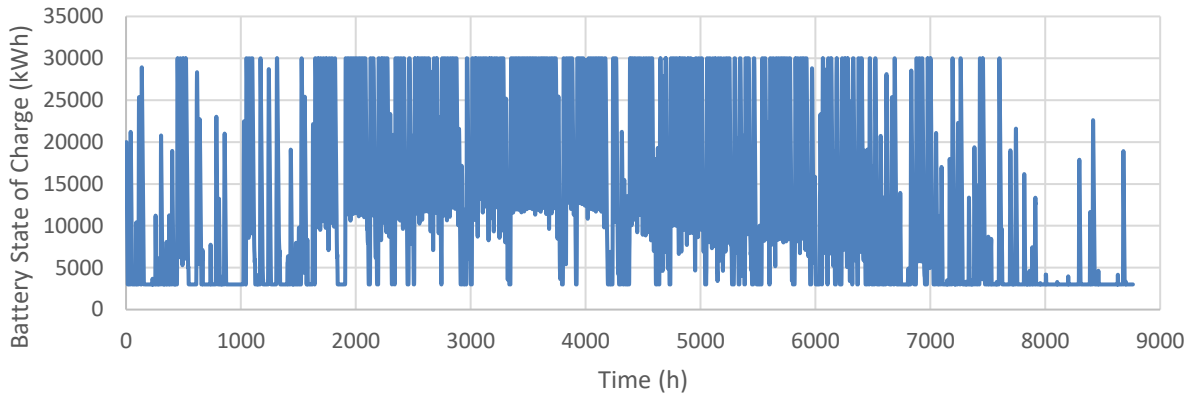
50 panels – 30 kWh

50 panels – 50 kwh
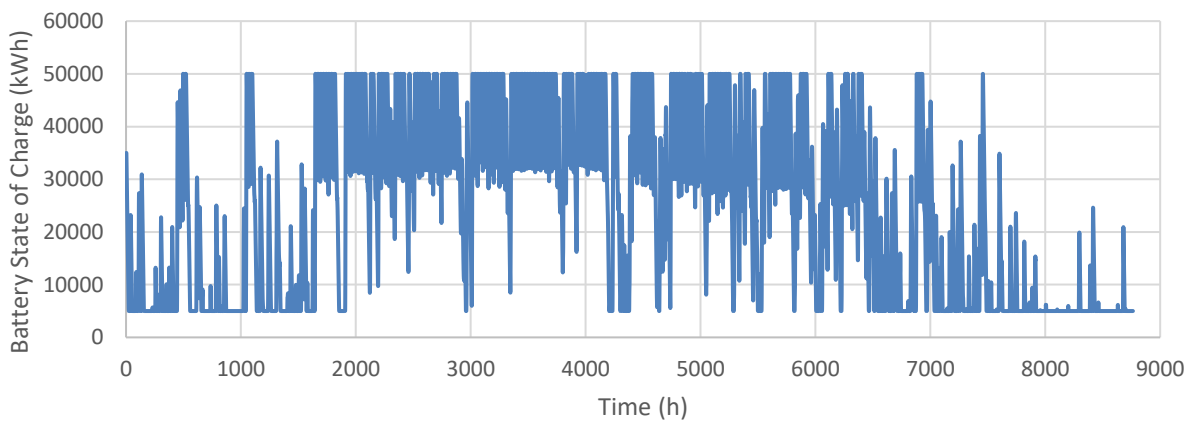
50 panels – 100 kwh
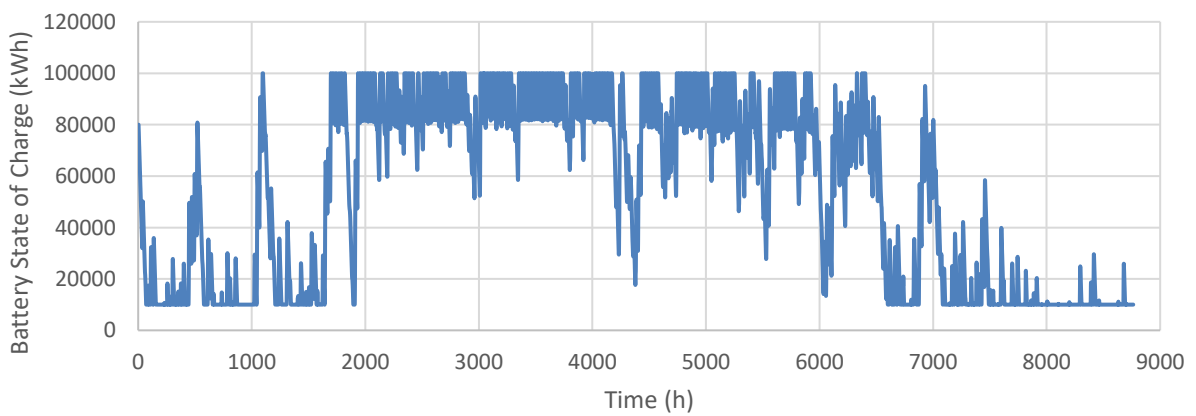
60 panels – 30 kwh
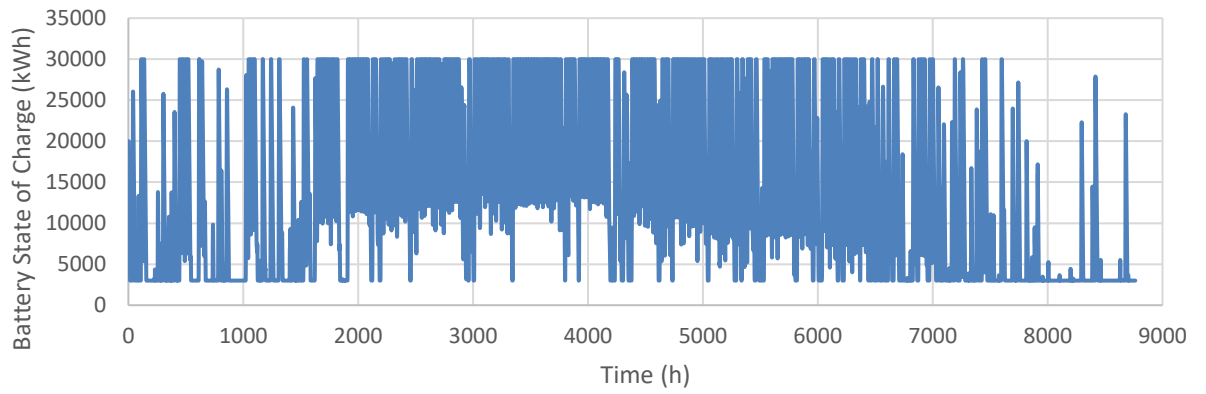
60 panels – 50 kWh

60 panels – 100 kWh

115
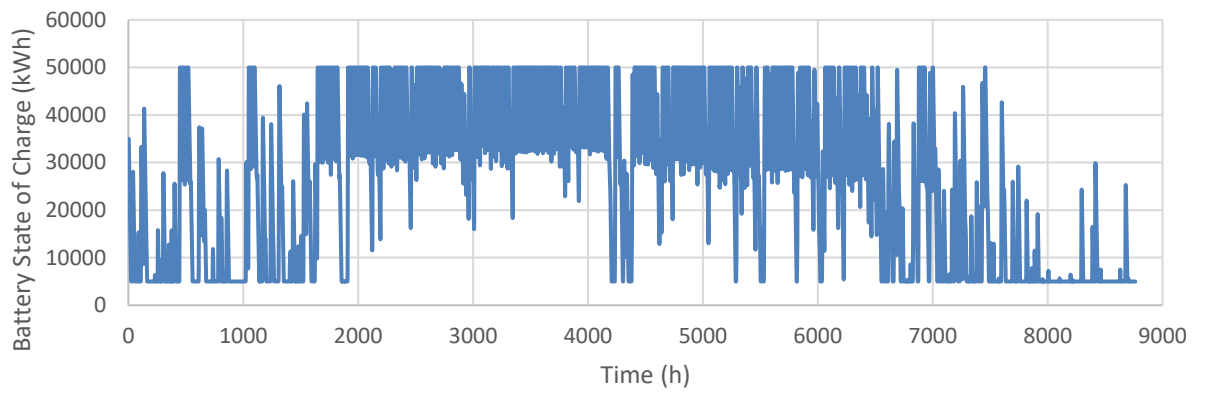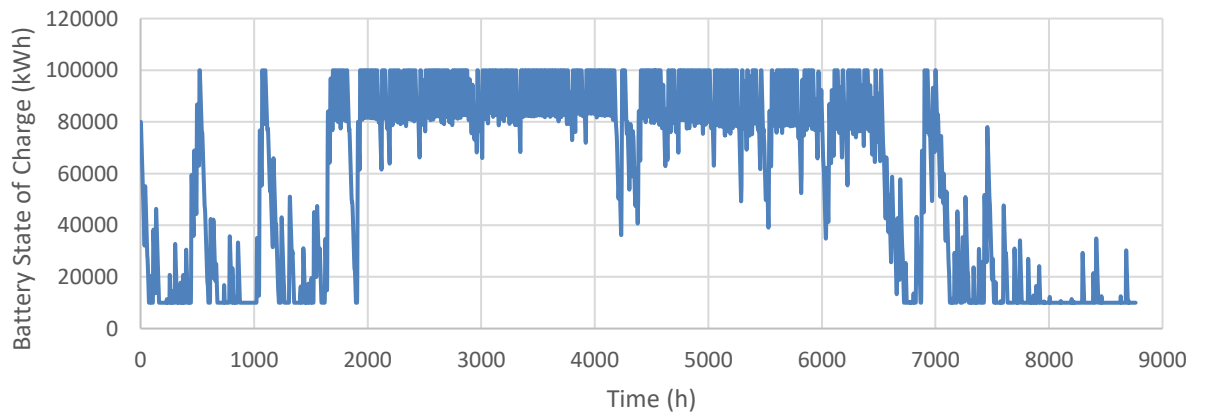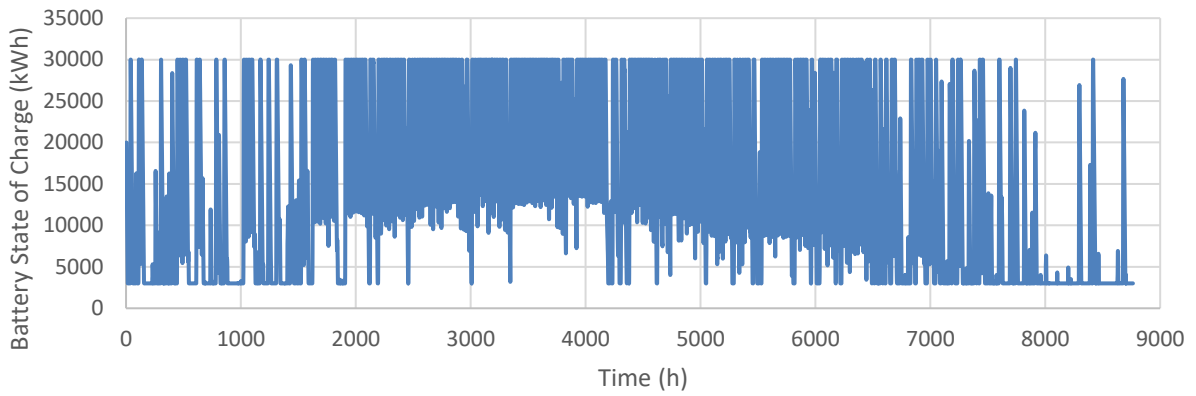
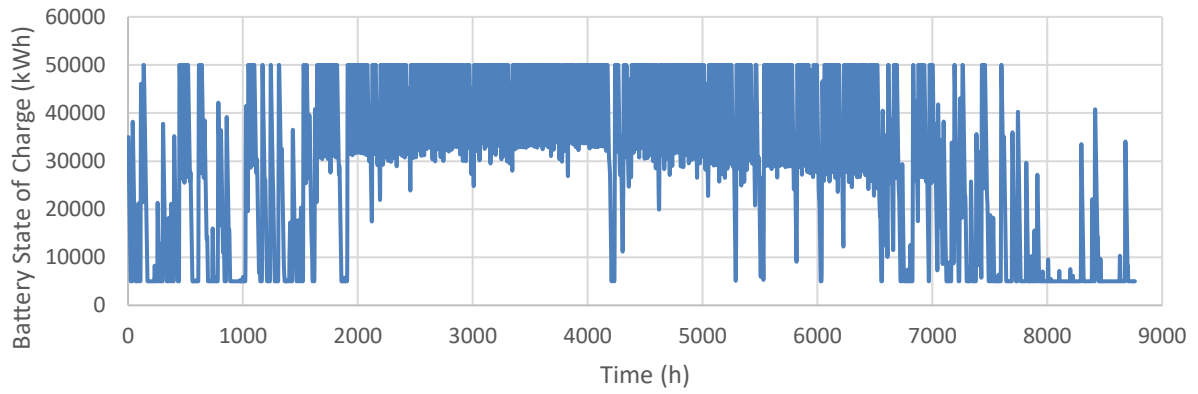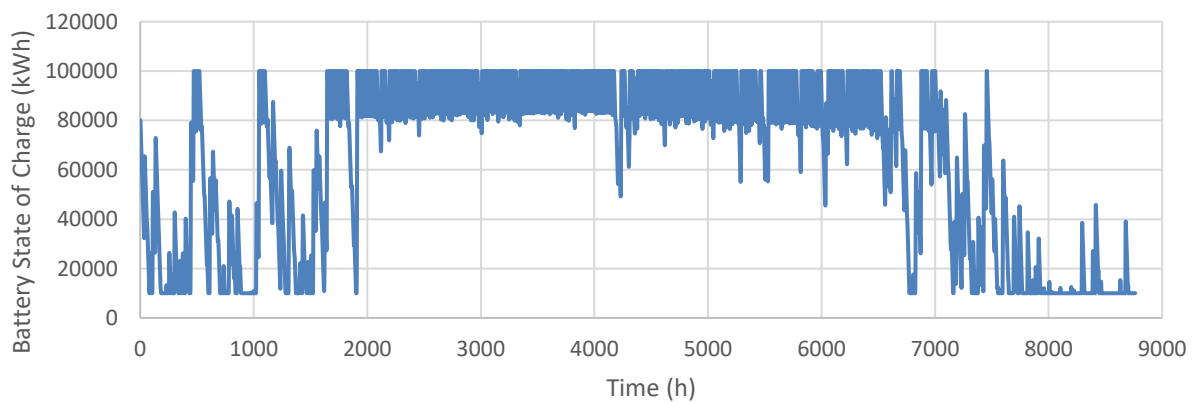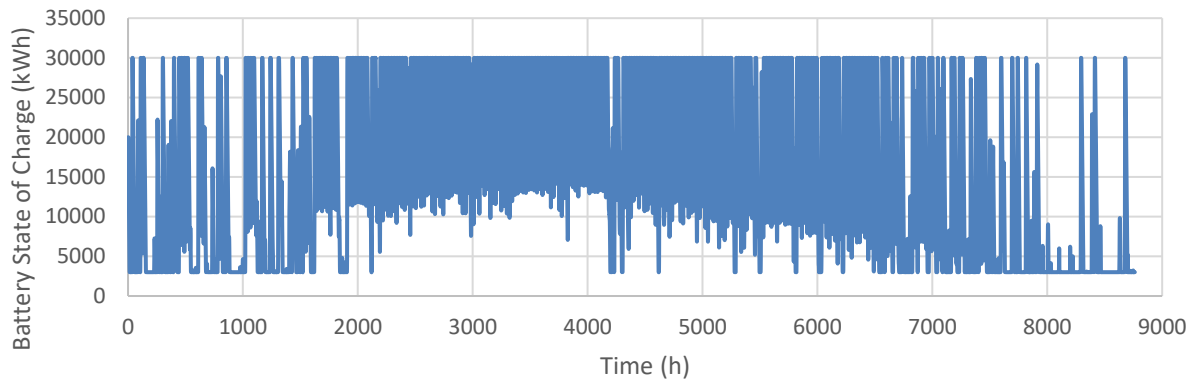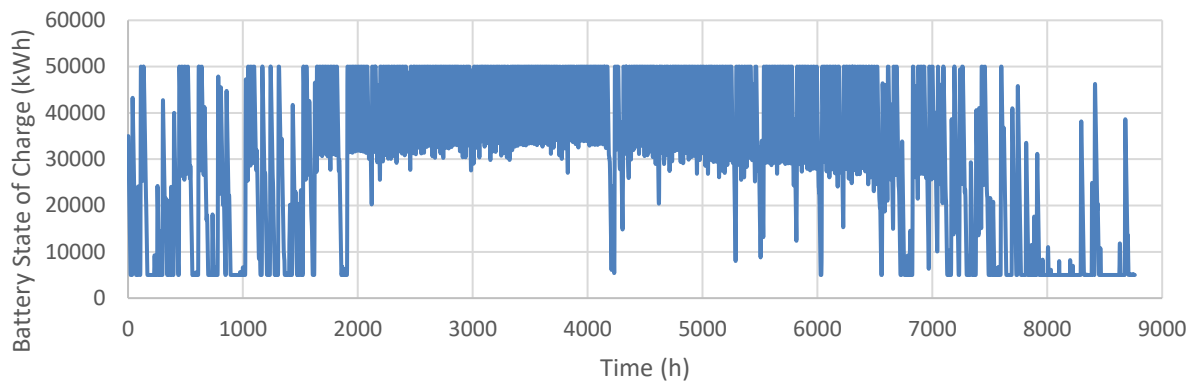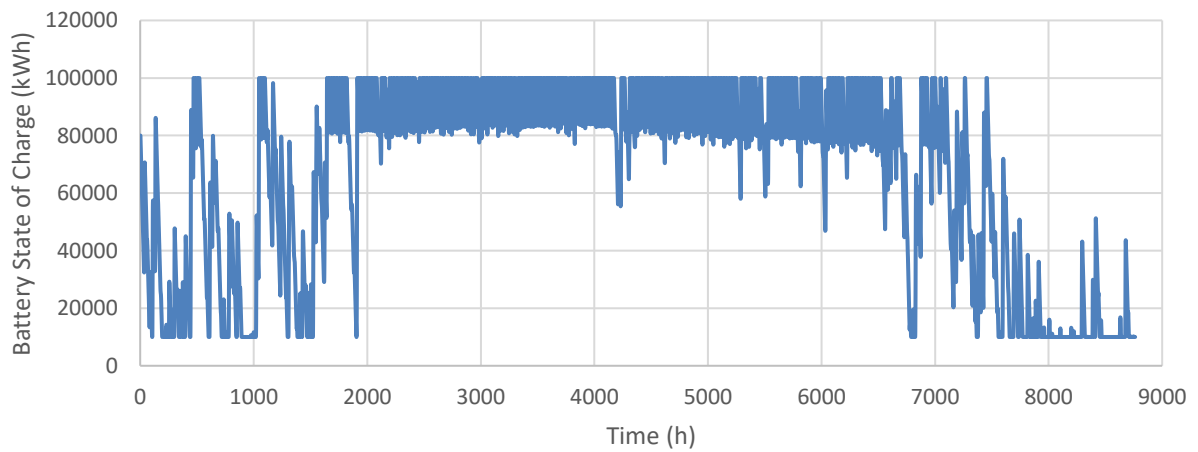## 70 panels – 30 kwh

70 panels – 50 kwh
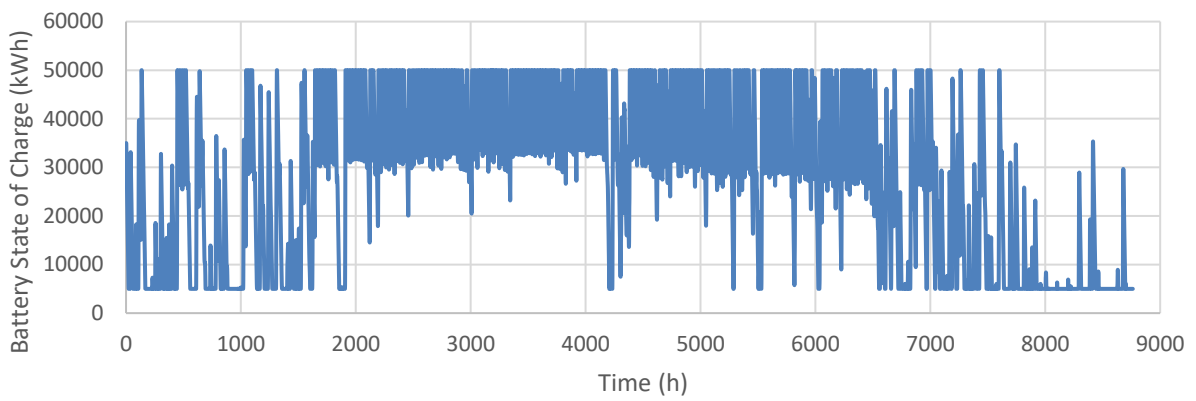
70 panels – 100 kwh
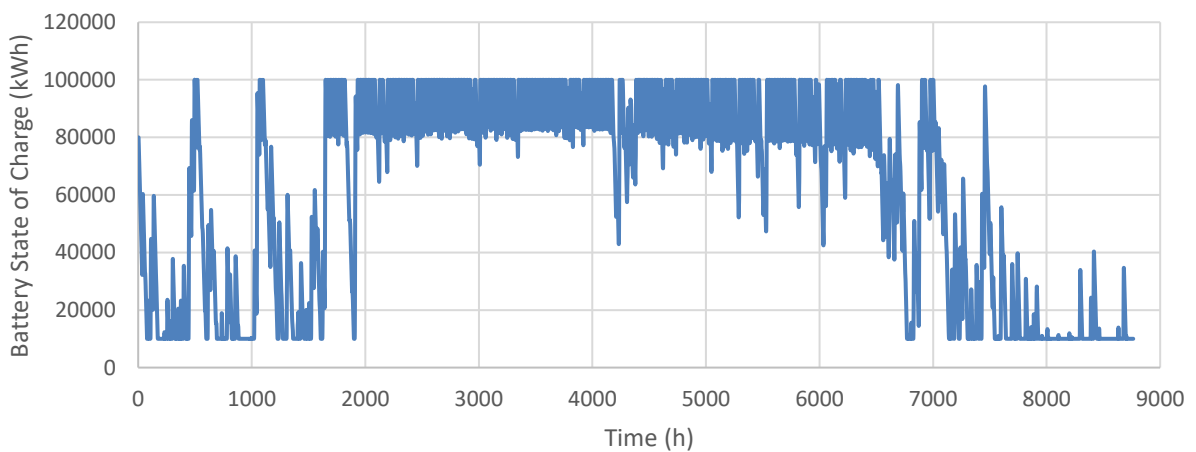
80 panels – 30 kwh
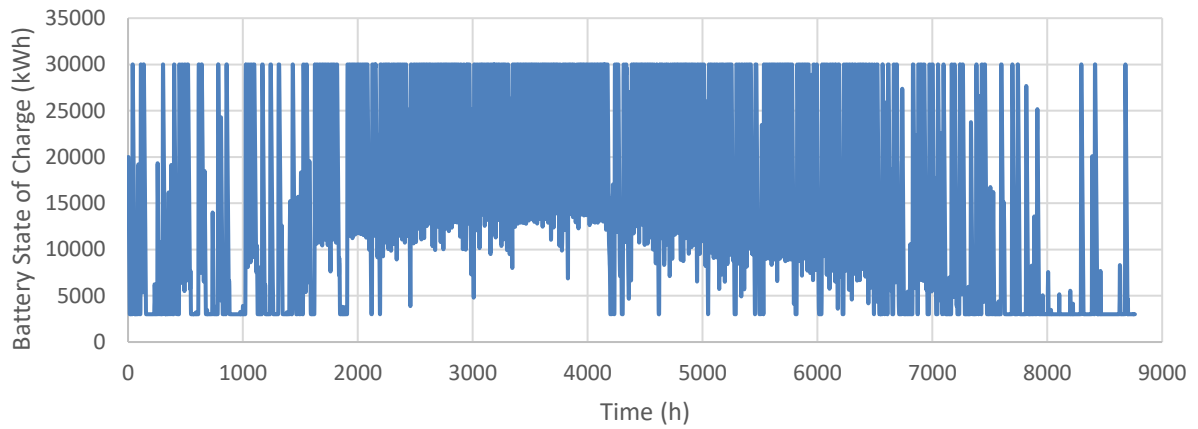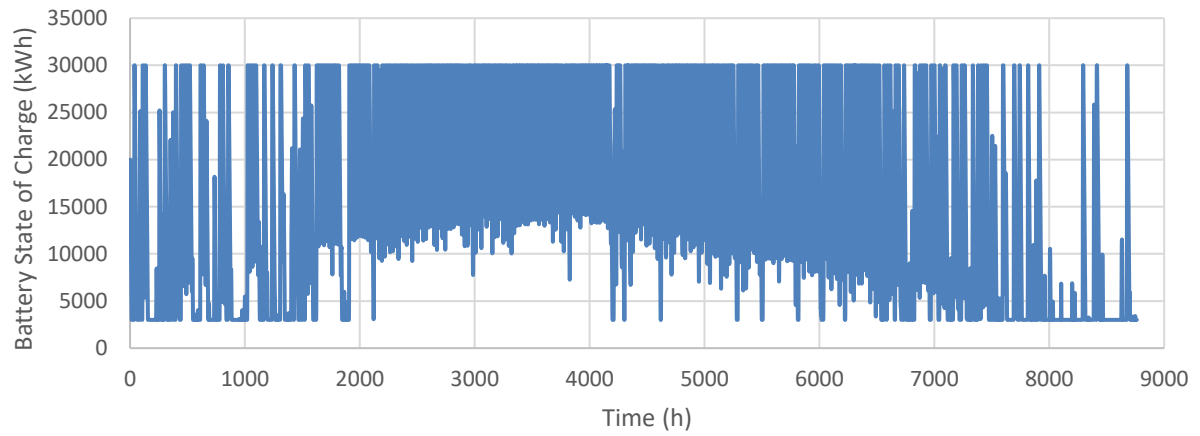

80 panels – 50 kwh

80 panels – 100 kwh

90 panels – 30 kwh

90 panels – 50 kwh
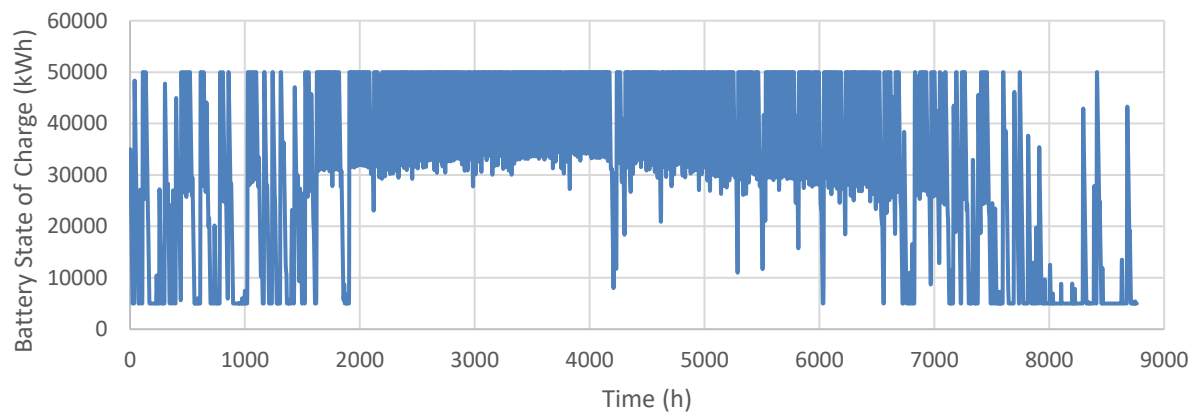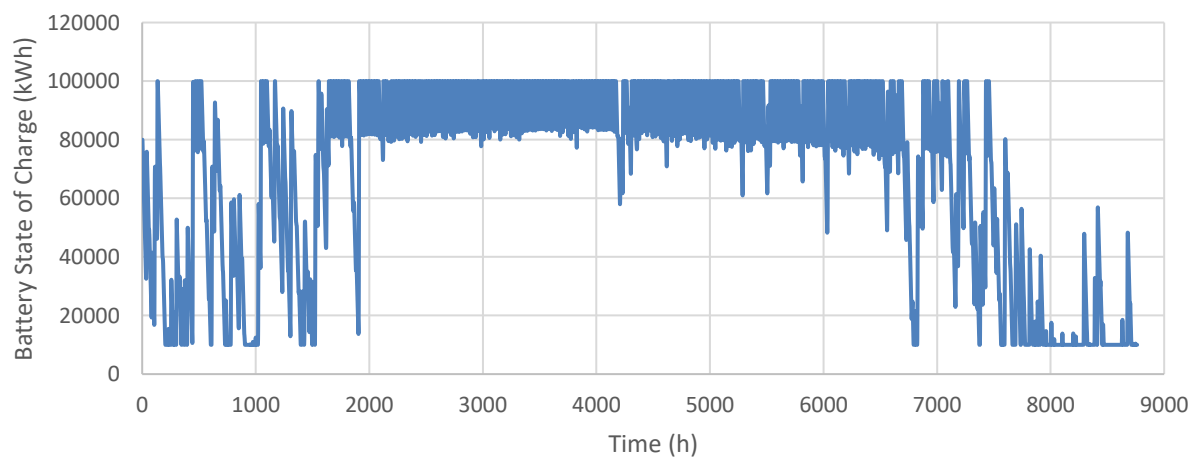

90 panels – 100 kwh

118

100 panels – 30 kwh

100 panels – 50 kwh

100 panels – 100 kwh

13.6 LCA

13.6.1 U-value matching for walls and roof, for different building materials

WALL	CLT		Mineral wool		
	thickness [mm]	thermal conductivity [W/(m*K)]	thickness [mm]	thermal conductivity [W/(m*K)]	U-value [W/(m²K)
Cross Laminated Timber	300	0.11	200	0.035	**0.1161**
	Concrete		Mineral wool		
	thickness [mm]	thermal conductivity [W/(m*K)]	thickness [mm]	thermal conductivity [W/(m*K)]	
Concrete	200	2	300	0.035	**0.1131**
	Mineral wool layer 1		Mineral wool layer 2		
	thickness [mm]	thermal conductivity [W/(m*K)]	thickness [mm]	thermal conductivity [W/(m*K)]	
Lightweight timber frame	100	0.035	200	0.035	**0.1144**

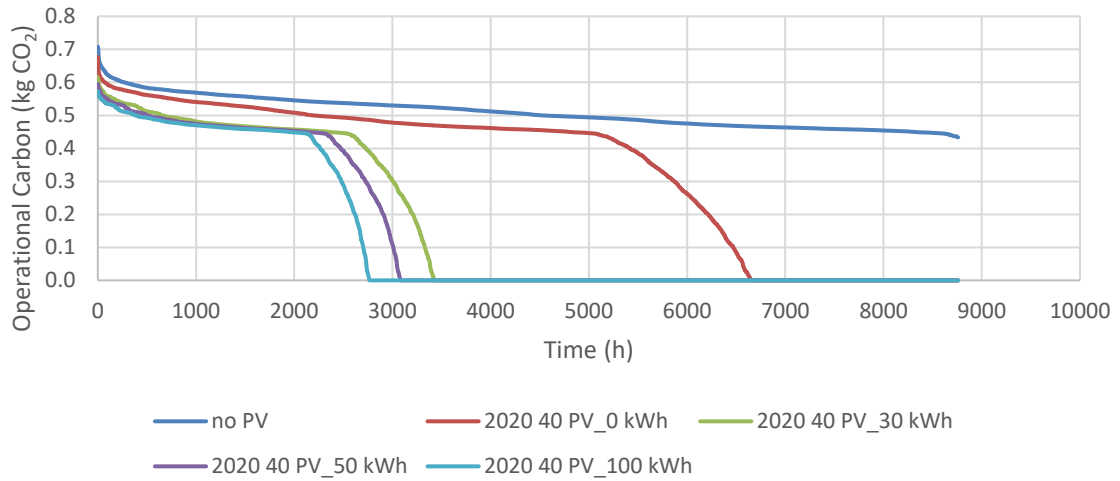| ROOF	CLT		Mineral wool		
	thickness [mm]	thermal conductivity [W/(m*K)]	thickness [mm]	thermal conductivity [W/(m*K)]	U-value [W/(m²K)
Cross Laminated Timber	200	0.11	250	0.035	**0.1095**
	Concrete		Mineral wool		
	thickness [mm]	thermal conductivity [W/(m*K)]	thickness [mm]	thermal conductivity [W/(m*K)]	
Concrete	200	2	320	0.035	**0.1062**
	Mineral wool layer 1		Mineral wool layer 2		
	thickness [mm]	thermal conductivity [W/(m*K)]	thickness [mm]	thermal conductivity [W/(m*K)]	
Lightweight timber frame	100	0.035	220	0.035	**0.1074**

13.6.2 Load Duration Curve

Example of 40 PVs, WITH different battery sizes for the years 2020, 2030, 2040 and 2050, considering the energy transition of the grid.
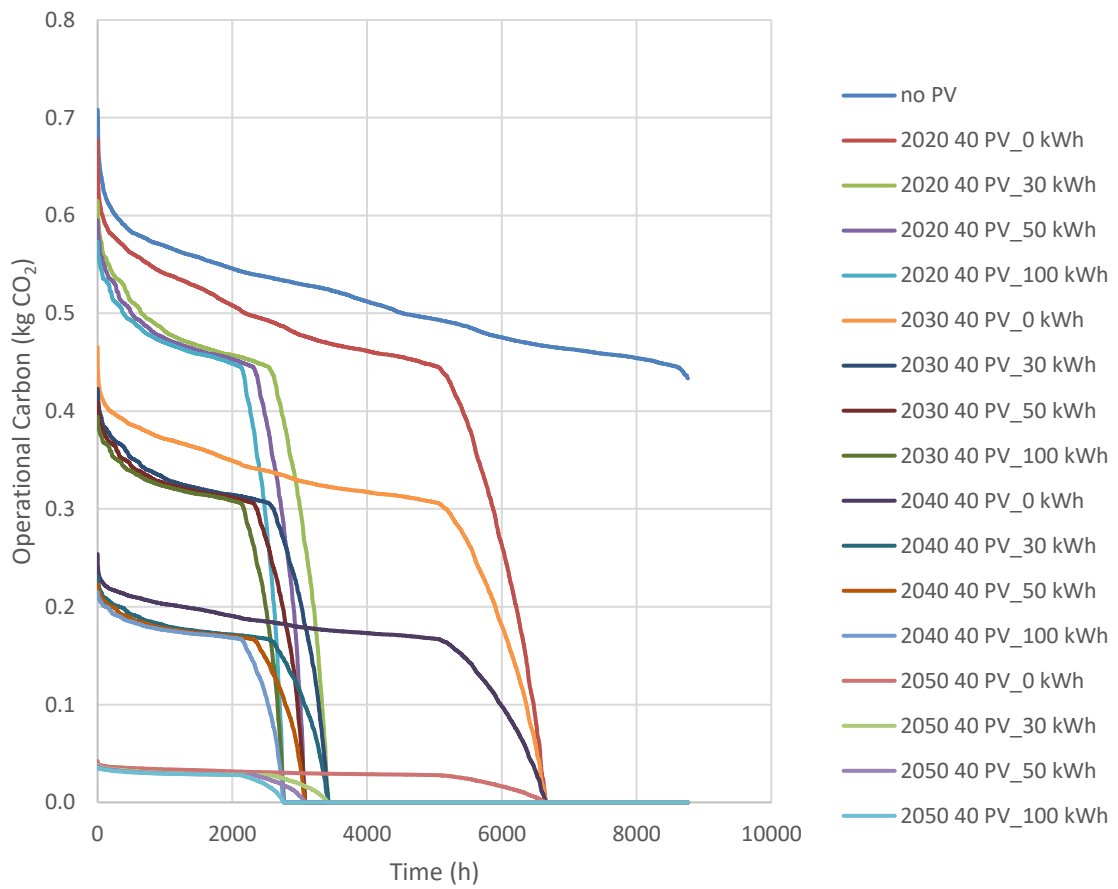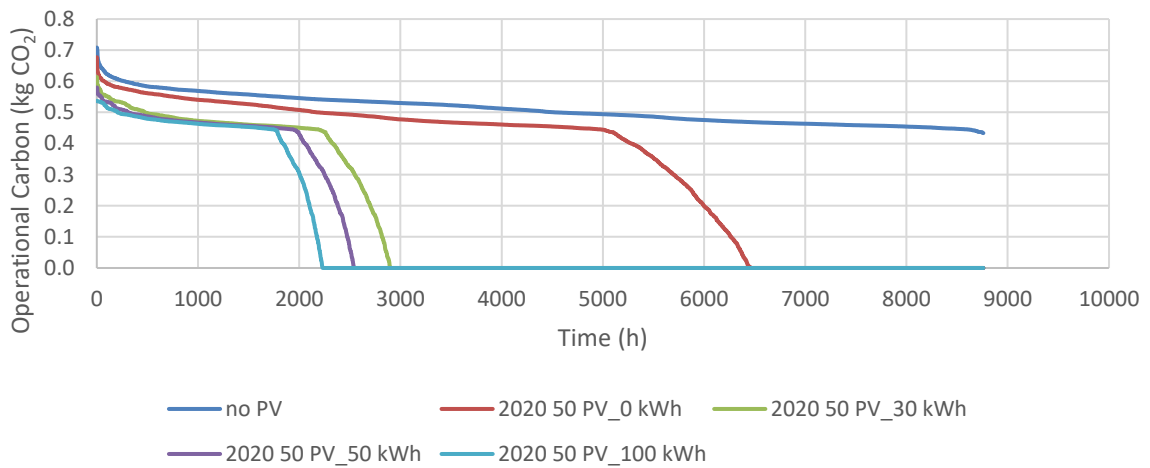
LCD of Operational Carbon – building without PVs, with PVs, and with PVs and batteries for year 2020
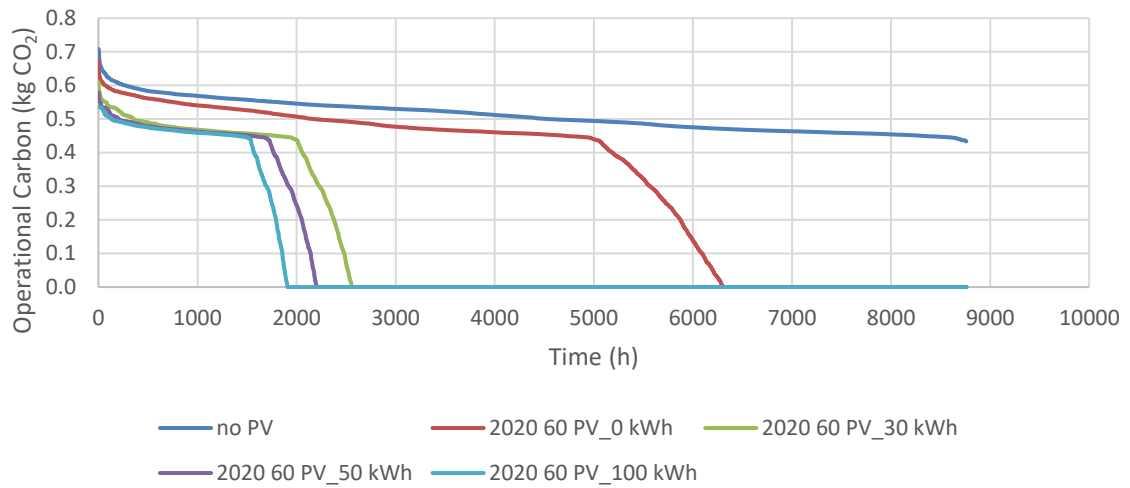
40 PV PANELS

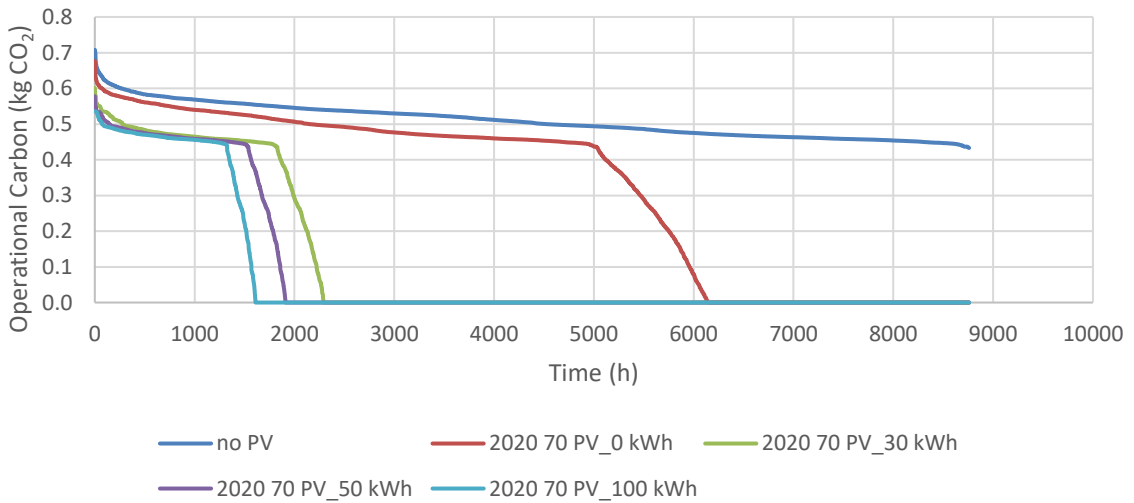## 50 PV PANELS

60 PV PANELS

70 PV PANELS

80 PV PANELS

90 PV PANELS

Operational Carbon (kg CO_2) vs Time (h)

Legend: no PV — 2020 90 PV_0 kWh — 2020 90 PV_30 kWh — 2020 90 PV_50 kWh — 2020 90 PV_100 kWh

100 PV PANELS

Operational Carbon (kg CO_2) vs Time (h)

Legend: no PV — 2020 100 PV_0 kWh — 2020 100 PV_30 kWh — 2020 100 PV_50 kWh — 2020 100 PV_100 kWh
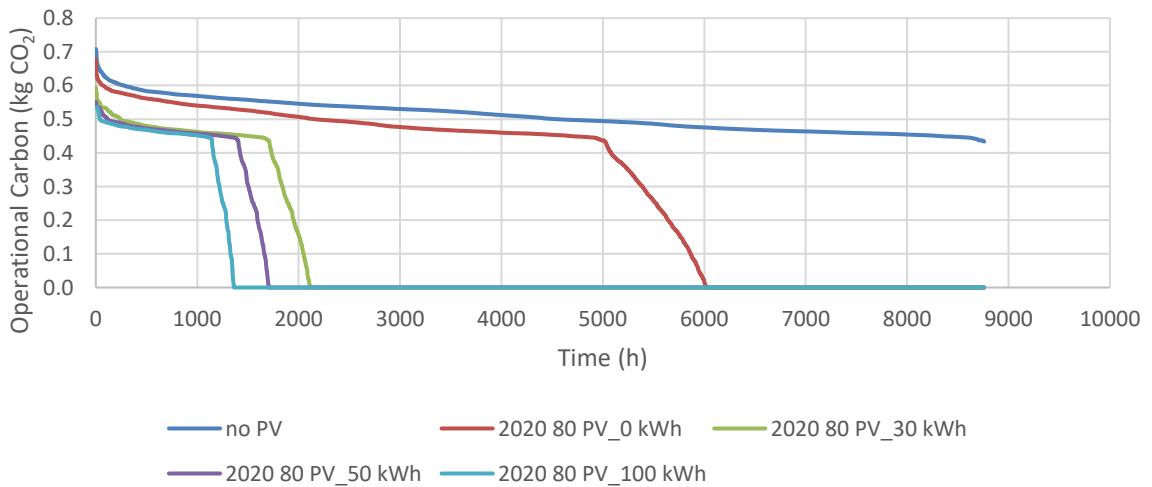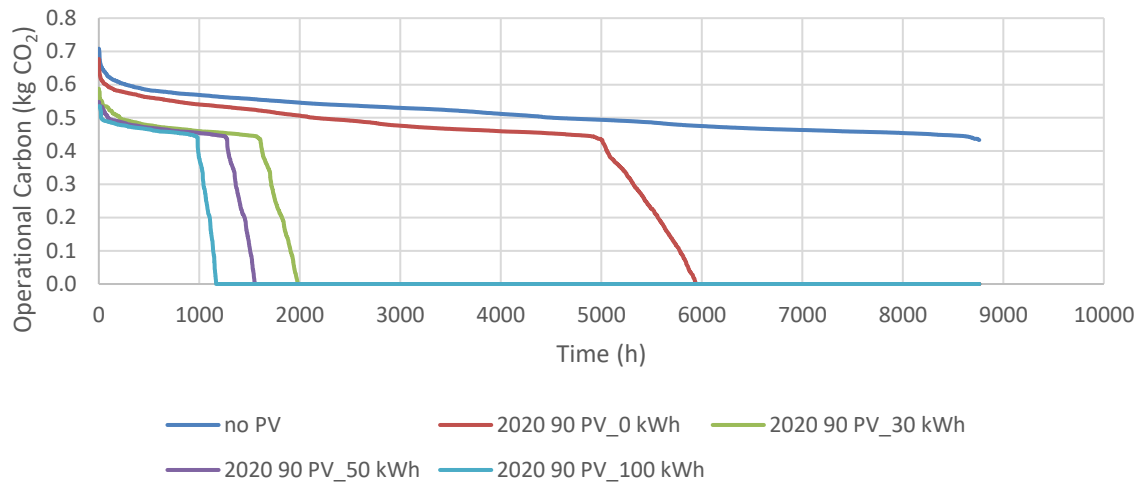
13.7 Cost Analysis

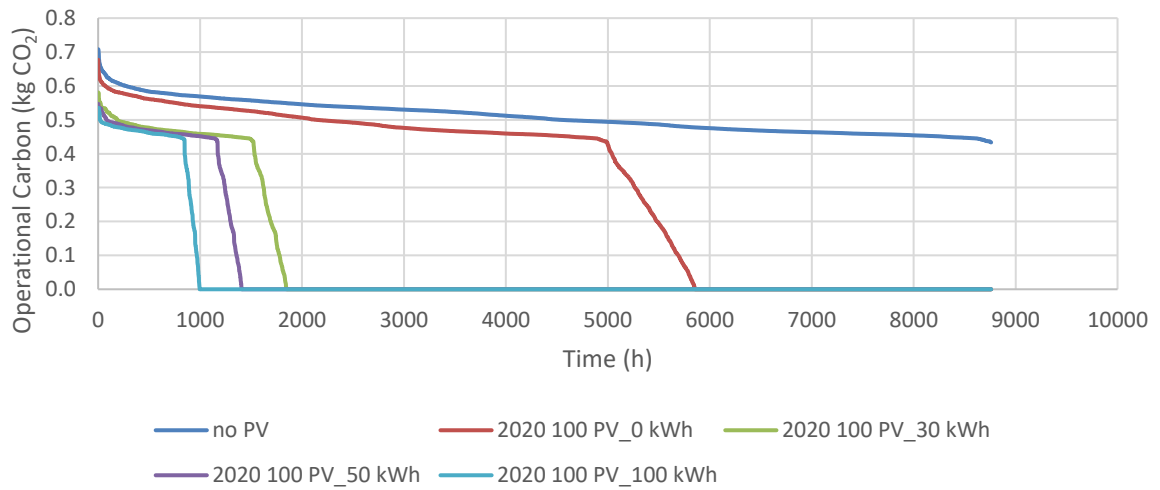|	Vault number – movable shelves			Fixed shelves	
	16	8	4		
Building surface	348.86	263.56	222.58	403.65	m²
ARCHITECTURAL HULL					
Materials					
CLT	190.81	140.90	112.38	194.36	m³
Rockwool	279.66	206.46	170.34	284.90	m³
Concrete floor	348.86	263.56	222.58	403.65	m³
Foundations	171.34	145.74	133.44	181.5	m¹
Price CLT	700				€/m³
+ *manufacturing surchage and business profit (25%)*	875				€/m³
CLT cost	**166,957**	**123,290**	**98,329**	**170,068**	€
Price Rockwool	9				€/m²
Calculation m2 with 12 cm thickn.	2,331	1,721	1,420	2,374	m²
Rockwool cost	**20,975**	**15,485**	**12,776**	**21,367**	€
Price concrete floor with EPS and reinforcement	115				€/m²
Concrete floor cost	40,119	30,310	25,596	46,420	€
Price foundations	60				€/m¹
Foundation cost	**10,280**	**8,744**	**8,006**	**10,890**	€
TOTAL materials	**240,845**	**179,550**	**146,127**	**251,119**	€
Price per m²	**690**	**681**	**657**	**622**	€/m²
INSTALLATION					
Installations (HVAC, Water, plumbing, electric)					
Cost per m² - HIGH	950				€/m²
Cost per m² - LOW	530				€/m²
HIGH	331,417	250,383	211,449	383,468	€
LOW	184,896	139,687	117,966	213,935	€
FIXED-EQUIPMENT					
Doors					
Number	16	8	4	20	
Price	1,500				€/unit
Total	**24,000**	**12,000**	**6,000**	**30,000**	€

Vents					
Number	16	8	4	20	
Price (€)	1,000				€/unit
Total	**16,000**	**8,000**	**4,000**	**20,000**	**€**
TERRAIN					
Cost per m² - HIGH	50				€/m²
Cost per m² - LOW	30				€/m²
HIGH	34,886	26,356	22,258	40,365	€
LOW	20,932	15,814	13,355	24,219	€
INDIRECT COSTS					
Cost per m² - HIGH	900				€/m²
Cost per m² - LOW	360				€/m²
HIGH	627,949	474,410	400,640	726,570	€
LOW	251,179	189,764	160,256	290,628	€
TOTAL COST - HIGH	1,275,097	950,699	790,473	1,451,522	€
TOTAL COST - LOW	737,852	544,815	447,704	829,901	€
ADDITIONAL COSTS					
percentage - HIGH	36%				€/m²
percentage - LOW	23%				€/m²
FINAL - HIGH	1,734,132	1,292,951	1,075,044	1,974,070	**€**
FINAL - LOW	907,558	670,122	550,676	1,020,778	**€**
Average	1,320,845	981,537	812,860	1,497,424	**€**
Per m² - HIGH	4,971	4,906	4,830	4,891	**€/m²**
Per m² - LOW	2,601	2,543	2,474	2,529	**€/m²**
Average	3,786	3,724	3,652	3,710	**€/m²**